MOLECULAR MECHANISMS OF MICROBIAL IRON RESPIRATION BY *SHEWANELLA ONEIDENSIS* MR-1

A Dissertation
Presented to
The Academic Faculty

By

Justin Lee Burns

In Partial Fulfillment
of the Requirements for the Degree
Doctor of Philosophy in the
School of Biology

Georgia Institute of Technology

May 2010

MOLECULAR MECHANISMS OF MICROBIAL IRON RESPIRATION BY *SHEWANELLA ONEIDENSIS* MR-1

Approved by:

Dr. Thomas J. DiChristina, Advisor
School of Biology
Georgia Institute of Technology

Dr. Roger Wartell
School of Biology
Georgia Institute of Technology

Dr. Nicholas Hud
School of Chemistry and Biochemistry
Georgia Institute of Technology

Dr. Ingeborg Schmidt-Krey
School of Biology
Georgia Institute of Technology

Dr. Andrew Neal
Center for Soils and Ecosystem Function
Rothamsted Research, United Kingdom

Date Approved: 31 March 2010

ACKNOWLEDGEMENTS

Many people have been a part of this work, either directly or indirectly, and I cannot possibly mention them all. I would like to first thank my advisor Tom DiChristina, for giving me the chance to start a research career after only my sophomore year at Georgia Tech. He provided not only financial support for the work I performed, but also moral support and constructive criticism whenever they were required. Additionally I would like to thank the members of my thesis committee for helping to shape my doctoral work and for providing collaborative efforts whenever required. Thank you to Roger Wartell, Inga Schmidt-Krey, Andy Neal and Nick Hud.

To the members of the DiChristina Lab, both former and current, Jason Dale, David Bates, Christine Fennessey, Seng Kew Wee, and Nadia Szeinbaum; it's been a pleasure to walk this part of the journey beside you through the disappointments and victories. To the other Ph.D. candidates, recent graduates, and researchers at Georgia Tech, including Rob Martinez, Jason Landrum, Morris Jones, Jake Leech, Melanie Beazley, Lin Hui, Kate Salome, Jordon Beckler; your friendship and camaraderie have made an immeasurable difference in my experience. Thank you also to the many undergraduates who have helped me in my graduate career.

Financial support for this work was provided by the Department of Energy, and the National Science Foundation.

TABLE OF CONTENTS

LIST OF TABLES

LIST OF FIGURES

LIST OF SYMBOLS AND ABBREVIATIONS

ADP	Adenosine diphosphate
ATP	Adenosine triphosphate
C42A	Cys42Ala knock-in complemented mutant of MTRB1
C45A	Cys45Ala knock-in complemented mutant of MTRB1
CBL	Cystathionine beta-lyase
DMRB	dissimilatory metal reducing bacteria
DMSO	dimethylsulfoxide
DNA	deoxyribonucleic acid
DOE	Department of Energy
E. coli	*Escherichia coli*
ETC	Electron transport chain
FeRB	iron-reducing bacteria
FMN	Flavinmononucleotide
IM	Inner Membrane
LB	Luria Bertani growth medium
MTRB1	*S. oneidensis* in-frame deletion mutant of *mtrB*
MFC	microbial fuel cell
MR-1	*S. oneidensis* MR-1 (wild-type)
NAD(P)H	Nicotinamide Adenine Dinucleotide (phophate) (reduced form)
OM	Outer Membrane
ORF	Open Reading Frame

PMF	Proton motive force
PSRA1	*S. oneidensis* in-frame deletion mutant of *psrA*
PSRA+	"knock-in" complemented PSRA1
RNA	ribonucleic acid
SDS	Sodium dodecyl sulfonate
SM	defined salts medium
S. oneidensis	*Shewanella oneidensis*
S. putrefaciens	*Shewanella putrefaciens*
ΔSO3800	*S. oneidensis* in-frame deletion mutant of SO3800
TEA	Terminal electron acceptor
TMAO	trimethylamine-*N*-oxide

SUMMARY

Microbial metal respiration is central to a variety of biogeochemically important processes including the weathering of clays, biotransformation of Fe- and Mn-bearing minerals, and reductive precipitation of radionuclides (e.g. U(VI) and Tc(VII)); the latter forming the basis for an alternative remediation strategy for radioactive-contaminated field sites. Compared to the wealth of knowledge of other respiratory processes including aerobic respiration and anaerobic respiration using NO_3^-, SO_4^{2-}, fumarate, and other compounds as electron acceptor, the components of the respiratory chain terminating with transition metals have yet to be conclusively identified. *Shewanella* spp. are present in a variety of freshwater and marine environments and can respire a variety of compounds which span the redox continuum. These include O_2, solid and soluble Fe(III), Mn(III), Mn(IV), NO_3^-, NO_2^-, $S_2O_3^{2-}$, S^0, DMSO, TMAO, fumarate, U(VI) and Tc(VII). Because of this extreme respiratory versatility, *Shewanella* spp. may predominate in redox-stratified subsurface environments where terminal electron acceptors vary on small temporal and spatial scales.

In the present study, a novel gene deletion system was constructed and used to examine the function of PsrA, the putative thiosulfate reductase in *S. oneidensis* MR-1. PsrA-null mutants (PSRA1) was unable to grow with $S_2O_3^{2-}$ or S^0 as terminal electron acceptor while retaining respiratory ability on all other electron acceptors tested. Additionally, PSRA1 retained mRNA transcripts for downstream genes *psrB* and *psrC*, indicating that the *psrA* mutation was in-frame and did not cause polar mutations. Using the newly constructed suicide vector, genes encoding proteins identified in the peripheral protein fraction, including those present in the Fe(III) terminal reductase complex, were

systematically deleted from the *S. oneidensis* MR-1 genome and the resulting mutant strains were tested for the ability to respire Fe(III). Two mutant strains (ΔSO3800 and MTRB1) were isolated and further characterized. SO3800 is a putative OM serine protease that displays sequence similarity to known bacterial adhesins. ΔSO3800 was deficient in adhesion to hematite (Fe_2O_3), yet retained Fe(III) respiratory ability. ΔSO3800 also displayed an increase in cell surface exopolymers and decreased electrophoretic mobility. MTRB1 contains a deletion in OM protein MtrB and is abolished in Fe(III) respiratory ability. MtrB contains a conserved N-terminal CXXC motif that may act as electron transfer motif or a structurally important disulfide bond. Both cysteines were independently changed to alanine via site-directed mutagenesis and subsequent "knock-in" complementation using the newly constructed suicide vector. Both MTRB1 and C42A displayed diminished Fe(III) respiratory ability and increased cytochrome content in the peripheral protein fraction while C45A displayed a phenotype similar to wild type. Potential mechanisms of Fe(III) respiration involving C42 and MtrB are proposed.

CHAPTER 1

INTRODUCTION

Iron is the fourth most abundant element in the Earth's crust, after silicon, aluminum and oxygen. Iron exists primarily in the +2 (ferrous) and +3 (ferric) oxidation states and oxidizes rapidly in the presence of oxygen or water. Iron is also an essential trace element for nearly all living organisms as it is an important cofactor in many proteins responsible for electron transfer (e.g. hydrogenases, cytochromes, iron-sulfur proteins), oxygen transport (e.g. hemoglobin, myoglobin), and other cell processes including the reduction of ribose to deoxyribose by ribonucleotide reductase (31, 33, 73). At circumneutral pH, however, iron primarily exists as highly crystalline and insoluble (oxy)hydroxides. The bioavailability of iron is an important topic in both prokaryotic and eukaryotic cell physiology.

Microbial metal respiration plays an important role in the biogeochemical cycling of iron in terrestrial, freshwater, and marine systems. Despite the environmental significance, however, the molecular mechanism of bacterial metal reduction remains poorly understood. Iron reduction activity exists in both archeal and eubacterial lineages, and is often deeply rooted in the modern, 16S-rRNA tree of life, suggesting that metal respiration may have been one of the first respiratory processes to evolve on early Earth. Members of the proteobacteria, including the genera *Shewanella* and *Geobacter* have been the most intensively studied FeRB, due to the cultivability outside the natural environment. Both genera are gram-negative, but recent data suggests that *Shewanella* and *Geobacter* spp. may have evolved different mechanisms for Fe respiration (13, 43).

With the recent release of the genome sequences of 22 *Shewanella* spp, and 8 *Geobacter* spp., intra-genus and inter-genus studies have become a viable alternative for exploring the molecular mechanism utilized by these groups.

DMRB also provide attractive models for environmental applications such as bioremediation of contaminant radionuclides and chlorinated compounds. *Shewanella* and *Geobacter* can respire U(VI) and Tc(VII) which are highly soluble and mobile in the higher oxidation state. Upon reduction, U(VI) precipitates to U(IV) and Tc(VII) precipitates to Tc(IV) and further to Tc(III). This forms the basis for the alternate remediation strategy employed by DOE at contaminated sites where DMRB predominate and may be stimulated by additions of electron donor (21-23, 44, 47, 66, 91, 98). Additionally, DMRB couple the oxidation of organic compounds to the reduction of contaminant chlorinated compounds such as tetrachloroethene (90). Tetrachloroethene and trichloroethene are ideal solvents in industrial application and their widespread use has increased their prevalence in environmental soils. The mechanism for reduction of chlorinated compounds is likely drastically different from that of metal oxides or radionuclides and further demonstrates the extreme respiratory versatility of these organisms.

Recently, DMRB have gained increasing attention as biological catalysts in microbially driven fuel cells (MFCs). Bacteria oxidize organic compounds and transfer electrons directly to the surface of carbon electrodes poised at a given redox potential (6, 41, 42, 69). MFCs have been successfully deployed *in situ* (69, 93) as well as in the laboratory (3, 6, 37, 39, 42, 101). Both cathodic (electrode as electron donor) and anodic (electrode as electron acceptor) MFCs are relatively recent additions to the known suite

of respiratory functions in DMRB and will likely drive future research into extracellular electron transfer (89). The development of MFCs for sustainable power production is the current focus of many sponsored programs, and the mechanism of electron transfer to and from electrode surfaces may be optimized for increased power generation.

Bacterial Respiratory Systems

Like all organisms, bacteria must conserve energy from the sum of all of the catabolic and anabolic processes required inside the cell. Bacteria conserve energy by forming high-energy phosphoanhydride bonds in the carrier molecule Adenosine-5'-triphosphate (ATP). ATP is generated from Adenosine-5'-diphosphate (ADP) and P_i through a condensation reaction in the bacterial ATP synthase complex driven by either substrate level or oxidative phosphorylation (46). ATP synthase is localized to the bacterial cytoplasmic membrane and consists of subunits that anchor the protein complex to the membrane and permit the controlled flow of protons (H^+) from outside the cell (gram-positive bacteria) or periplasmic space (gram-negative bacteria) and the synthesis components which bind ADP and P_i and form the high-energy bond between the γ- and β-phosphoryl groups (5, 34, 87).

Substrate-level phosphorylation consists of reactions that produce electron carrier molecules such as NAD(P)H from sugars such as glucose. Oxidative phosphorylation is often termed electron-transport chain linked-phosphorylation because it requires the transfer of electrons from compounds with more negative redox potential (reducing) to those with more positive redox potential (oxidizing). This is accomplished via transfer through membrane-bound electron carriers and the formation of a proton gradient across the membrane. The proton motive force (PMF) drives ATP synthesis via ATP synthase

as mentioned previously (34, 46). Respiratory chain components are typically organized in decreasing redox potential to optimize transfer from electron carriers to terminal electron acceptors and maximize the number of protons that can be translocated across the cytoplasmic membrane. Electron chain components consist of flavoproteins (containing riboflavin, or flavinmononucleotide), FeS-cluster proteins (containing one or more covalently bound 2Fe-2S or 4Fe-4S clusters), quinones (containing redox active ketone moieties), and cytochromes (containing one of the four heme groups *a, b, c,* or *d*) (46).

Respiration with molecular oxygen (O_2) as terminal electron acceptor has been exhaustively studied in both prokaryotes *(E. coli* and *Paracoccus denitrificans*) and eukaryotes (mitochondria) and the path of electron flow during oxidative phosphorylation is clear (58, 75, 76, 88) (Figure 1.1). Although specific mechanistic differences exist in some prokaryotes, the flow of electrons resulting in the reduction of O_2 to H_2O begins in eukaryotes with the oxidation of NADH by NADH oxidoreductase or Complex I. Complex I oxidizes NADH using FMN as a cofactor and ultimately reduces ubiquinone and translocates 4 protons from the mitochondrial matrix to the intermembrane space. During the reduction of ubiquinone to ubiquinol, 2 additional protons are consumed from the matrix, which also contributes to the formation of PMF. Complex II in mitochondria contains flavinadeninedinucleotide, FeS clusters and heme and oxidizes succinate to fumarate and contributes to electron transport by generating more ubiquinol from ubiquinone. Complex II acts as a second entry point into the ETC and participates not only in oxidative phosphorylation, but also in the citric acid cycle (77, 88).

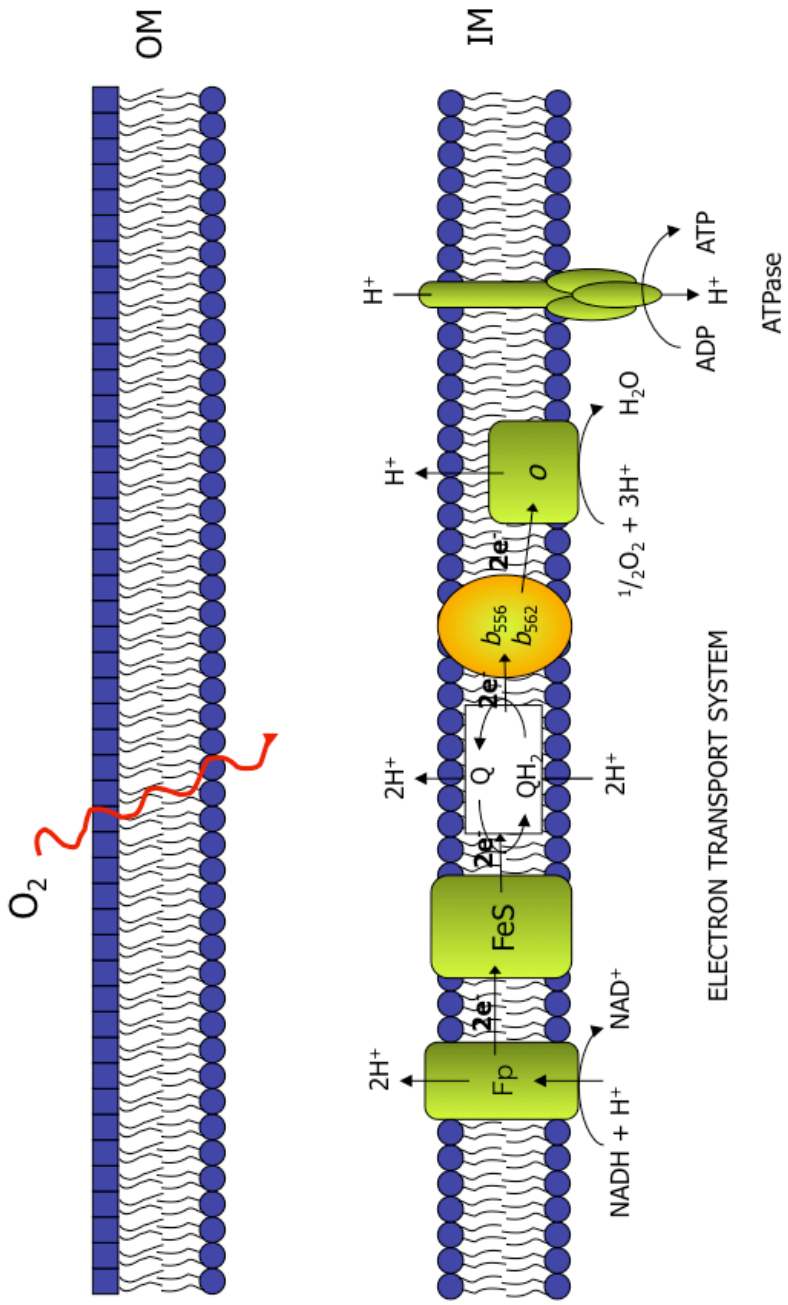

Figure 1.1 Model of typical Aerobic respiratory chain.

Complex III (cytochrome bc_1 complex) oxidizes ubiquinol produced from Complexes I and II and transfers electrons to cytochrome *c*. During the process ubiquinol is oxidizes in a stepwise process, forming an intermediate semiquinone in the transition state. Following reduction of cytochrome *c*, electrons flow to complex IV (cytochrome *c* oxidase) and the ETC terminates with the reduction of O_2 to H_2O. Complex IV also pumps 4 protons across the inner mitochondrial membrane and consumes 4 additional protons in the reduction of O_2. Generation of PMF drives ATP synthesis as it is relieved through ATP synthase, localized on the inner mitochondrial membrane. Prokaryotic electron transport chains terminating with the reduction of O_2 share similar components with those of the mitochondria, however they differ in the respect that electron donors other than NADH may be employed (38, 58, 64, 75). *E. coli*, for example, may use glucose, NADH, formate, lactate or even hydrogen (H_2) as electron donor. ETC components may be mixed and matched with others to facilitate energy generation in the changing conditions that bacteria experience in natural environmental systems.

Changing environmental conditions present bacterial cells with not only different electron donors, but also alternate electron acceptors, which are respired when oxygen becomes deplete. *E. coli* uses NO_3^-, NO_2^-, dimethylsulfoxide, or fumarate as alternate terminal electron acceptors during respiration (46). Anaerobic respiration in the bacterial domain utilizes compounds that virtually span the entire redox continuum including those mentioned for *E. coli* and others including the transition metals Fe(III) and Mn(IV). Respiratory terminal reductases for NO_3^-, NO_2^-, DMSO, TMAO, $S_2O_3^{2-}$, fumarate, and

CO_2 have previously been identified and some have been crystallized and their structures determined (8, 18, 30, 78, 85).

Electron Transport Chain Physiology of Metal Reducing Members of the Genus *Shewanella*

Metal reducing members of the genus *Shewanella* display remarkable respiratory versatility, respiring compounds that span the redox range found in natural systems including O_2, Fe(III), Mn(IV), U(VI), Tc(VII), NO_3^-, NO_2^-, DMSO, TMAO, fumarate, $S_2O_3^{2-}$, S^0, humic acids, and potentially several others (13). SO_4^{2-} is notably absent from the suite of terminal electron acceptors and appears to be utilized by strictly anaerobic organisms (50). This extreme respiratory versatility is likely due to the fact that *Shewanella* spp. contain a highly branched electron transport chain organized in a modular fashion. Primary dehydrogenases oxidize electron donors (lactate, formate, H_2) and transfer electrons to a membrane-bound quinone pool while translocating protons from the cytoplasm to the periplasm. Reduced quinols transfer electrons to a central branch point *c*-type cytochrome CymA. CymA is a small, tetraheme cytochrome that is localized on the periplasmic face of the inner membrane (51, 52, 55, 79, 80). CymA oxidizes quinol and transfers electrons to several different respiratory pathways including those terminating with NO_3^-, NO_2^-, DMSO, Fe(III), Mn(IV), and fumarate (Figure. 1.2). The respiratory pathways terminating with TMAO or $S_2O_3^{2-}$ have dedicated quinol oxidases and inner membrane bound terminal reductase complexes. Currently, CymA is believed to transfer electrons to a number of soluble, periplasmically-localized *c*-type cytochromes including a small tetraheme cytochrome (STC), and decaheme *c*-type cytochrome MtrA. MtrA is strictly required for respiration of insoluble metal oxides (27,

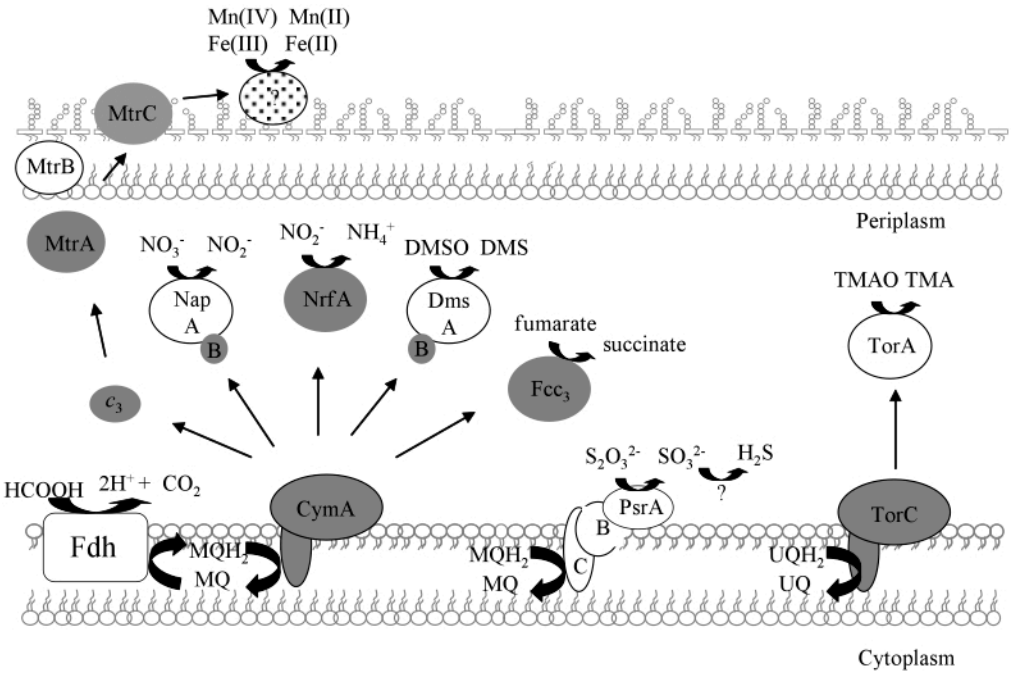

Figure 1.2. Model for branched electron transport chain in *S. oneidensis*

67, 84) and is postulated to transfer electrons to the outer membrane decaheme cytochromes OmcA and MtrC. OmcA and MtrC share limited sequence similarity, suggesting overlapping roles in Fe(III) and Mn(IV) respiration. *In vivo* studies, however, demonstrate no loss of respiratory ability when the *omcA* gene is interrupted or removed from the *S. oneidensis* genome (56, 57, 71, 82, 100, 103). MtrC mutants display decreased respiratory ability with metal oxides. *In vitro* biochemical studies with OmcA and MtrC demonstrate Fe(III) reduction activity by either cytochrome when artificially reduced via surrogate electron donor (26, 45, 71, 82). It is important to note, however, that for OmcA or MtrC to be an Fe(III) terminal reductase, heme groups covalently bound to the protein must come within ~14 angstroms of the mineral surface being reduced for efficient electron transfer to occur (17, 35, 36, 72, 100, 102-104). MtrB is an additional OM-localized protein that is also strictly required for metal respiration in *S. oneidensis*. Previous studies indicate that MtrB is an OM beta-barrel protein that may participate in localization of OM cytochromes MtrC and OmcA. A previously constructed MtrB-null mutant mislocalized both OM cytochromes, although to differing extents. Additionally, the cytochromes were more susceptible to proteolytic cleavage when whole cells were treated with Proteinase K (2, 53, 54).

Reduction mechanisms which utilize cell-surface proteins in direct contact with mineral oxide surfaces play a pivotal role in Fe(III) and Mn(IV) respiration in *Shewanella* spp. Because proteins are synthesized in the cytoplasm of the cell, the pathways for protein secretion to the bacterial cell surface likely play an important role in metal reduction. Recent studies demonstrated that a functional Type II protein secretion system (T2SS) is required for metal respiration in both *S. putrefaciens* and *S. oneidensis* (14, 83).

A representative model of the Fe(III) respiratory chain is given in Figure 1.3. T2SS in other gram negative bacteria are responsible for a myriad of functions including secretion of cholera toxin in *Vibrio cholerae*, secretion of the plant cell-wall degrading enzyme pullulanase in *Klebsiella oxytoca*, and secretion of endotoxin A and elastase in *Pseudomonas aeruginosa* (15, 74, 81). T2SS in enteropathic and enterohemorrhagic *E. coli* contributes to adherence and intestinal colonization (29). T2SS mutants in *S. putrefaciens* were unable to localize OM cytochromes OmcA and MtrC from the periplasmic space, where heme groups are covalently attached to the apocytochrome, to the outer surface of the OM where they presumably make contact with insoluble Fe(III) (14). T2SS mutants also mislocalize a protein complex loosely associated with the external face of the OM that displays Fe(III) reduction activity in non-denaturing PAGE separations, suggesting that a functional Fe(III)-reductase complex is secreted in complete form, following assembly in the periplasmic space (14).

Despite the involvement of a T2SS in metal respiration in *Shewanella*, cells may reduce insoluble metal oxides without direct contact via the use of small, diffusible, redox-active molecules termed electron shuttles. Electron shuttles can be naturally occurring compounds such as humic or fulvic acids that contain reducible moities and diffuse into the cell, and are reduced internally. The shuttles subsequently diffuse from the cell and chemically (abiotically) reduce the mineral oxide. *Shewanella* cells were able to reduce insoluble 2-line ferrihydrite suspended in dialysis tubing with 1000 Da molecular weight cutoff, indicating that the electron shuttle is extremely small (mass $\leq$ 1 kDa) and likely not a protein produced and excreted by the cell (40). The quinonoid compound anthraquinone-2,6-disulfonate (AQDS) acts as a surrogate electron shuttle in

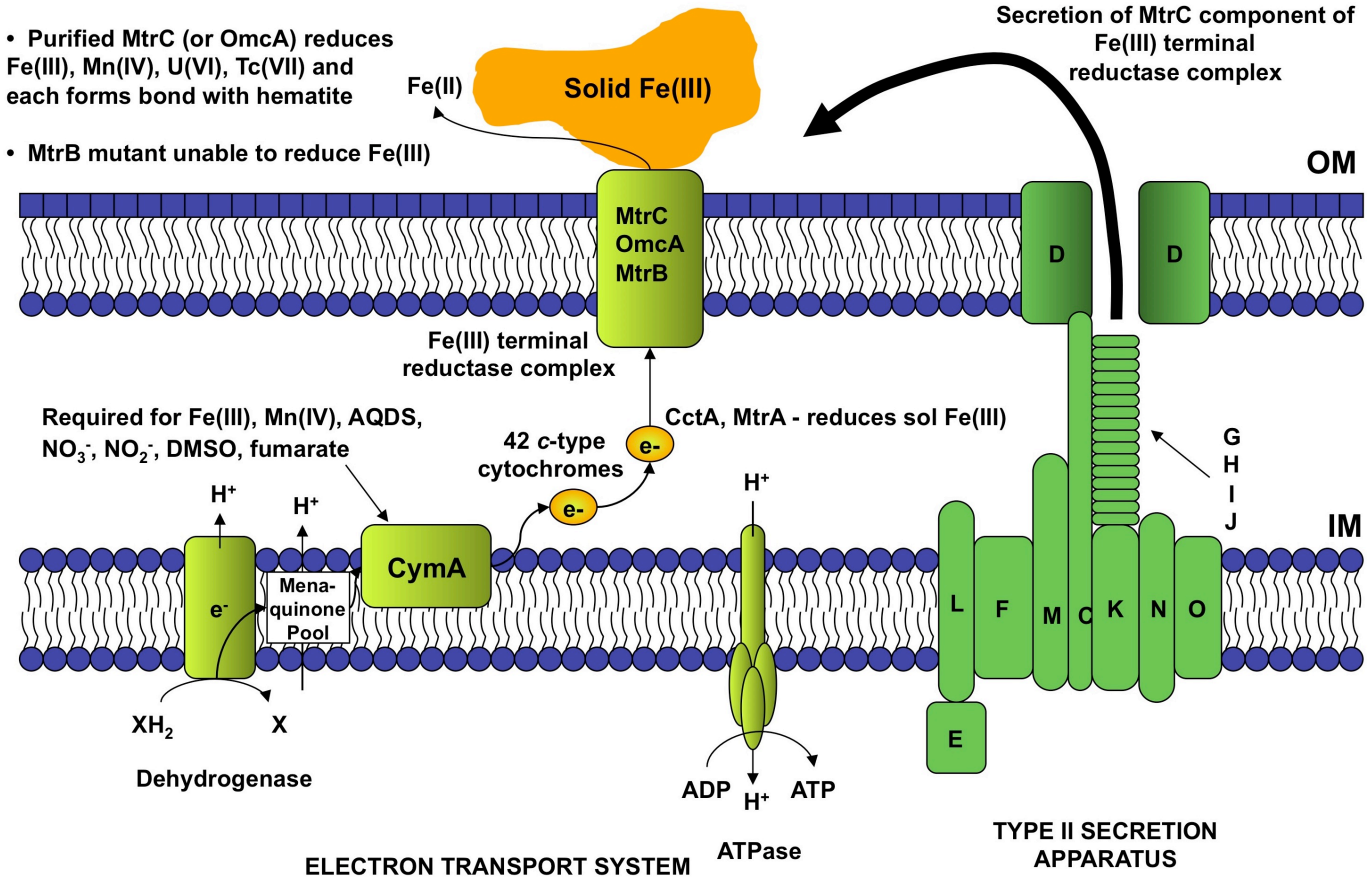

Figure 1.3 Postulated model of Fe(III) respiratory pathway in S. oneidensis

laboratory experiments. The addition of AQDS at levels 3 orders of magnitude lower than levels of Fe(III) in the same culture (1000X lower) enhanced Fe(III) respiration in the wild-type strain (7).

S. oneidensis has been postulated to respire Fe(III) at a distance via the production of an endogenous electron shuttle in the forms of riboflavin, melanin, or menaquinone. (40, 48, 63, 95, 96). Riboflavin is a common redox-active cofactor that participates in a variety of biochemical processes inside the cell. Flavins are essential components of the respiratory electron transport chain (mentioned above) and also in conserved enzymes such as pyridoxal phosphate (Vitamin B6) synthase, niacin (vitamin B3) synthase, and glutathione oxidoreductase (GOR), which helps maintain redox balance inside the cell (49). Melanin was observed in culture media following growth with excess L-tyrosine (a melanin precursor). Melanin contains redox active quinone groups similar to AQDS and may act in a similar manner (94, 95). Endogenously produced quinones are typically membrane soluble and remain bound in the IM to serve as electron carriers in varios ETCs. A recent study, however discovered that menaquinone could serve as an electron shuttle for *S. oneidensis* (63). Several recent studies indicate that *Geobacter* spp. require direct contact with the Fe(III) oxide surface, while *Shewanella* spp. may utilize both direct contact and electron shuttles for more efficient reduction (28, 40, 60-62, 83, 84).

In addition to direct contact and electron shuttling mechanisms, metal-respiring bacteria may employ electrically active pili ("nanowires") that are comprised of small, repeating pseudopilin subunits (PilA) that may carry electrons long distances from the cell, reportedly several microns (24, 68). *Geobacter* mutants deficient for *pilA* were unable to respire solid Fe(III) and displayed decreased adhesion to Fe(III) oxides. PilA is

an integral component of a secondary T2SS originally termed a Type IV pilus (T4P). T4P was originally discovered as a mechanism for motility in gram-negative bacteria. T4P functions similarly to T2SS, and may component share both sequence and structural similarity (11, 16, 20). T4P functions by extruding a pilus through an outer membrane secretin (PilQ) and attaching the tip to a solid surface. The extension process is driven by ATP hydrolysis via PilB. A secondary ATP-driven motor PilT, then retracts the pilus, causing the cell to move in a twitching manner (twitching motility). T2SS do not possess a secondary motor for retraction, and the primary motor (GspE) functions to drive the piston for protein secretion (11). Nanowires are thought to function by stringing together individual OM cytochromes along the pilus to form an electrical conduit that extends great distances from the cell. However, Scanning Tunneling Microscopy (STM) revealed that electrically conductive pili are not exclusive to DMRB, and exist in other bacteria that do not respire metals and do not possess the OM cytochromes present in *Shewanella* and *Geobacter* (24).

As a final mechanism, *Shewanella* spp. may also non-reductively solublize Fe(III) from mineral oxide surfaces through secretion of an organic ligand (19, 32, 92). Soluble, organic Fe(III) is significantly more bioavailable and may be transported into bacterial cells through specific uptake mechanisms, depending on the Fe(III) chelate. Gram-negative bacterial cells often make use of soluble Fe(III) forms for assimilation and possess dedicated transporters for Fe(III) citrate (65, 99). Additionally, bacteria secrete endogenously produced siderophores to scavenge Fe(III) from the environment, and also from host cells where competition for Fe(III) is a key determining factor in bacterial cell infection (1, 10, 59, 97). Although siderophores are commonly employed to import

Fe(III) into cells, it seems unlikely that they are used for dissimilatory applications (19, 97). Siderophores coordinate Fe(III) with an extremely high binding constant, to prevent loss of Fe(III) and outcompete other organic ligands which may be present. Fe(III) chelates with high binding constants are not preferred by *S. putrefaciens* during dissimilatory respiration (25). Recent studies suggest that an as-of-yet unidentified organic ligand plays an important role in Fe(III) respiration in *S. oneidensis* (32, 92). Interestingly, riboflavin (Vitamin B_2) has been proposed as not only an endogenously produced electron shuttle, but may also nonreductively dissolve insoluble Fe(III) oxides before reduction (48). Some researchers in the field maintain that "shelators" are the best explanation for the reduction of insoluble Fe(III) in the environment, although their use *in situ* has yet to be conclusively shown. A main objective of my PhD research is to determine the molecular mechanism of anaerobic Fe(III) respiration by *Shewanella oneidensis*.

Genetic system for in-frame gene deletion in *Shewanella*

With the recent release of 22 *Shewanella* genome sequences, a reliable method for constructing mutant strains is necessary. Previous genetic systems in *Shewanella* included using techniques for making random mutations such as chemical mutagens (ethylmethane sulfonate; EMS, 5'-bromouracil) and transposon mutagenesis. Chemical mutagens were employed for isolating base transitions in bacterial genomes. Single nucleotide changes were isolated following optimization of the chemical mutagen exposure time and concentration. Single-hit kinetics was used to identify a 90% kill ratio and based on genome size, optimized for a single base change per genome, per cell (12).

To identify the mutation (before genome sequence was available) host cell genomic DNA is partially digested with a single restriction endonuclease (to generate random fragments) and subsequently cloned into a cosmid vector. Cosmid vectors are unique in that they are packaged into empty phage head particles that are used to infect donor cells. Following confirmation that the genomic clone library contains random fragments and that no single clone is overrepresented, the "clone bank" is mobilized from the host cells harboring the library to recipient cells containing the random mutation. Transconjugates are then subjected to the same screening technique used to identify the original random mutation and those with complementing genomic fragments display positive phenotypes. As a final step to identify the original genetic mutation, the complementing fragment must then be subcloned to identify the smallest complementing fragment and then sequenced to determine the gene(s) required to restore function to the mutant strain. The entire process is often extremely laborious and time consuming. Additionally, random point mutations may result in nonsense mutations where a single codon is changed to a stop and ceases translation. This often results in polar mutations for genes arranged in operons or genes that are cotranscribed (14). However, provided that the screening technique is designed well, the random mutagenesis approach provides valuable insight into mechanisms that are novel and where no genetic system is in place. Random mutagenesis is often the first approach utilized in systems where no genome sequence data is available.

Transposon mutagenesis is another random mutagenesis technique that involves transfer of a mobile genetic element into a host cell where it may interrupt genes in the host cell genome. Transposons contain inverted repeat sequences at the termini, contain

a selectable marker (such as antibiotic resistance), and facilitate insertion into host genomes via proteins called transposases (86). Some transposons encode the necessary transposase on the transposon itself, negating the requirements for an accessory vector expressing the transposase. Most commercially available transposon mutagenesis systems employ the use of either Tn5 or *Himar*-homing transposons (9, 70, 86). These transposons are usually transferred to host cells by direct transformation or conjugation with a plasmid vector containing the transposon and encoding the transposase (86). Transposon mutagenesis is an attractive system because sequencing the DNA region flanking the transposon can directly identify the interrupted gene. Transposon mutagenesis, however, also has several pitfalls: 1) the antibiotic resistance marker requires an extra energetic requirement not present in the wild-type strain, 2) bacteria may contain endogenous insertion elements and transposases which can cause genomic rearrangements upon transposon insertion, and 3) transposons are inherently unstable and may "hop" around the host genome or even remove segments of the genome which can forever mask the original mutation (4). Also, like chemical mutagenesis, transposons may result in polar mutations of downstream genes, complicating functional analysis of the mutation.

Genomic sequence data permits greater flexibility during genetic studies by permitting construction of targeted genomic manipulations. While random mutagenesis provides valuable information about unknown systems and processes, targeted approaches permit hypothesis-driven research once preliminary information is known. Genes identified in random mutagenesis screens may be confirmed via targeted deletion without the adverse side effects of antibiotic resistance and polar mutation. Traditionally,

genomic manipulations require homologous recombination between *in vitro* synthesized constructs and host cell genomic DNA. Targeted mutations consist of deletions, insertions, and site-directed changes. Targeted insertions are plagued by the same problems as transposon mutagenesis, however they do not require the use of an externally encoded transposase, but instead rely on homologous recombination and subsequent antibiotic resistance selection. Targeted deletions may either be gene replacements, in which the target open reading frame is replaced with one containing a selectable marker (such as antibiotic resistance, green fluorescent protein, or beta-galactosidase), or deletions in which the target ORF is removed from the genome without replacement by another marker. Markerless gene deletions are isogenic to the wild-type strain and thus permit growth and other phenotypic analyses without the energetic requirements of antibiotic resistance. A main objective of my PhD research is to develop a gene deletion system for *Shewanella oneidensis.*

RESEARCH OBJECTIVES

The main objective of the present study was to identify genes and proteins required for anaerobic Fe(III) respiration by *Shewanella oneidensis* MR-1. Experimental strategies followed to carry out this objective include 1) construction of a novel suicide vector for generating markerless, in-frame gene deletions; 2) identification of cell surface proteins putatively involved in anaerobic Fe(III) respiration; 3) generation of in-frame deletions of genes encoding the identified cell surface proteins, and tests of the resulting mutants for anaerobic Fe(III) respiratory ability; and 4) identification of specific amino acid residues required for Fe(III) respiratory capability in the cell surface proteins.

REFERENCES

1. Andrews, S.C., A.K. Robinson, and F. Rodriguez-Quinones, Bacterial iron homeostasis. Fems Microbiology Reviews, 2003. **27**(2-3): p. 215-237.

2. Beliaev, A.S. and D.A. Saffarini, *Shewanella putrefaciens mtrB* encodes an outer membrane protein required for Fe(III) and Mn(IV) reduction. Journal of Bacteriology, 1998. **180**(23): p. 6292-7.

3. Biffinger, J., et al., Characterization of Electrochemically Active Bacteria Utilizing a High-Throughput Voltage-Based Screening Assay. Biotechnology and Bioengineering, 2009. **102**(2): p. 436-444.

4. Bordi, C., et al., Effects of ISSo2 insertions in structural and regulatory genes of the trimethylamine oxide reductase of *Shewanella oneidensis*. Journal of Bacteriology, 2003. **185**(6): p. 2042-2045.

5. Boyer, P.D., The ATP synthase - A splendid molecular machine. Annual Review of Biochemistry, 1997. **66**: p. 717-749.

6. Bretschger, O., et al., Current production and metal oxide reduction by Shewanella oneidensis MR-1 wild type and mutants. Applied and Environmental Microbiology, 2007. **73**(21): p. 7003-7012.

7. Burns, J. and T. DiChristina, Exogenous Electron Shuttling Pathway Rescues Fe(III) Respiratory Capability in Type II Protein Secretion and Outer Membrane Cytochrome Deficient Mutants of *Shewanella oneidensis* MR-1. Submitted, 2010.

8. Campbell, W.H., Nitrate reductase structure, function and regulation: Bridging the gap between biochemistry and physiology. Annual Review of Plant Physiology and Plant Molecular Biology, 1999. **50**: p. 277-+.

9. Chiang, S.L. and J.J. Mekalanos, Use of signature-tagged transposon mutagenesis to identify Vibrio cholerae genes critical for colonization. Molecular Microbiology, 1998. **27**(4): p. 797-805.

10. Crosa, J.H., Genetics and molecular biology of siderophore-mediated iron transport in bacteria. Microbiological Reviews, 1989. **53**(4): p. 517-530.

11. Desvaux, M., et al., The general secretory pathway: a general misnomer? Trends in Microbiology, 2004. **12**(7): p. 306-309.

12. DiChristina, T.J. and E.F. DeLong, Isolation of anaerobic respiratory mutants of *Shewannella putrefaciens* and genetic analysis of mutants deficient in anaerobic growth on Fe3+. Journal of Bacteriology, 1994. **176**(5): p. 1468-1474.

13. DiChristina, T.J., J.K. Fredrickson, and J.M. Zachara, Enzymology of electron transport: energy generation with geochemical consequences. Reviews in Mineralogy and Geochemistry, 2005. **59**: p. 27-52.

14. DiChristina, T.J., C.M. Moore, and C.A. Haller, Dissimilatory Fe(III) and Mn(IV) reduction by *Shewanella putrefaciens* requires *ferE*, a homolog of the *pulE* (*gspE*) type II protein secretion gene. Journal of Bacteriology, 2002. **184**(1): p. 142-151.

15. Durand, E., et al., Type II protein secretion in Pseudomonas aeruginosa: the pseudopilus is a multifibrillar and adhesive structure. Journal of Bacteriology, 2003. **185**(9): p. 2749-2758.

16. Economou, A., et al., Secretion by numbers: Protein traffic in prokaryotes. Mol Microbiol, 2006. **62**(2): p. 308-19.

17. Eggleston, C.M., et al., Binding and direct electrochemistry of OmcA, an outer-membrane cytochrome from an iron reducing bacterium, with oxide electrodes: A candidate biofuel cell system. Inorganica Chimica Acta, 2008. **361**(3): p. 769-777.

18. Einsle, O., et al., Structure of cytochrome c nitrite reductase. Nature, 1999. **400**(6743): p. 476-480.

19. Fennessey, C.M., et al., Siderophores are not Involved in Fe(III) Solubilization During Anaerobic Fe(III) Respiration by *Shewanella oneidensis* MR-1. Applied and Environmental Microbiology, 2010.

20. Filloux, A., The underlying mechanisms of type II protein secretion. Biochimica Et Biophysica Acta-Molecular Cell Research, 2004. **1694**(1-3): p. 163-179.

21. Finneran, K.T., et al., Potential for Bioremediation of uranium-contaminated aquifers with microbial U(VI) reduction. Soil & Sediment Contamination, 2002. **11**(3): p. 339-357.

22. Finneran, K.T., M.E. Housewright, and D.R. Lovley, Multiple influences of nitrate on uranium solubility during bioremediation of uranium-contaminated subsurface sediments. Environ Microbiol, 2002. **4**(9): p. 510-6.

23. Ganesh, R., et al., Reduction of hexavalent uranium from organic complexes by sulfate- and iron-reducing bacteria. Applied and Environmental Microbiology, 1997. **63**(11): p. 4385-4391.

24. Gorby, Y.A., et al., Electrically conductive bacterial nanowires produced by *Shewanella oneidensis* strain MR-1 and other microorganisms. Proceedings of the National Academy of Sciences of the United States of America, 2006. **103**(30): p. 11358-11363.

25. Haas, J.R. and T.J. DiChristina, Effects of Fe(III) chemical speciation on dissimilatory Fe(III) reduction by *Shewanella putrefaciens*. Environmental Science and Technology, 2002. **63**(3): p. 373-380.

26. Hartshorne, R.S., et al., Characterization of Shewanella oneidensis MtrC: a cell-surface decaheme cytochrome involved in respiratory electron transport to extracellular electron acceptors. Journal of Biological Inorganic Chemistry, 2007. **12**(7): p. 1083-1094.

27. Hartshorne, R.S., et al., Characterization of an electron conduit between bacteria and the extracellular environment. Proc Natl Acad Sci U S A, 2009.

28. Hernandez, M.E. and D.K. Newman, Extracellular electron transfer. Cell Mol Life Sci, 2001. **58**(11): p. 1562-71.

29. Ho, T.D., et al., Type 2 secretion promotes enterohemorrhagic Escherichia coli adherence and intestinal colonization. Infection and Immunity, 2008. **76**(5): p. 1858-1865.

30. Iverson, T.M., et al., Structure of the Escherichia coli fumarate reductase respiratory complex. Science, 1999. **284**(5422): p. 1961-1966.

31. Johnson, D.C., et al., Structure, function, and formation of biological iron-sulfur clusters. Annual Review of Biochemistry, 2005. **74**: p. 247-281.

32. Jones, M., et al., *Shewanella oneidensis* mutants selected for their inability to produce soluble organic-Fe(III) are unable to respire Fe(III) as anaerobic electron acceptor. Environmental Microbiology, 2010.

33. Jordan, A. and P. Reichard, Ribonucleotide reductases. Annual Review of Biochemistry, 1998. **67**: p. 71-98.

34. Junge, W., H. Lill, and S. Engelbrecht, ATP synthase: an electrochemical transducer with rotatory mechanics. Trends in Biochemical Sciences, 1997. **22**(11): p. 420-423.

35. Kerisit, S., M. Dupuis, and K.M. Rosso, Electron-transfer reactions at water- and cytochrome-iron oxide interfaces. Geochimica Et Cosmochimica Acta, 2008. **72**(12): p. A465-A465.

36. Kerisit, S., et al., Molecular computational investigation of electron-transfer kinetics across cytochrome-iron oxide interfaces. Journal of Physical Chemistry C, 2007. **111**(30): p. 11363-11375.

37. Kim, H.J., et al., A mediator-less microbial fuel cell using a metal reducing bacterium, *Shewanella putrefaciens*. Enzyme and Microbial Technology, 2002. **30**(2): p. 145-152.

38. Krause, F., et al., "Respirasome"-like supercomplexes in green leaf mitochondria of spinach. Journal of Biological Chemistry, 2004. **279**(46): p. 48369-48375.

39. Lanthier, M., K.B. Gregory, and D.R. Lovley, Growth with high planktonic biomass in *Shewanella oneidensis* fuel cells. FEMS Microbiol Lett, 2008. **278**(1): p. 29-35.

40. Lies, D.P., et al., Shewanella oneidensis MR-1 uses overlapping pathways for iron reduction at a distance and by direct contact under conditions relevant for biofilms. Applied and Environmental Microbiology, 2005. **71**(8): p. 4414-4426.

41. Logan, B.E., et al., Microbial fuel cells: methodology and technology. Environmental Science & Technology, 2006. **40**(17): p. 5181-5192.

42. Lovley, D.R., Bug juice: harvesting electricity with microorganisms. Nature Reviews Microbiology, 2006. **4**(7): p. 497-508.

43. Lovley, D.R., D.E. Holmes, and K.P. Nevin, Dissimilatory Fe(III) and Mn(IV) reduction. Advances in Microbial Physiology, 2004. **49**: p. 219-285.

44. Lovley, D.R., et al., Microbial Reduction of Uranium. Nature, 1991. **350**(6317): p. 413-416.

45. Lower, B.H., et al., Specific bonds between an iron oxide surface and outer membrane cytochromes MtrC and OmcA from Shewanella oneidensis MR-1. J Bacteriol, 2007. **189**(13): p. 4944-52.

46. Madigan, M., J. Martinko, and J. Parker, *Brock Biology of Microorganisms*. 10 ed. 2003, Upper Saddle River, NJ: Prentice Hall/Pearson Education. various pagings.

47. Marshall, M.J., et al., *c*-Type cytochrome-dependent formation of U(IV) nanoparticles by *Shewanella oneidensis*. PLoS Biol, 2006. **4**(9): p. e268.

48. Marsili, E., et al., *Shewanella* secretes flavins that mediate extracellular electron transfer. Proceedings of the National Academy of Sciences of the United States of America, 2008. **105**(10): p. 3968-3973.

49. Meister, A. and M.E. Anderson, Glutathione. Annual Review of Biochemistry, 1983. **52**: p. 711-760.

50. Methe, B.A., et al., Genome of Geobacter sulfurreducens: metal reduction in subsurface environments. Science, 2003. **302**(5652): p. 1967-9.

51. Murphy, J.N. and C.W. Saltikov, The *cymA* gene, encoding a tetraheme *c*-type cytochrome, is required for arsenate respiration in *Shewanella* species. Journal of Bacteriology, 2007. **189**(6): p. 2283-2290.

52. Myers, C.R. and J.M. Myers, Cloning and sequence of cymA a gene encoding a tetraheme cytochrome c required for reduction of iron(III), fumarate, and nitrate by Shewanella putrefaciens MR-1. Journal of Bacteriology, 1997. **179**(4): p. 1143-1152.

53. Myers, C.R. and J.M. Myers, MtrB is required for proper incorporation of the cytochromes OmcA and OmcB into the outer membrane of Shewanella putrefaciens MR-1. Appl Environ Microbiol, 2002. **68**(11): p. 5585-94.

54. Myers, C.R. and J.M. Myers, Cell surface exposure of the outer membrane cytochromes of *Shewanella oneidensis* MR-1. Letters in Applied Microbiology, 2003. **37**(3): p. 254-258.

55. Myers, J.M. and C.R. Myers, Role of the tetraheme cytochrome CymA in anaerobic electron transport in cells of Shewanella putrefaciens MR-1 with normal levels of menaquinone. Journal of Bacteriology, 2000. **182**(1): p. 67-75.

56. Myers, J.M. and C.R. Myers, Role for outer membrane cytochromes OmcA and OmcB of *Shewanella putrefaciens* MR-1 in reduction of manganese dioxide. Appl Environ Microbiol, 2001. **67**(1): p. 260-9.

57. Myers, J.M. and C.R. Myers, Overlapping role of the outer membrane cytochromes of *Shewanella oneidensis* MR-1 in the reduction of manganese(IV) oxide. Lett Appl Microbiol, 2003. **37**(1): p. 21-5.

58. Myllykallio, H., et al., Electron-transfer supercomplexes in photosynthesis and respiration. Trends in Microbiology, 2000. **8**(11): p. 493-494.

59. Neilands, J.B., Siderophores - structure and function of microbial iron transport compounds. Journal of Biological Chemistry, 1995. **270**(45): p. 26723-26726.

60. Nevin, K.P. and D.R. Lovley, Lack of production of electron-shuttling compounds or solubilization of Fe(III) during reduction of insoluble Fe(III) oxide by Geobacter metallireducens. Applied and Environmental Microbiology, 2000. **66**(5): p. 2248-2251.

61. Nevin, K.P. and D.R. Lovley, Potential for nonenzymatic reduction of Fe(III) via electron shuttling in subsurface sediments. Environmental Science & Technology, 2000. **34**(12): p. 2472-2478.

62. Nevin, K.P. and D.R. Lovley, Mechanisms for accessing insoluble Fe(III) oxide during dissimilatory Fe(III) reduction by Geothrix fermentans. Applied and Environmental Microbiology, 2002. **68**(5): p. 2294-2299.

63. Newman, D.K. and R. Kolter, A role for excreted quinones in extracellular electron transfer. Nature, 2000. **405**(6782): p. 94-97.

64. Niebisch, A. and M. Bott, Purification of a cytochrome bc-aa3 supercomplex with quinol oxidase activity from Corynebacterium glutamicum. Identification of a fourth subunity of cytochrome aa3 oxidase and mutational analysis of diheme cytochrome c1. J Biol Chem, 2003. **278**(6): p. 4339-46.

65. Ogierman, M. and V. Braun, Interactions between the outer membrane ferric citrate transporter FecA and TonB: Studies of the FecA TonB box. Journal of Bacteriology, 2003. **185**(6): p. 1870-1885.

66. Ortiz-Bernad, I., et al., Resistance of solid-phase U(VI) to microbial reduction during in situ bioremediation of uranium-contaminated groundwater. Applied and Environmental Microbiology, 2004. **70**(12): p. 7558-7560.

67. Pitts, K.E., et al., Characterization of the *Shewanella oneidensis* MR-1 decaheme cytochrome MtrA: expression in *Escherichia coli* confers the ability to reduce soluble Fe(III) chelates. Journal of Biological Chemistry, 2003. **278**(30): p. 27758-65.

68. Reguera, G., et al., Extracellular electron transfer via microbial nanowires. Nature, 2005. **435**(7045): p. 1098-1101.

69. Reimers, C.E., et al., Microbial fuel cell energy from an ocean cold seep. Geobiology, 2006. **4**(2): p. 123-136.

70. Rollefson, J.B., C.E. Levar, and D.R. Bond, Identification of Genes Involved in Biofilm Formation and Respiration via Mini-Himar Transposon Mutagenesis of Geobacter sulfurreducens. Journal of Bacteriology, 2009. **191**(13): p. 4207-4217.

71. Ross, D.E., S.L. Brantley, and M. Tien, Kinetic characterization of terminal reductases OmcA and MtrC involved in respiratory electron transfer for dissimilatory iron reduction in *Shewanella oneidensis* MR-1. Appl Environ Microbiol, 2009: p. doi 10.1128/AEM.00544-09.

72. Rosso, K.M., et al., Nonlocal bacterial electron transfer to hematite surfaces. Geochimica Et Cosmochimica Acta, 2003. **67**(5): p. 1081-1087.

73. Rouault, T.A. and R.D. Klausner, Iron-sulfur clusters as biosensors of oxidants and iron. Trends in Biochemical Sciences, 1996. **21**(5): p. 174-177.

74. Russel, M., Macromolecular assembly and secretion across the bacterial cell envelope: Type II protein secretion systems. Journal of Molecular Biology, 1998. **279**(3): p. 485-499.

75. Schagger, H., Respiratory chain supercomplexes of mitochondria and bacteria. Biochim Biophys Acta, 2002. **1555**(1-3): p. 154-9.

76. Schagger, H., et al., Significance of respirasomes for the assembly/stability of human respiratory chain complex I. Journal of Biological Chemistry, 2004. **279**(35): p. 36349-36353.

77. Schagger, H. and K. Pfeiffer, The ratio of oxidative phosphorylation complexes I-V in bovine heart mitochondria and the composition of respiratory chain supercomplexes. Journal of Biological Chemistry, 2001. **276**(41): p. 37861-37867.

78. Schindelin, H., et al., Crystal structure of DMSO reductase: Redox-linked changes in molybdopterin coordination. Science, 1996. **272**(5268): p. 1615-1621.

79. Schwalb, C., S.K. Chapman, and G.A. Reid, The membrane-bound tetrahaem c-type cytochrome CymA interacts directly with the soluble fumarate reductase in *Shewanella.* Biochem Soc Trans, 2002. **30**(4): p. 658-62.

80. Schwalb, C., S.K. Chapman, and G.A. Reid, The tetraheme cytochrome CymA is required for anaerobic respiration with dimethyl sulfoxide and nitrite in *Shewanella oneidensis.* Biochemistry, 2003. **42**(31): p. 9491-9497.

81. Scott, M.E., Z.Y. Dossani, and M. Sandkvist, Directed polar secretion of protease from single cells of Vibrio cholerae via the type II secretion pathway. Proceedings of the National Academy of Sciences of the United States of America, 2001. **98**(24): p. 13978-13983.

82. Shi, L., et al., Isolation of a high-affinity functional protein complex between OmcA and MtrC: Two outer membrane decaheme *c*-type cytochromes of *Shewanella oneidensis* MR-1. Journal of Bacteriology, 2006. **188**(13): p. 4705-4714.

83. Shi, L., et al., Direct involvement of type II secretion system in extracellular translocation of *Shewanella oneidensis* outer membrane cytochromes MtrC and OmcA. Journal of Bacteriology, 2008. **190**(15): p. 5512-5516.

84. Shi, L., et al., Respiration of metal (hydr)oxides by *Shewanella* and *Geobacter:* a key role for multihaem *c*-type cytochromes. Mol Microbiol, 2007. **65**(1): p. 12-20.

85. Shima, S., et al., Structure and function of enzymes involved in the methanogenic pathway utilizing carbon dioxide and molecular hydrogen. Journal of Bioscience and Bioengineering, 2002. **93**(6): p. 519-530.

86. Simon, R., U. Priefer, and A. Puhler, A Broad Host Range Mobilization System for Invivo Genetic-Engineering - Transposon Mutagenesis in Gram-Negative Bacteria. Bio-Technology, 1983. **1**(9): p. 784-791.

87. Stock, D., A.G.W. Leslie, and J.E. Walker, Molecular architecture of the rotary motor in ATP synthase. Science, 1999. **286**(5445): p. 1700-1705.

88. Stroh, A., et al., Assembly of respiratory complexes I, III, and IV into NADH oxidase supercomplex stabilizes complex I in Paracoccus denitrificans. J Biol Chem, 2004. **279**(6): p. 5000-7.

89. Strycharz, S.M., et al., Graphite electrode as a sole electron donor for reductive dechlorination of tetrachlorethene by *Geobacter lovleyi.* Appl Environ Microbiol, 2008. **74**(19): p. 5943-7.

90. Sung, Y., et al., Geobacter lovleyi sp nov strain SZ, a novel metal-reducing and tetrachloroethene-dechlorinating bacterium. Applied and Environmental Microbiology, 2006. **72**(4): p. 2775-2782.

91. Suzuki, Y., et al., Radionuclide contamination - Nanometre-size products of uranium bioreduction. Nature, 2002. **419**(6903): p. 134-134.

92. Taillefert, M., et al., *Shewanella putrefaciens* produces an Fe(III)-solubilizing ligand during anaerobic respiration on insoluble Fe(III) oxides Journal of Inorganic Biochemistry, 2007. **101**(11): p. 1760-1767.

93. Tender, L.M., et al., The first demonstration of a microbial fuel cell as a viable power supply: Powering a meteorological buoy. Journal of Power Sources, 2008. **179**(2): p. 571-575.

94. Turick, C.E., F. Caccavo, Jr., and L.S. Tisa, Electron transfer from Shewanella algae BrY to hydrous ferric oxide is mediated by cell-associated melanin. FEMS Microbiol Lett, 2003. **220**(1): p. 99-104.

95. Turick, C.E., L.S. Tisa, and F. Caccavo, Jr., Melanin production and use as a soluble electron shuttle for Fe(III) oxide reduction and as a terminal electron acceptor by Shewanella algae BrY. Appl Environ Microbiol, 2002. **68**(5): p. 2436-44.

96. von Canstein, H., et al., Secretion of flavins by Shewanella species and their role in extracellular electron transfer. Appl Environ Microbiol, 2007.

97. Vraspir, J.M. and A. Butler, Chemistry of marine ligands and siderophores. Annual Review of Marine Science, 2009. **1**: p. 43-63.

98. Wade, R. and T.J. DiChristina, Isolation of U(VI) reduction-deficient mutants of *Shewanella putrefaciens.* FEMS Microbiol Lett, 2000. **184**(2): p. 143-148.

99. Wagegg, W. and V. Braun, Ferric Citrate Transport in Escherichia-Coli Requires Outer-Membrane Receptor Protein Feca. Journal of Bacteriology, 1981. **145**(1): p. 156-163.

100. Wang, Z.M., et al., Kinetics of reduction of Fe(III) complexes by outer Membrane cytochromes MtrC and OmcA of *Shewanella oneidensis* MR-1. Applied and Environmental Microbiology, 2008. **74**(21): p. 6746-6755.

101. Watanabe, K., Recent Developments in Microbial Fuel Cell Technologies for Sustainable Bioenergy. Journal of Bioscience and Bioengineering, 2008. **106**(6): p. 528-536.

102. Wigginton, N.S., et al., Examining the electron transfer properties of an outer membrane cytochrome from Shewanella oneidensis using scanning tunneling microscopy. Abstracts of Papers of the American Chemical Society, 2005. **230**: p. U1727-U1728.

103. Wigginton, N.S., et al., Electron tunneling properties of outer-membrane decaheme cytochromes from *Shewanella oneidensis*. Geochimica Et Cosmochimica Acta, 2007. **71**(3): p. 543-555.

104. Wigginton, N.S., et al., Long-Range Electron Transfer across Cytochrome-Hematite (alpha-Fe2O3) Interfaces. Journal of Physical Chemistry C, 2009. **113**(6): p. 2096-2103.

CHAPTER 2

ANAEROBIC RESPIRATION OF ELEMENTAL SULFUR AND THIOSULFATE BY *SHEWANELLA ONEIDENSIS* MR-1 REQUIRES *PSRA*, A HOMOLOG OF THE *PHSA* GENE OF *SALMONELLA ENTERICA* SEROVAR TYPHIMURIUM LT2

Abstract

Shewanella oneidensis MR-1, a facultatively anaerobic γ-proteobacterium, respires a variety of anaerobic terminal electron acceptors, including the inorganic sulfur compounds sulfite (SO_3^{2-}), thiosulfate ($S_2O_3^{2-}$), tetrathionate ($S_4O_6^{2-}$), and elemental sulfur (S^0). The molecular mechanism of anaerobic respiration of inorganic sulfur compounds by *S. oneidensis* however, is poorly understood. In the present study, a three-gene cluster was identified in the *S. oneidensis* genome whose translated products displayed 59-73% amino acid similarity to *phsABC*, a gene cluster required for S^0 and $S_2O_3^{2-}$ respiration by *Salmonella typhimurium* LT2. Homologs of *phsA* (annotated as *psrA*) were identified in the genomes of *Shewanella* strains that reduce S^0 and $S_2O_3^{2-}$, yet were missing from the genomes of *Shewanella* strains unable to reduce these electron acceptors. A new suicide vector was constructed and used to generate a markerless, in-frame deletion of *psrA,* the gene encoding the putative thiosulfate reductase. The *psrA* deletion mutant (PSRA1) retained expression of downstream genes *psrB* and *psrC*, but was unable to respire S^0 or $S_2O_3^{2-}$ as terminal electron acceptor. Based on these results, we postulate that PsrA functions as the main subunit of the *S. oneidensis* $S_2O_3^{2-}$ terminal

reductase whose end products [sulfide (HS^-) or SO_3^{2-}] participate in an intraspecies sulfur cycle that drives S^0 respiration.

Introduction

Microbial reduction of inorganic sulfur compounds is central to the biogeochemical cycling of sulfur and other elements such as carbon and metals (29). The ability to reduce elemental sulfur (S^0) is found in members of both prokaryotic domains (20), including mesophilic δ-proteobacteria (*Desulfovibrio vulgaris, Pelobacter carbinolicus, Geobacter sulfurreducens*) (6, 9, 36, 51), thermophilic δ-proteobacteria (*Desulfurella acetivorans)*, (39), γ-proteobacteria (*Shewanella putrefaciens)* (41), ε-proteobacteria (*Wolinella succinogenes*) (49), cyanobacteria (*Oscillatoria limnetica)* (45), and hyperthermophilic archaea (1, 53). Partially reduced inorganic sulfur compounds such as tetrathionate ($S_4O_6^{2-}$), thiosulfate ($S_2O_3^{2-}$) and sulfite (SO_3^{2-}) are also important electron acceptors in the biogeochemical cycling of sulfur (29, 51). $S_4O_6^{2-}$-reducing bacteria, for example, may produce $S_2O_3^{2-}$ as a metabolic end product of $S_4O_6^{2-}$ reduction, while $S_2O_3^{2-}$ disproportionation is a key reaction catalyzed by sulfate-reducing bacteria (SRB), resulting in the formation of sulfate (SO_4^{2-}) and sulfide (S^{2-}) (26).

S. oneidensis MR-1, a facultatively anaerobic γ-proteobacterium, respires a variety of compounds as anaerobic electron acceptor, including the inorganic sulfur compounds S^0, SO_3^{2-}, $S_2O_3^{2-}$, $S_4O_6^{2-}$, transition metals (e.g., Fe(III) and Mn(IV)) and radionuclides (e.g., U(VI) and Tc(VII)) (8, 21, 41, 44, 50, 55, 56). The majority of studies on anaerobic respiration by *S. oneidensis* have focused on the mechanism of electron transport to transition metals and radionuclides (11, 14, 34, 46, 58, 59), while the

mechanism of electron transport to inorganic sulfur compounds has not been thoroughly examined.

Microbial S^0 respiration is postulated to occur via two pathways, both of which are based on an intraspecies sulfur cycle. In the first pathway (catalyzed by members of the genus *Salmonella* (20)), $S_2O_3^{2-}$ is reduced, yielding HS^- and SO_3^{2-} (24). SO_3^{2-} diffuses from the cell and reacts chemically with extracellular S^0 to form $S_2O_3^{2-}$, which re-enters the periplasm and is re-reduced, thereby sustaining an intraspecies sulfur cycle. In the second pathway (catalyzed by *W. succinogenes* (24)), water-soluble polysulfides (S_n^{2-}, n>2), formed by chemical interactions of S^0 at pH>7 (52), are reduced step-wise in the periplasm to S_{n-1}^{2-} and HS^-. Similar to the first pathway, microbially produced HS^- diffuses from the cell and reacts chemically with S^0 to produce additional S_n^{2-}, which re-enters the periplasm and is re-reduced to sustain an analogous intraspecies sulfur cycle (24).

Genetic analyses of $S_2O_3^{2-}$ reduction-deficient mutants of *S. typhimurium* have demonstrated that *phsA* (denoting production of hydrogen sulfide) is required for HS^- production during $S_2O_3^{2-}$ respiration (10, 17, 22). In addition, *phsA*-deficient mutants are unable to reduce S^0 as electron acceptor (24). The *phsA* homolog of *W. succinogenes* (annotated as *psrA* for polysulfide reduction) is required for S^0 respiration (32, 37). *W. succinogenes psrA* is the first gene of a three-gene cluster (including *psrA, psrB* and *psrC)* whose products encode a polysulfide reductase, a quinol oxidase and a membrane anchor, respectively (15). In addition, the structure of the polysulfide reductase complex (PsrABC) from *Thermus thermophilus* has recently been solved, and results indicate that PsrC acts as a quinol oxidase that transfers electrons step-wise via PsrB and PsrA to S_n^{2-}

during anaerobic S^0 respiration (27). The main objectives of the present study were to 1) identify the *S. typhimurium phsA* homolog in the *S. oneidensis* genome, 2) employ a newly constructed suicide cloning vector for in-frame gene deletion mutagenesis in *S. oneidensis* to delete the *S. typhimurium phsA* homolog of *S. oneidensis*, and 3) test the *S. oneidensis psrA* deletion mutant for respiratory activity on a combination of two electron donors and 11 electron acceptors, including the inorganic sulfur compounds $S_4O_6^{2-}$, $S_2O_3^{2-}$, and S^0.

Materials and Methods

Growth Media and Cultivation Conditions. *S. oneidensis* MR-1 was cultured at 30°C in Luria Bertani medium (10 g L^{-1} NaCl, 5 g L^{-1} yeast extract, 10 g L^{-1} tryptone) for genetic manipulations. For anaerobic growth experiments, cells were cultured in a defined salts medium (SM) (44) supplemented with lactate (18 mM) or formate (30 mM) as carbon/energy source. Anaerobic growth experiments were carried out in 13 mL Hungate tubes (Bellco Glass, Inc) filled with 10 mL of SM and sealed with black butyl rubber stoppers under an N_2 atmosphere. Growth experiments were performed in two parallel, yet independent incubations. In a second set of anaerobic growth experiments with S^0 and $S_2O_3^{2-}$, *S. oneidensis* cultures were incubated with continual flushing of the headspace with N_2 to remove bacterially-produced HS^- (37). Electron acceptors were added from filter-sterilized stocks (synthesized as described previously (13), except where indicated, at the following final concentrations: O_2 (atmospheric); NO_3^-, 10 mM; Fe(III) citrate, 50 mM; hydrous ferric oxide (HFO), Mn(III)-pyrophosphate, 10 mM (30); 40 mM; trimethylamine-*N*-oxide (TMAO), 25 mM; $S_2O_3^{2-}$, 10 mM; $S_4O_6^{2-}$, 2 mM;

fumarate, 30 mM; dimethylsulfoxide (DMSO), 25 mM; and S^0, 20 mM (41). When required, antibiotics were supplemented at the following final concentrations: gentamycin, 15 μg mL^{-1} and chloramphenicol, 25 μg mL^{-1}. For growth of *Escherichia coli* β2155 λ pir (12), diaminopimelate (DAP) was supplemented at a final concentration of 100 μg mL^{-1}.

Analytical Techniques. Cell growth was monitored by direct cell counts via epifluorescence microscopy and by measuring terminal electron acceptor depletion or end product accumulation. Acridine orange-stained cells were counted (Carl Zeiss AxioImager Z1 Microscope) according to previously described procedures (35). Cell numbers at each time point were calculated as the average of 10 counts from two parallel yet independent anaerobic incubations. NO_2^- was measured spectrophotometrically with sulfanilic acid-*N*-1-naphthyl-ethylene-diamine dihydrochloride solution (40). Fe(III) reduction was monitored by measuring Fe(II) production with the ferrozine technique (54). Mn(III)-pyrophosphate concentration was measured colorimetrically as previously described (30). $S_2O_3^{2-}$ and $S_4O_6^{2-}$ concentrations were measured by cyanolysis as previously described (28). Growth on O_2, TMAO, DMSO, and fumarate were monitored by cell growth only. Control experiments consisted of incubations with cells that were heat-killed at 80°C for 30 minutes prior to inoculation or by omission of terminal electron acceptor.

Nucleotide and amino acid sequence analyses. Genome sequence data for *S. oneidensis* MR-1 (21), *S. typhimurium* LT2 (38) and *W. succinogenes* (5) was obtained from the comprehensive microbial resource (J. Craig Venter Institute, http://cmr.jcvi.org). *S. oneidensis* proteins that displayed significant similarity to *S. typhimurium* PhsA

Table 2.1: Strains and Plasmids used in this study.

Strain	Features	Source
Shewanella oneidensis		
MR-1	Wild-type strain	ATCC
PSRA1	in-frame deletion mutant	This study
PSRA+	"knock-in" complemented mutant	This study
Escherichia coli		
EC100D *pir*-116	*F- mcrA* Δ(*mrr-hsdRMS-mcrBC*) ϕ80d*lacZΔM15* Δ*lacX*74 *recA*1 *endA*1 *araD*139 Δ(*ara, leu*)7697 *galU galK* λ- *rpsL nupG pir*-116(DHFR)	Epicentre
β2155 λ pir	*thrB1004 pro thi strA hsdS lacZΔM15* (F9 *lacZ*Δ*M15 lacI*q *traD36 proA*1 *proB*1) Δ*dapA::erm pir::*RP4 Km^R	(12)
Plasmids		
pKO2.0	4.5 kb γR6K, *mob*RP4 *sacB* Gm^R *lacZ*	This study
pKNOCK-Gm	1.6 kb γR6K, *mob*RP4 Gm^R	(2)
pBBR1MCS	Cm^R lacZ	(31)
pJQ200	ColE1 *sacB* Gm^R	(48)
pKOPSRA	pKO2.0 containing psrA in-frame deletion	This study
pKOPSRA+	pKO2.0 containing WT *psrA*	This study

(designated PsrA in the *S. oneidensis* genome), tetrathionate reductase (TtrA) and anaerobic sulfite reductase (AsrA) were identified via BLAST analysis (3). Functional motifs were analyzed via Pfam (http://pfam.sanger.ac.uk) and ClustalW (33). The *S. oneidensis* PsrA sequence was used as the query sequence for BLAST analysis of several other recently sequenced *Shewanella* genomes, including *S. putrefaciens* 200, *S. putrefaciens* CN32, *S. putrefaciens* W3-18-1, *S. amazonensis* SB2B, *S. denitrificans* OS217, *S. baltica* OS155, *S. frigidimarina* NCIMB400, *S. pealeana* ATCC 700345, *S. woodyi* ATCC 51908, *S.* sp. ANA-3, *S.* sp. MR-4, *S.* sp. MR-7, *S. loihica* PV-4, *S. halifaxens* HAW-EB4, *S. piezotolerans* WP3, *S. sediminis* HAW-EB3, and *S. benthica* KT99. Preliminary genome sequence data for these strains was obtained from the Department of Energy, Joint Genome Institute (http://www.jgi.doe.gov).

Construction of suicide vector pKO2.0. The strategy for construction of suicide vector pKO2.0 is outlined in Figure. 2.1. The R6K *oriV* and the RP4 *oriT* of pKNOCK-Gm (2) were PCR-amplified with *Nhe*I restriction sites engineered onto the ends of the *oriV-oriT* fragment. The chloramphenicol acetyltransferase gene (*cat*) and the LacZ-containing multiple cloning site (MCS) were PCR-amplified from pBBR1MCS (31) with *Nhe*I sites also engineered onto the ends (see Supplemental Table 1 for corresponding primers). The resulting PCR products were ligated to form pKOCat-MCS. The open reading frames encoding *sacB* and gentamycin acetyltransferase (conferring gentamycin resistance; Gm^R) were PCR-amplified from pJQ200 (48) as a contiguous fragment with *ApaL*I and *Mun*I restriction sites engineered onto the ends. The *cat* gene was removed from pKOCat-MCS by inverse PCR, resulting in a fragment containing the R6K *oriV*,

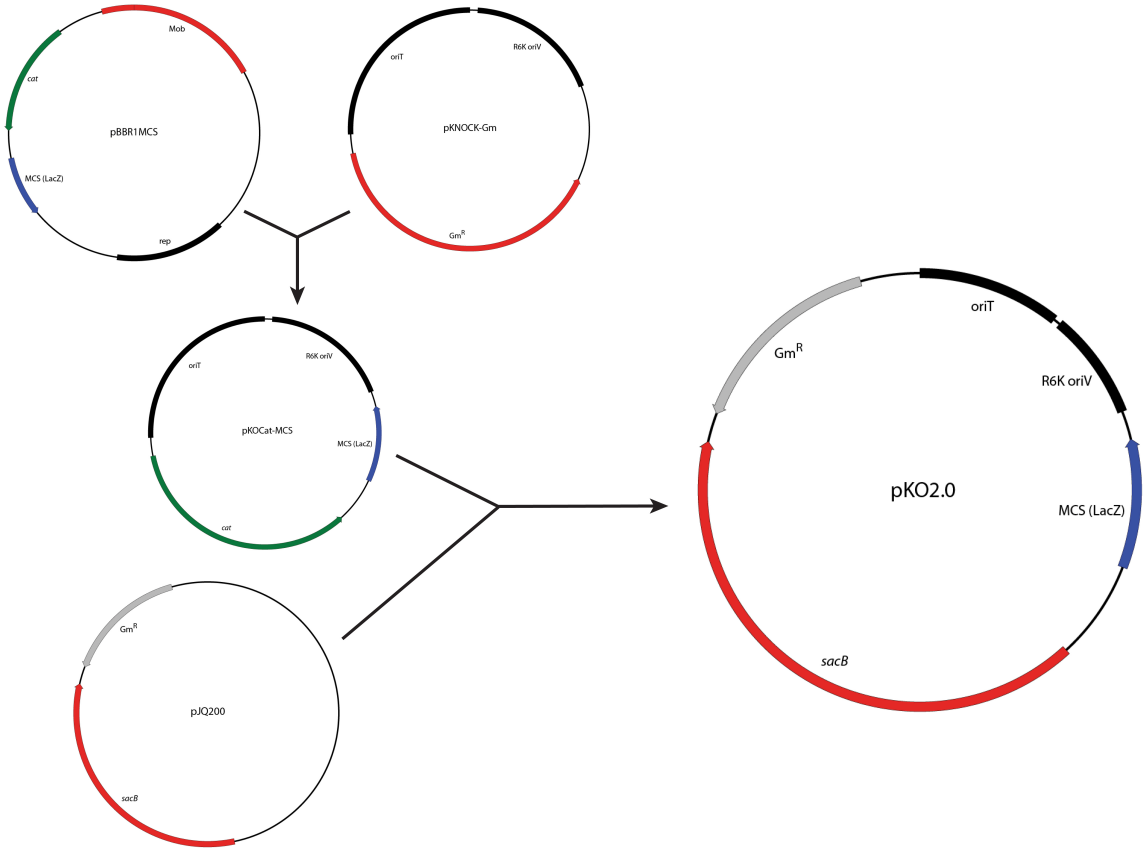

Figure 2.1 Stepwise construction of suicide vector pKO2.0. Individual steps in construction of pKO2.0 are described in the text

RP4 *oriT*, and the LacZ-MCS with *ApaL*I and *Mun*I sites on the ends. These two fragments were ligated to form pKO2.0 (R6K, *oriT*, LacZ-MCS, Gm^R *sacB*).

In-frame gene deletion mutagenesis. *psrA* was deleted from the *S. oneidensis* genome by the following method. Regions corresponding to ~750 bp upstream and downstream of the *psrA* ORF were PCR-amplified using iProof ultra high-fidelity polymerase (Bio-Rad, Hercules, CA). Primers used for construction of the *psrA* deletion mutant are listed in Table 2.2. PCR cycling routines consisted of 98°C for 30 sec., 35 cycles of 98°C for 15 sec., 60°C for 30 sec., and 72°C for 30 sec., concluding with a final extension step at 72°C for 7 min. PCR reactions (50 μL total volume) were performed on a Bio-Rad iCycler (Bio-Rad, Hercules CA) and contained 20 ng of *S. oneidensis* genomic DNA (DNAzol, Invitrogen), 250 μM of dNTPs, and 50 ng of each oligonucleotide. The resulting fragments were separated by agarose gel electrophoresis, isolated from the gel (QIAquik gel extraction kit, QIAGEN) and subsequently joined using overlap-extension PCR (25) to generate a DNA fragment containing regions homologous to the regions flanking *psrA*. This region was cloned into the newly constructed knockout vector pKO2.0, and the resulting plasmid (pKOPSRA) was electroporated into *E. coli* EC100D *pir*-116 (Epicentre) (Bio-Rad Xcell Electroporation system, Bio-Rad, Hercules, CA). Recipients were detected on LB agar medium containing gentamycin (Gm) and 40 μg mL^{-1} X-Gal (5-bromo-4-chloro-3-indolyl-β-D-galactopyranoside). The recombinant plasmid was confirmed by detection of a ~1.5 kb insertion following digestion with *Bam*HI. Following confirmation, pKO2.0-Δ*psrA* was electroporated into *E. coli* β2155 λ pir (12) (Bio-Rad Xcell Electroporation system, Bio-Rad, Hercules, CA) and the resulting donor strain was mated biparentally with *S. oneidensis* on LB agar medium supplemented

with DAP. Following an 18-hour incubation, the mating mix was resuspended in LB liquid medium and subsequently plated onto LB agar medium containing Gm.

S. oneidensis MR-1 colonies with pKOPSRA integrated into the genome were screened by PCR using primers flanking the recombination region. The resulting strain (MR-1::pKOPSRA) was grown in LB medium with NaCl omitted and subsequently transferred to LB agar medium with NaCl omitted and containing 10% sucrose (w/v). Colonies were patched to LB agar medium containing Gm to confirm loss of pKO2.0, and the deletion in *psrA* was confirmed in the Gm-sensitive colonies via PCR using primers flanking the recombination region. One mutant strain (PSRA1) was also confirmed by direct DNA sequencing of the targeted region (University of Nevada, Reno Genomics Center).

Confirmation of in-frame deletions. Liquid cultures of *S. oneidensis* wild-type and deletion mutant strains were grown to mid-log phase (corresponding to 1.8 X 10^9 cells mL^{-1}) in LB and total RNA was extracted with PureZol reagent (Bio-Rad, Hercules, CA) according to the manufacturer's instructions. RNA (~150 ng μL^{-1}) was further purified (RNeasy Kit, QIAGEN) with on-column DNase I treatment according to the manufacturer's instructions. RNA was reversely transcribed with High Capacity cDNA Reverse Transcription Kit (Applied Biosystems). RT reactions (20 μL) consisted of 150 ng RNA, 50 U MultiScribe Reverse Transcriptase, 4 mM dNTPs and random hexamers. Cycling routines consisted of 25°C for 10 min., 37°C for 120 min. and 85°C for 5 min. The resulting cDNA was PCR-amplified with primers specific for internal regions of *psrA, psrB* and *psrC* (Table 2.2). RNA polymerase factor *rpoA* served as a positive

control. Negative controls consisted of identical reactions with reverse transcriptase omitted.

Knock-in complementation analysis of PSRA1. PSRA1 was complemented via a strategy analogous to that followed in the gene deletion protocol. Wild-type *psrA* was PCR-amplified from MR-1 genomic DNA with *psrA*-specific primers PSRAD1 and PSRAD4. The resulting amplicon contained the entire ORF and ~750 bp of upstream and downstream DNA for subsequent recombination into PSRA1. The amplicon was cloned into pKO2.0 using identical restriction sites and the resulting construct was subsequently transformed into *E. coli* strains as described above. "Knock-in" complementation was performed as described for in-frame deletion above, except that PSRA1 was used as recipient strain. Insertion into the proper location of the genome was confirmed via PCR amplification with flanking primers PSRADTF, PSRADTR (Table 2.2) followed by DNA sequencing (University of Nevada, Reno Genomics Center). The resulting "knock-in" complemented strain was designated PSRA+.

Table 2.2: Primers used in this study.

Name	Sequence
PSRAD1	GACTGGATCCCACAGCTTATTTGGTCGTACCGA
PSRAD2	ATATCTTTTCGTCATTTGAGCCTCCAAGGTTACCTCCATCACACTCA
PSRAD3	TGAGTGTGATGGAGGTAACCTTGGAGGCTCAAATGACGAAAAGATAT
PSRAD4	GACTGTCGACACAAGCCAAGCCTAAGCTGATGG
PSRADTF	GCGTGCATTTTGAACGACAG
PSRADTR	GCTTTCTAAAGGGCATAAGCAGC
RT-PSRAF	GTCGCCGATAAAGCCGATGAATGGTA
RT-PSRAR	GGCATATCTTTTACGCCGGGCTTAC
RT-PSRBF	TATGGCGAAATGCCCAATCTGC
RT-PSRBR	AAGCGGGTGTCCTTACAGAAGT
RT-PSRCF	AGTCACGACAAGACGTTAGCCA
RT-PSRCR	GCTTTGGCCCGCATACACAATA
RT-RPOAF	GTTCAACACGAGCTGCTTCTA
RT-RPOAR	GGCTTAGCAGTGACTATCGAG

RESULTS

Construction of new suicide vector pKO2.0. Suicide vector pKO2.0 was constructed in a step-wise fashion, integrating the hallmark components of previously constructed vectors. The R6K *oriV* and RP4 *oriT* origins from pKNOCK-Gm and the chloramphenicol resistance marker (*cat*) and the LacZ-containing polylinker (MCS) from the broad-host range vector pBBR1MCS were independently PCR-amplified and joined to form pKOCat-MCS (Figure. 2.1). The *cat* gene was subsequently removed via inverse PCR and the resulting product (containing R6K*ori*, *oriT*, and MCS) was ligated with the PCR product containing the Gentamycin resistance gene (Gm^R) and *sacB* encoding levansucrase (Figure. 2.1).

Identification of *S. oneidensis* gene products that display similarity to the PhsA homolog of *S. typhimurium*. BLAST analysis revealed that the *S. oneidensis* MR-1 genome contained a three gene cluster (annotated as *psrABC*) whose translated products displayed 59-73% and 65-80% amino acid similarity to the *phsABC* (*psrABC*) clusters of *S. typhimurium* LT2 and *W. succinogenes*, respectively (Table 2.3). The three gene *psr* cluster in *S. oneidensis* MR-1 has the same genomic organization as the three gene *psr* clusters in both *S typhimurium* and *W. succinogenes* (data not shown). ClustalW multiple alignments of PsrA functional domains with those of other proteobacteria indicated that *S. oneidensis* PsrA contains the conserved 4Fe-4S cluster and molybdopterin guanine-dinucleotide (MGD) binding motifs postulated to contribute to PsrA activity (Figure. 2.2). PsrA contained the predicted Pfam domains consistent with other members of the polysulfide (thiosulfate) reductase family of proteins, including the 4Fe-4S cluster

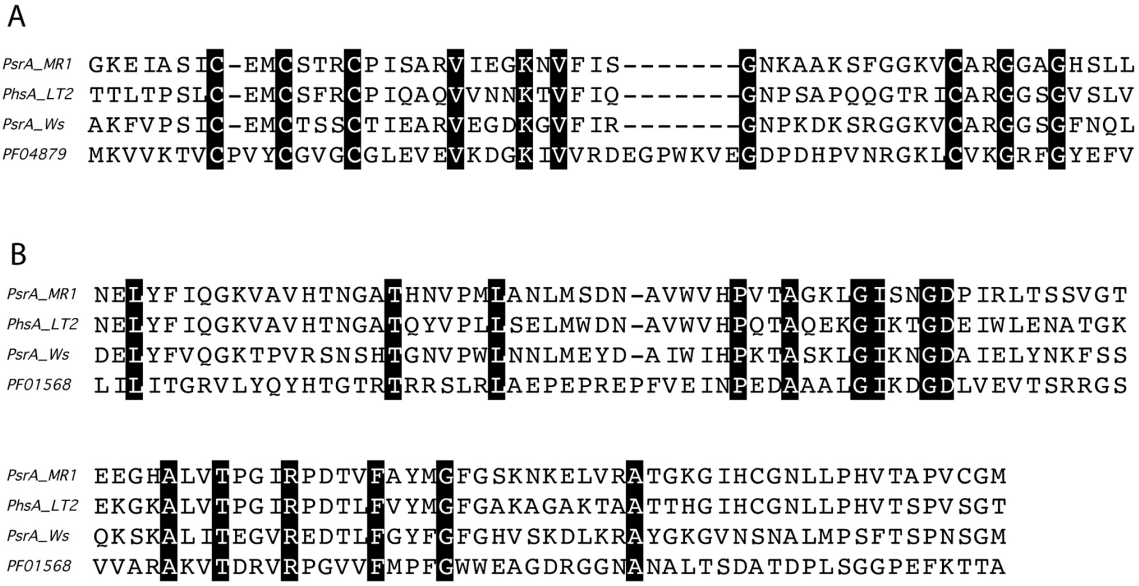

Figure 2.2. Identification of conserved PFam domains in PsrA family of proteins. ClustalW multiple alignment of PsrA-family proteins containing conserved PFam Domains. A) multiple alignment of PFam domain PF04879 (Fe4S4-binding domain) with *S. oneidensis* MR-1 PsrA (PsrA_MR1), *S. typhimurium* LT2 PhsA (PhsA_LT2), and *W. succinogenes* PsrA (PsrA_Ws). B) multiple alignment of PFam domain PF01568 (bis-MGD binding domain). Identical residues are shaded.

(PF04879) and MGD binding motifs (PF01568) (Figure. 2.2). Proteins homologous to the *S. typhimurium* TtrA (tetrathionate reductase) or AsrA (anaerobic sulfite reductase) were not detected in the *S. oneidensis* genome (data not shown).

$S_2O_3^{2-}$-reducing members of the genus *Shewanella* contain Psr homologs with high amino acid sequence similarity. The *psrABC* cluster was also identified in the recently sequenced genomes of *Shewanella* strains that respire S^0 and $S_2O_3^{2-}$, including *S. putrefaciens* CN32, *S. putrefaciens* 200, *S. putrefaciens* W3-18-1, *S. amazonensis* SB2B, *S. frigidimarina* NCIMB400, *S. baltica* OS155, *S. pealeana*, *S. sp.* ANA-3, *S. loihica* PV-4, *S. sp.* MR-4, *S. sp.* MR-7, *S. benthica*, *S. halifaxens*, *S. piezotolerans*, and *S. sediminis*. The *psr* gene cluster was missing from the genomes of *S. denitrificans* OS217 and *S. woodyi*, a finding that correlated with the inability of these two strains to respire $S_2O_3^{2-}$ (57). PsrA (85-98%), PsrB (90-99%) and PsrC (66-99%) amino acid sequence similarities were highly conserved among $S_2O_3^{2-}$-respiring *Shewanella* spp. (Table 2.3).

Construction and confirmation of in-frame deletion mutant strain PSRA1 and Knock-in complementation strain PSRA+. *S. oneidensis psrA* was deleted in-frame via application of the newly developed pKO2.0-based gene deletion system. Regions flanking *psrA* were PCR-amplified and joined to construct a region used for gene deletion. This region was cloned into pKO2.0 (designated pKOPSRA) and subsequently mobilized into *S. oneidensis* via conjugal transfer. Single integrants were selected by resistance to Gm and confirmed via PCR using test primers flanking the recombination region. The second step involved resolution of the single integration by counterselection on media containing sucrose. Several sucrose-resistant colonies were screened by PCR, and selected for further study. A single strain (designated PSRA1)

Table 2.3. Identities and similarities between PsrA, PsrB, and PsrC homologs identified in the 21 sequenced *Shewanella* strains, *S. typhimurium* LT2, and best-hit in GenBank.

	Shewanella spp.[a]			*S. typhimurium* LT2[b]			GenBank[c]			
Protein	Sim	ID	E value	Sim	ID	E value	Best Hit	Sim	ID	E value
PsrA	85-98	75-96	0.0	73	56	0.0	*W. succinogenes*	65	47	0.0
PsrB	90-99	79-98	10^{-87}-10^{-107}	71	54	10^{-57}	*W. succinogenes*	80	65	10^{-63}
PsrC	66-99	51-96	10^{-57}-10^{-137}	59	40	10^{-38}	*W. succinogenes*	67	45	10^{-62}

[a] Percent sequence similarity (Sim), percent identity (ID), and expect value (E value) between *S. oneidensis* Psr predicted amino acid sequences obtained from TIGR. Ranges were determined by pairwise comparison with translated sequence data from draft genome sequences of recently sequenced *Shewanella*, including *S. putrefaciens* 200, *S. putrefaciens* CN32, *S. putrefaciens* W3-18-1, *S. amazonensis* SB2B, *S. denitrificans* OS217, *S. baltica* OS195, *S. frigidimarina* NCIMB400, *S. pealeana* ATCC 700345, *S. woodyi* ATCC 51908, *S.* sp. ANA-3, *S.* sp. MR-4, *S.* sp. MR-7, *S. loihica* PV-4, *S. halifaxens*, *S. piezotolerans*, *S. benthica*, and *S. sediminis*.

[b] Percent sequence similarity (Sim), percent identity (ID), and expect value (E value) between *S. oneidensis* when compared to *S. typhimurium* LT2.

[c] Organism outside the genus *Shewanella* or *Salmonella* with the ortholog of highest similarity (Best hit) determined by BLASTP analysis of GenBank nonredundant database.

displaying a PCR product corresponding to an in-frame *psrA* deletion was chosen and tested for expression of downstream genes *psrB* and *psrC* via RT-PCR. Transcripts for *psrB* and *psrC* were detected in PSRA1, while transcripts for *psrA* were not (Figure. 2.3).

To avoid problems associated with *in trans* complementation (e.g., inadvertent overexpression), newly constructed suicide vector pKO2.0 was used to generate a "knock-in" genetic complementation strain, designated PSRA+. *psrA* and regions upstream and downstream (identical to those used to construct PSRA1) was PCR-amplified and cloned into pKO2.0 as described above. pKOPSRA+ was used to re-insert the *psrA* gene into PSRA1 as described for construction of the in-frame deletion with the exception that PSRA1 was used as the recipient strain. Insertion of wild-type *psrA* back into PSRA1 was confirmed via DNA sequencing and RT-PCR analyses as described above (Figure. 2.3).

Anaerobic growth capabilities of *S. oneidensis* strains PSRA1 and PSRA+. Wild-type *S. oneidensis*, deletion mutant PSRA1, and complemented mutant PSRA+ were tested for anaerobic respiration on a combination of two electron donors (lactate or formate) and a set of alternate electron acceptors. PSRA1 was severely impaired in its ability to respire anaerobically on $S_2O_3^{2-}$ and S^0 with lactate or formate (Figures. 2.4 and 2.5), yet retained the ability to grow on all other combinations of electron donors and electron acceptors including O_2, DMSO, Fe(III)-citrate, HFO, NO_3^-, fumarate, Mn(III)-pyrophosphate, and TMAO (Figure. 2.6). Anaerobic growth of wild-type *S. oneidensis* and PSRA+ on S^0-containing solid growth medium was accompanied by the production of a clearing zone in the colony periphery. The clearing zone, indicative of S^0 reduction was more pronounced with formate rather than lactate as electron donor (Figure. 2.5).

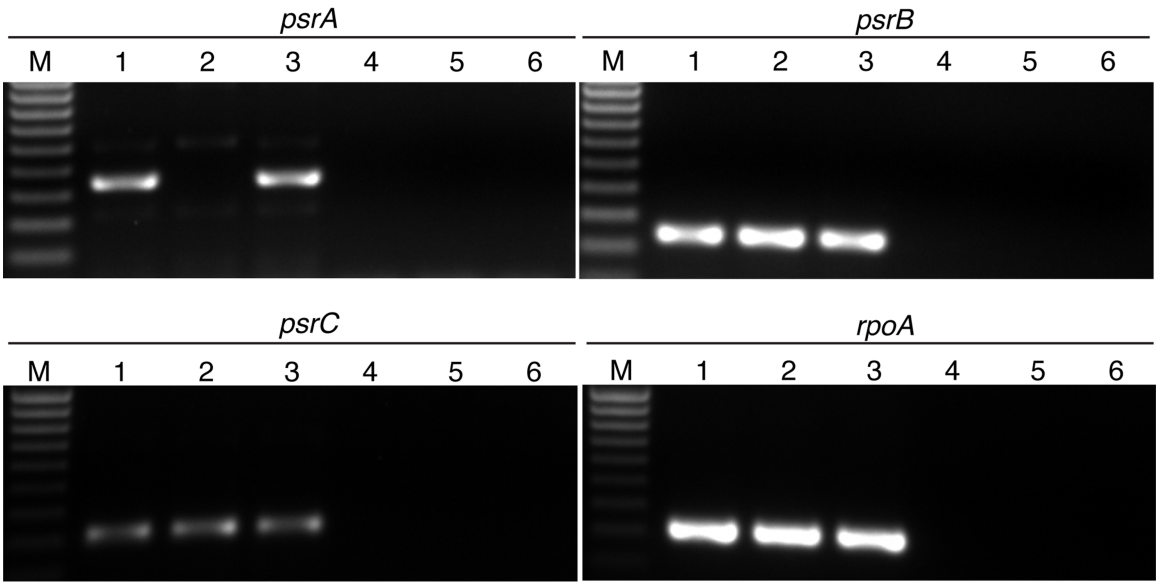

Figure 2.3. Reverse transcriptase PCR of genes in the *psr* operon. PCR products generated from cDNA from Wild-type (lane 1), PSRA1 (lane 2), or PSRA+ (lane 3) were separated electrophoretically and visualized via staining with ethidium bromide. Transcripts for *psr* or housekeeping (*rpoA*) genes are indicated above gel lanes. Negative control lanes 4, 5, and 6 include cDNA from wild-type, PSRA1, and PSRA+, respectively with reverse transcriptase omitted from the cDNA synthesis reaction.

Neither cell mass, nor a clearing zone were observed in anaerobic incubations of PSRA1 on S^0-containing solid growth medium.

PSRA1 retained $S_4O_6^{2-}$ respiratory activity, and consequently produced $S_2O_3^{2-}$, although not at wild-type rates (Figure. 2.7). With formate as electron donor, the wild-type strain and PSRA+ depleted $S_4O_6^{2-}$ to low levels and switched to anaerobic respiration of the produced $S_2O_3^{2-}$ (noted by a depletion of $S_2O_3^{2-}$ after 24 hours). With lactate as electron donor, the wild-type strain and PSRA+ reduced $S_4O_6^{2-}$ to $S_2O_3^{2-}$, however neither strain was able to respire the produced $S_2O_3^{2-}$. PSRA1, on the other hand, reduced $S_4O_6^{2-}$ and produced $S_2O_3^{2-}$, but was unable to respire the produced $S_2O_3^{2-}$ with either lactate or formate as electron donor. As a result, PSRA1 displayed a marked decrease in growth rate and $S_4O_6^{2-}$ reduction activity. (Figure. 2.7).

Discussion

Metal-respiring members of the genus *Shewanella* provide attractive models for determining the molecular mechanism of anaerobic respiration of metals, metalloids and radionuclides. Genetic manipulations in *Shewanella* can be performed aerobically prior to subsequent phenotypic tests under anaerobic conditions. With the recent release of the genomic sequences of 21 *Shewanella* strains (Joint Genome Institute, http://www.jgi.doe.gov), targeted, in-frame gene deletion mutagenesis may now be carried out to examine the molecular mechanism of anaerobic respiration. Earlier genetic manipulation techniques such as transposon and chemical mutagenesis have been problematic for a variety of reasons, including polar effects on downstream genes, inadvertent genomic rearrangements and deletions, and altered growth rates due to the energetic requirements for maintaining antibiotic resistance markers (7, 13, 43). The

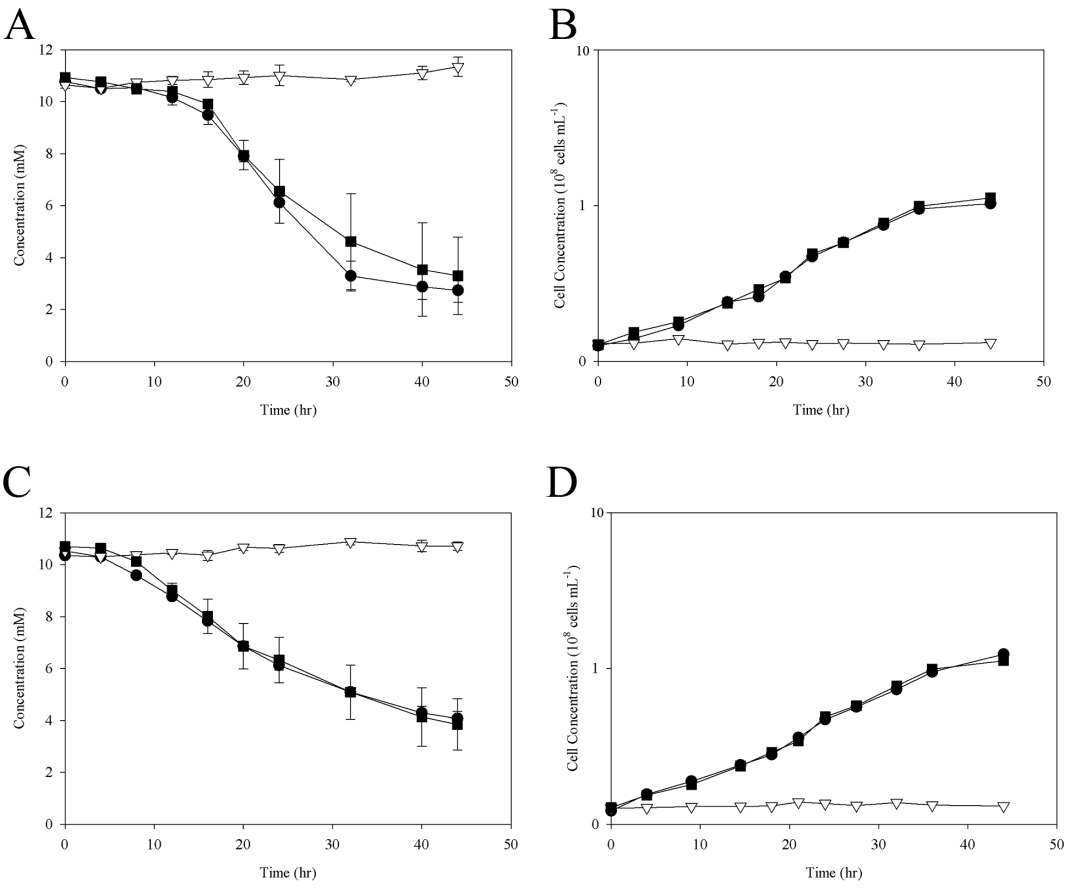

Figure 2.4. $S_2O_3^{2-}$ reduction phenotypes of wild-type (MR-1), *psrA* deletion mutant (PSRA1) and "knock-in" complemented (PSRA+) strains. A) $S_2O_3^{2-}$ concentration as a function of time for wild-type (filled circles), PSRA1 (open triangles), and PSRA+ (filled squares) with lactate (18 mM) as electron donor. B) cell-growth as a function of time with lactate as electron donor (symbols are identical to A). C) $S_2O_3^{2-}$ concentration as a function of time with formate (30 mM) as electron donor (symbols are identical to A). D) cell-growth as a function of time with formate as electron donor (symbols are identical to A).

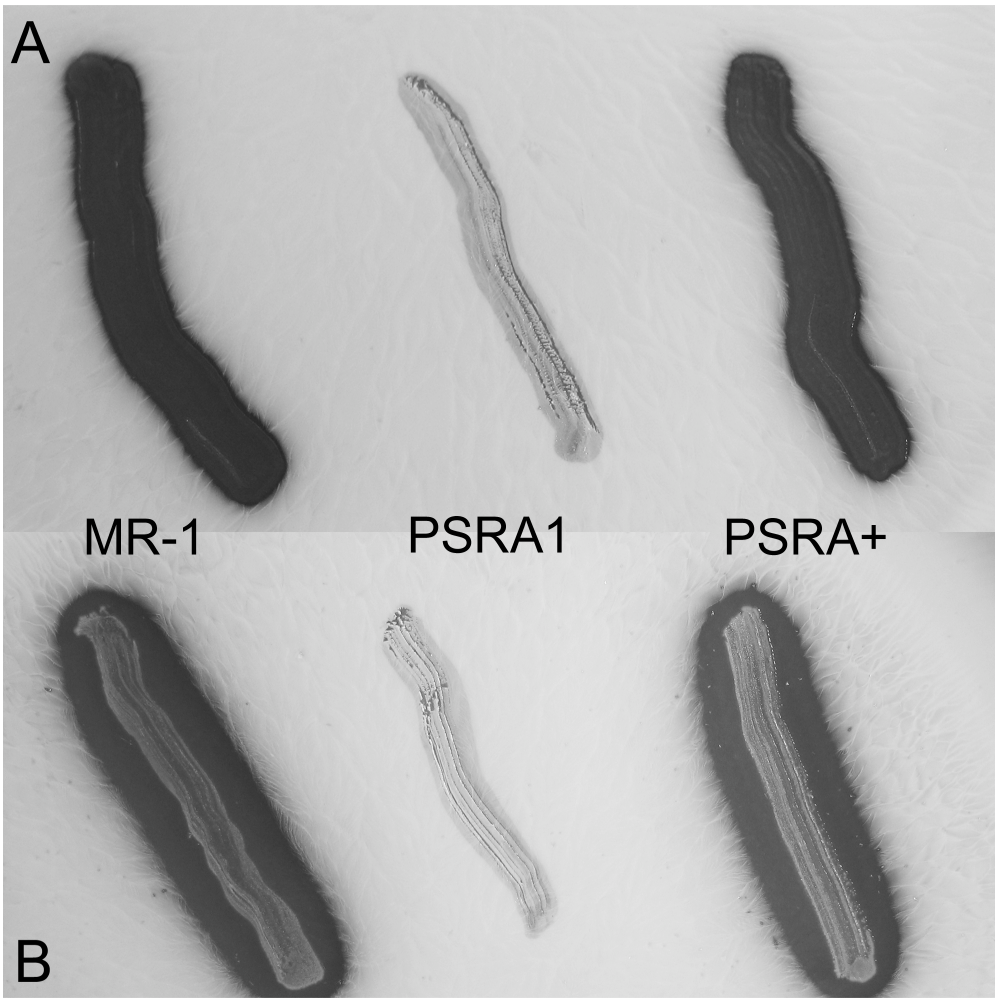

Figure 2.5. S^{v} respiratory phenotypes of wild-type (MR-1), *psrA* deletion mutant (PSRA1) and "knock-in" complemented (PSRA+) strains. Anaerobic cell growth on solid medium containing S^0 (40 mM) as electron acceptor with either lactate (10 mM) (A) or formate (30 mM) (B) as electron donor (90% N_2, 10% CO_2 atmosphere). Following a 48-hour anaerobic incubation, plates were visualized against a black background to observe the clearing zone associated with S^0 reduction by MR-1 and PSRA+ (but not by PSRA1).

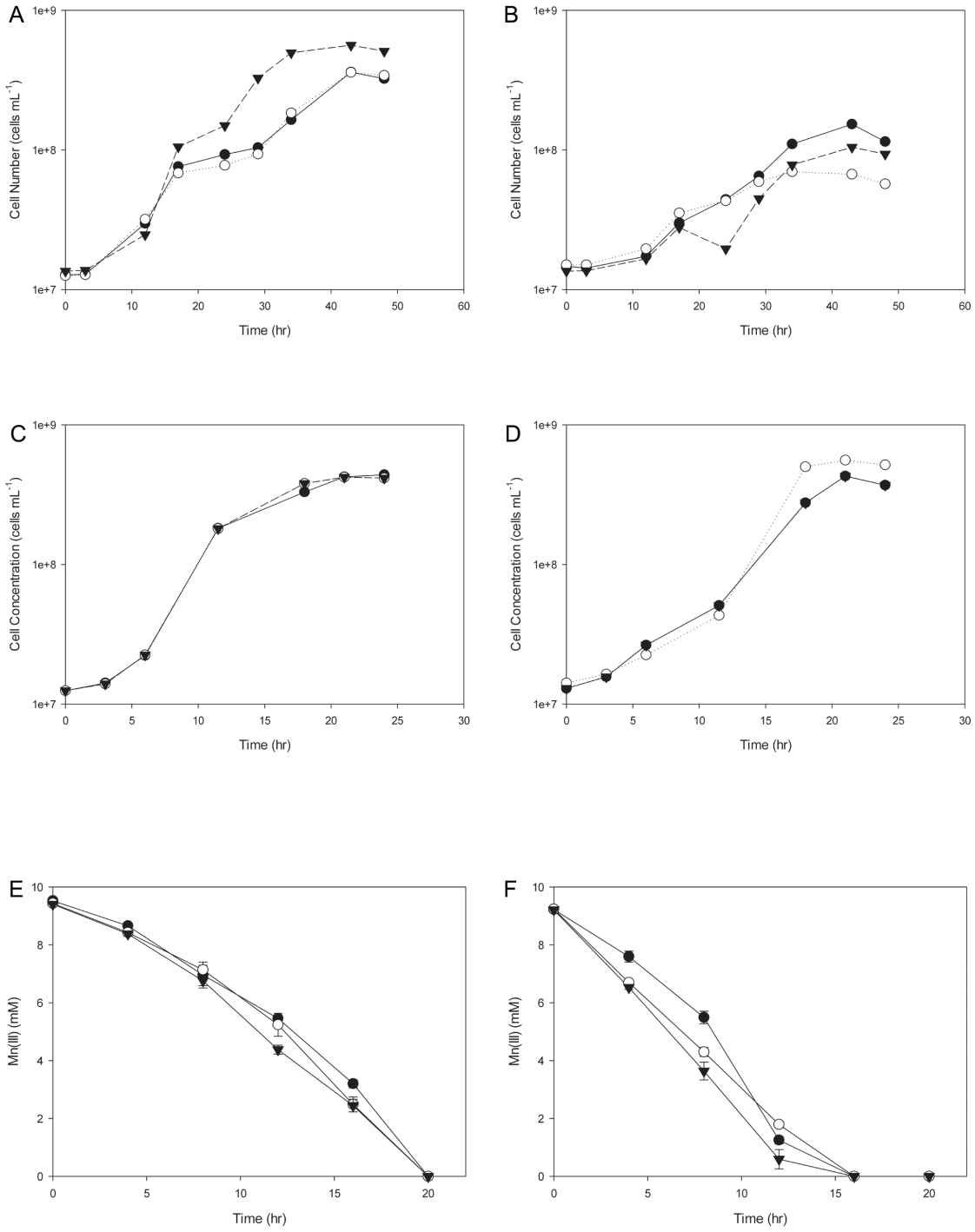

Figure 2.6. Growth on a set of alternate electron acceptors. wild-type (filled circles), PSRA1 (open circles), and PSRA+ (filled triangles). A) and B) cell density as a function of time with DMSO as TEA C) and D) cell density as a function of time with fumarate as TEA. E) and F) Mn(II) concentration as a function of time with Mn(III)-pyrophosphate as TEA. G) and H) Fe(II) concentration as a function of time with Fe(III)-citrate as TEA. I) and J) Fe(II) concentration as a function of time with HFO as TEA. K) and L) NO_2^- concentration as a function of time with NO_3^- as TEA. M) and N) cell density as a function of time with TMAO as TEA. O) cell density as a function of time with O_2 as TEA and lactate as electron donor.

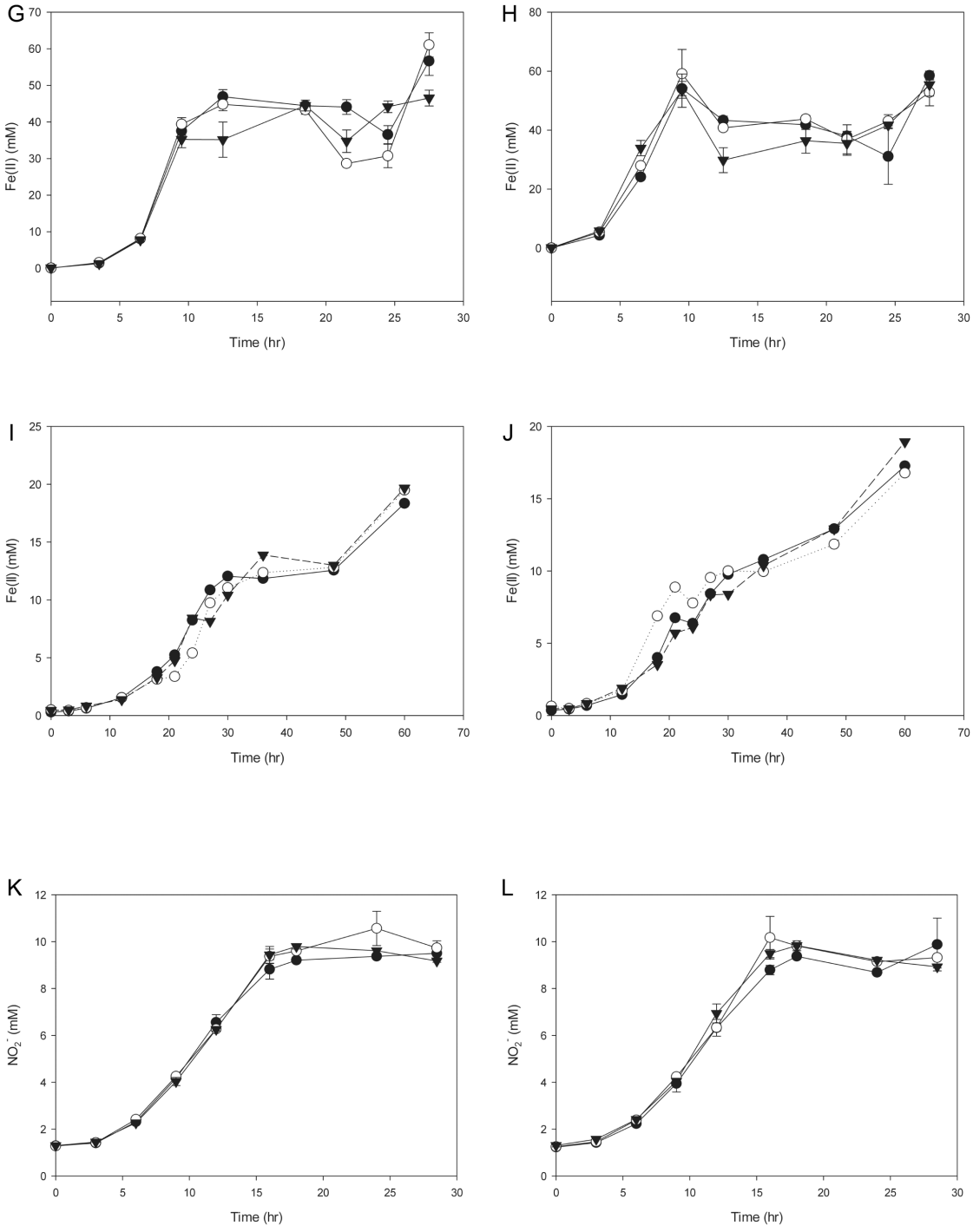

Figure 2.6 continued.

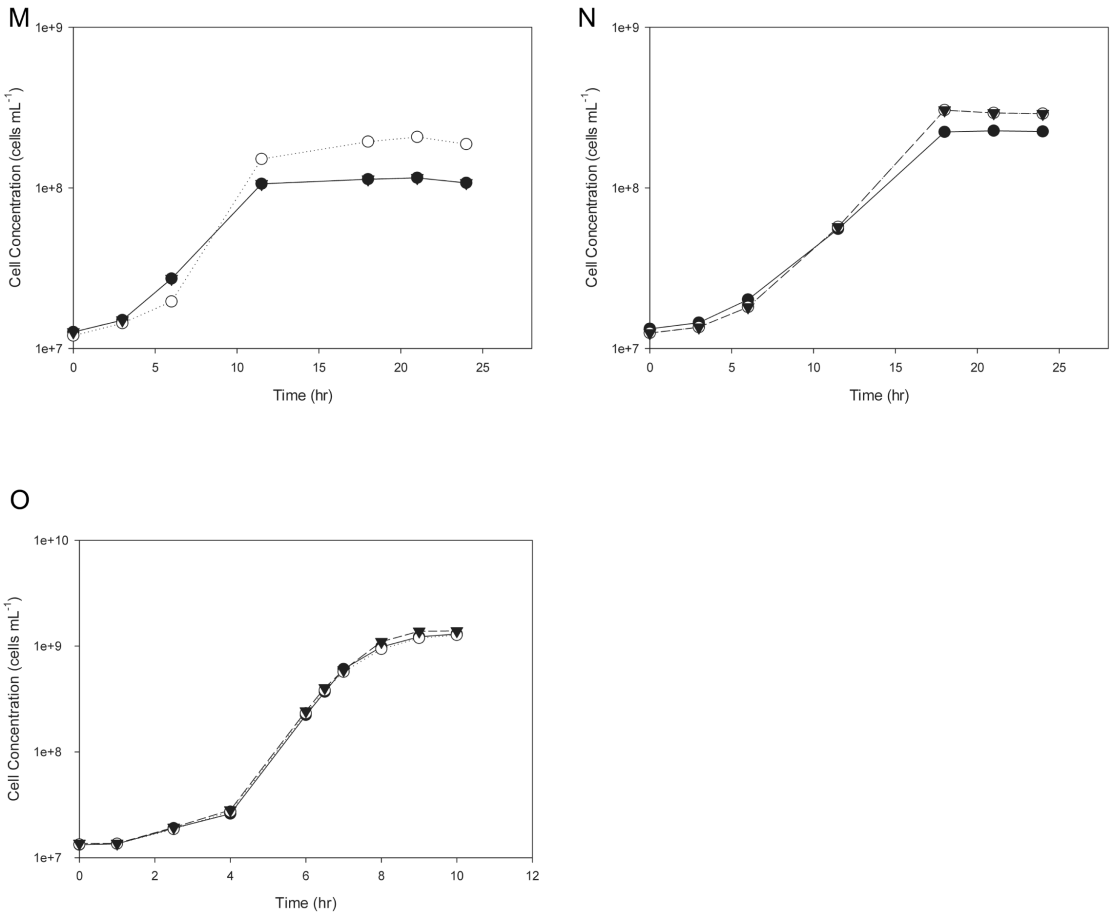

Figure 2.6 continued.

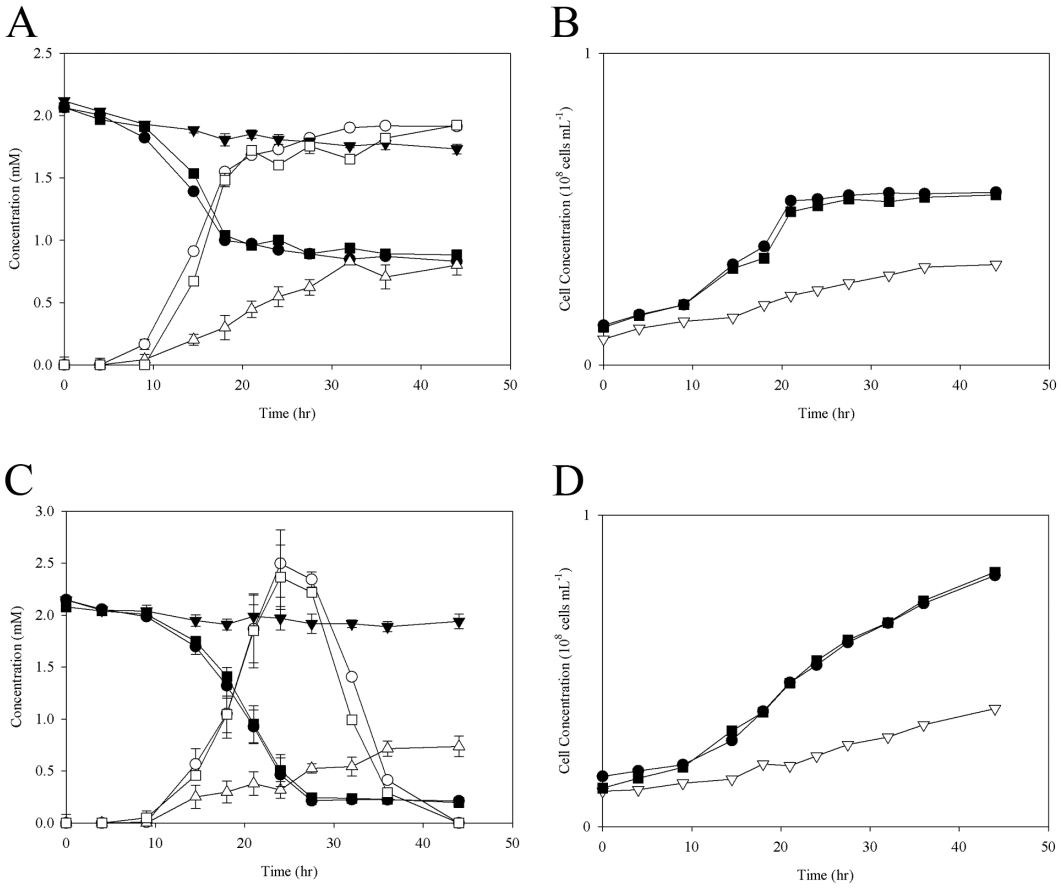

Figure 2.7. $S_4O_6^{2-}$-respiratory phenotypes of wild-type (MR-1), *psrA* deletion mutant (PSRA1) and "knock-in" complemented (PSRA+) strains. A) and C) $S_4O_6^{2-}$ reduction by wild-type (filled circles), PSRA1 (filled triangles), or PSRA+ (filled squares) strains with lactate (18 mM) (A) or formate (30 mM) (C) as electron donor. Respiration of $S_4O_6^{2-}$ results in an accumulation of $S_2O_3^{2-}$ by wild-type (open circles), PSRA1 (open triangles), or PSRA+ (open squares) strains. B) and D) cell-growth as a function of time for wild-type (filled circles), PSRA1 (open triangles), or PSRA+ (filled squares) with lactate (B) or formate (D) as electron donor. In some cases, error bars are smaller than the symbol.

suicide vector constructed in the present study (pKO2.0) contains features ideal for generating in-frame, markerless gene deletions in *Shewanella*: pKO2.0 replicates efficiently in *E. coli* donor strains but not *S. oneidensis*, contains an appropriate broad-host-range origin of transfer (*oriT*), and encodes a functional counterselection marker (*sacB*) (16, 18, 19). In addition, pKO2.0 is ~5 kb smaller in size than previously constructed vectors (18) and contains a LacZ-polylinker for more efficient ligation of DNA constructs. *Shewanella* deletion mutants may therefore be constructed more efficiently due to increased transformation efficiency and elimination of problems with blunt-end cloning (19). pKO2.0 was used to construct in-frame deletions of the gene encoding the putative *psrA* homolog identified in the *S. oneidensis* genome.

The majority of studies on anaerobic respiration by *S. oneidensis* have focused on the mechanism of electron transport to transition metals and radionuclides, while the mechanism of electron transport to metalloids such as inorganic sulfur compounds remains poorly understood (8, 11, 14, 46, 56). Previous studies demonstrated that several members of the *Shewanella* genus couple the oxidation of organic matter (or hydrogen) to the dissimilatory reduction of S^0, a process that does not require direct contact between the cell and the S^0 particle (41, 47). S^0 respiration in *S. typhimurium* and *W. succinogenes* involves a PhsA (PsrA)- dependent intraspecies sulfur cycle. In *S. typhimurium*, PhsA reduces $S_2O_3^{2-}$ to HS^- and SO_3^{2-}. The produced SO_3^{2-} diffuses from the cell and reacts chemically with S^0 to form additional $S_2O_3^{2-}$, which re-enters the periplasm and is reduced by PhsA to HS^- and SO_3^{2-}, thereby sustaining an intraspecies sulfur cycle. In *W. succinogenes*, PsrA reduces S_n^{2-} step-wise to S_{n-1}^{2-} and HS^-. The HS^- diffuses from the cell and reacts with S^0 to form additional S_n^{2-}, which re-enters the

periplasm and is re-reduced (24). In this manner, the terminal reduction step for S^0 respiration by *S. typhimurium* and *W. succinogenes* is driven by the abiotic interaction of S^0 with either SO_3^{2-} or HS^- and not by direct enzymatic reduction of S^0.

In the present study, all predicted PsrA homologs identified in the recently sequenced *Shewanella* genomes contain Pfam domains indicative of the Phs (Psr) family of thiosulfate reductases, including 4Fe-4S cluster and MGD binding motifs. *psrA*-like genes are not found in the genomes of *S. denitrificans* or *S. woodyi*, two *Shewanella* species unable to respire S^0 or $S_2O_3^{2-}$ (57). Interestingly, *S. denitrificans* and *S. woodyi* are also unable to respire Fe(III) oxides as terminal electron acceptor (57), a pattern of electron acceptor utilization reflecting the close association of the S^0 and Fe(III) reduction phenotypes in metal-respiring bacteria (57).

To determine if *S. oneidensis psrA* is required for S^0 and $S_2O_3^{2-}$ respiration, the *S. typhimurium phsA* homolog identified in the *S. oneidensis* genome was deleted in-frame with the new pKO2.0-based in-frame gene deletion system, and the resulting mutant was tested for anaerobic respiration on a combination of two electron donors and a set of 11 alternate electron acceptors, including S^0 and $S_2O_3^{2-}$. *S. oneidensis* deletion mutant PSRA1 is unable to respire anaerobically on $S_2O_3^{2-}$ or S^0 as electron acceptor, yet retains respiratory activity on 9 other electron acceptors tested, including $S_4O_6^{2-}$. Following depletion of $S_4O_6^{2-}$, wild-type *S. oneidensis* switches to anaerobic respiration of the produced $S_2O_3^{2-}$. PSRA1, on the other hand, is unable to respire the produced $S_2O_3^{2-}$ and, as a result, displays decreased cell growth and $S_4O_6^{2-}$ depletion rates (Figure. 2.7). This finding indicates that $S_4O_6^{2-}$ is reduced to HS^- step-wise with $S_2O_3^{2-}$ as an intermediate. Cells respiring $S_4O_6^{2-}$ with lactate as electron donor were unable to reduce the produced

$S_2O_3^{2-}$ (Figure. 2.7A). Reasons for this finding are not clear, but may be due to repression of the Psr system by residual (1 mM) $S_4O_6^{2-}$ remaining in the system. A similar growth pattern was recently reported for cytochrome *c* maturation (*ccmB*) mutants of *S. putrefaciens* 200 that are unable to reduce NO_2^- but retain NO_3^- reduction activity (11). *S. putrefaciens* CCMB1 (mutant with an in-frame deletion of *ccmB*) mutant stoichiometrically converts NO_3^- to NO_2^-, but is unable to respire the produced NO_2^- and growth halts.

$S_4O_6^{2-}$-respiring bacteria generally contain the three-gene cluster *ttrBAC*, in which *ttrA* encodes the major subunit (TtrA) of typical $S_4O_6^{2-}$ terminal reductases. TtrA contains ferredoxin and MGD binding motifs, similar to the polysulfide (thiosulfate) reductases PhsA and PsrA (23). The ability of PSRA1 to respire $S_4O_6^{2-}$ indicates that PsrA does not function as the $S_4O_6^{2-}$ reductase in *S. oneidensis*. Interestingly, the genomes of other $S_4O_6^{2-}$-respiring members of the genus *Shewanella* contain the traditional *ttrBAC* gene cluster, while *S. oneidensis* does not (21). A possible candidate for $S_4O_6^{2-}$ reductase in *S. oneidensis* is an atypical octaheme *c*-type cytochrome (SO4144) that displays $S_4O_6^{2-}$, NO_2^-, and NH_2OH reduction activities *in vitro* (4, 42). The physiological role of SO4144 *in vivo* remains to be examined.

Results of the present study indicate that pKO2.0 is an effective suicide vector for generating markerless, in-frame gene deletions in *S. oneidensis* MR-1. The vector is also suitable for generating "knock-in" complements of the deletion mutants, thereby avoiding problems associated with genetic complementation *in trans*. The results also indicate that PsrA is required for *S. oneidensis* to respire anaerobically on either S^0 or $S_2O_3^{2-}$ as electron acceptor, most likely functioning as the $S_2O_3^{2-}$ terminal reductase. The large

clearing zone observed in the periphery of wild-type *S. oneidensis* colonies incubated anaerobically on solid medium amended with S^0 corroborates previous findings that direct contact is not required for S^0 respiration by *S. oneidensis* (41). *S. oneidensis* may therefore respire S^0 via an intraspecies sulfur cycle catalyzed by extracellular, abiotic (purely chemical) interactions between S^0 and either HS^- or SO_3^{2-} produced during anaerobic S^0 respiration. Results of the present study are unable to differentiate between the HS^- and SO_3^{2-}-catalyzed pathways. One potential strategy for differentiating between the HS^- and SO_3^{2-}cycling pathways is to construct of SO_3^{2-} reductase deletion mutants. An increase in the diameter of clearing zones in the periphery of SO_3^{2-} reductase deletion mutants incubated anaerobically on S^0-amended solid growth medium is an indication that SO_3^{2-} contributes to S^0 mobilization in *S. typhimurium* (24) (produced SO_3^{2-} is not reduced and is therefore more readily available to interact with extracellular S^0 resulting in a larger clearing zone). This experimental strategy is not currently possible in *S. oneidensis*, however, since a genome-wide scan indicated that genes encoding traditional dissimilatory SO_3^{2-} terminal reductases (DsrA or AsrA) are missing from the *S. oneidensis* genome. Current work is focused on identifying the novel SO_3^{2-} reductase in *S. oneidensis* and examination of the S^0 reduction activity of the corresponding SO_3^{2-} reductase deletion mutants.

REFERENCES

1. Adams, M.W., Biochemical diversity among sulfur-dependent, hyperthermophilic microorganisms. FEMS Microbiol Rev, 1994. **15**(2-3): p. 261-77.

2. Alexeyev, M.F., The pKNOCK series of broad-host-range mobilizable suicide vectors for gene knockout and targeted DNA insertion into the chromosome of Gram-negative bacteria. Biotechniques, 1999. **26**(5): p. 824-825.

3. Altschul, S.F., et al., Gapped BLAST and PSI-BLAST: a new generation of protein database search programs. Nucleic Acids Res, 1997. **25**(17): p. 3389-3402.

4. Atkinson, S.J., et al., An octaheme c-type cytochrome from *Shewanella oneidensis* can reduce nitrite and hydroxylamine. FEBS Lett, 2007. **581**(20): p. 3805-3808.

5. Baar, C., et al., Complete genome sequence and analysis of *Wolinella succinogenes*. Proc Natl Acad Sci USA, 2003. **100**(20): p. 11690-11695.

6. Biebl, H. and N. Pfennig, Growth of sulfate-reducing bacteria with sulfur as electron acceptor. Arch Microbiol, 1977. **112**(1): p. 115-117.

7. Bordi, C., et al., Effects of ISSo2 insertions in structural and regulatory genes of the trimethylamine oxide reductase of *Shewanella oneidensis*. J Bacteriol, 2003. **185**(6): p. 2042-2045.

8. Burnes, B.S., M.J. Mulberry, and T.J. DiChristina, Design and application of two rapid screening techniques for isolation of Mn(IV) reduction-deficient mutants of *Shewanella putrefaciens*. Appl Environ Microbiol, 1998. **64**(7): p. 2716-2720.

9. Caccavo, F., Jr., et al., *Geobacter sulfurreducens* sp. nov., a hydrogen- and acetate-oxidizing dissimilatory metal-reducing microorganism. Appl Environ Microbiol, 1994. **60**(10): p. 3752-3759.

10. Clark, M.A. and E.L. Barrett, The *phs* gene and hydrogen sulfide production by *Salmonella typhimurium*. J Bacteriol, 1987. **169**(6): p. 2391-2397.

11. Dale, J.R., R. Wade, Jr., and T.J. DiChristina, A conserved histidine in cytochrome *c* maturation permease CcmB of *Shewanella putrefaciens* is required for anaerobic growth below a threshold standard redox potential. J Bacteriol, 2007. **189**(3): p. 1036-1043.

12. Dehio, C. and M. Meyer, Maintenance of broad-host-range incompatibility group P and group Q plasmids and transposition of Tn5 in *Bartonella henselae*

following conjugal plasmid transfer from *Escherichia coli.* J Bacteriol, 1997. **179**(2): p. 538-540.

13. DiChristina, T.J. and E.F. Delong, Isolation of anaerobic respiratory mutants of *Shewanella putrefaciens* and genetic analysis of mutants deficient in anaerobic growth on Fe^{3+}. J Bacteriol, 1994. **176**(5): p. 1468-1474.

14. DiChristina, T.J., J.K. Fredrickson, and J.M. Zachara, Enzymology of electron transport: Energy generation with geochemical consequences. Reviews in Mineralogy and Geochemistry, 2005. **59**: p. 27-52.

15. Dietrich, V. and O. Klimmek, The function of methyl-menaquinone-6 and polysulfide reductase membrane anchor (PsrC) in polysulfide respiration of *Wolinella succinogenes.* Eur J Biochem, 2002. **269**(4): p. 1086-1095.

16. Donnenberg, M.S. and J.B. Kaper, Construction of an Eae deletion mutant of enteropathogenic *Escherichia coli* by using a positive-selection suicide vector. Infect Immun, 1991. **59**(12): p. 4310-4317.

17. Fong, C.L., et al., Cloning of the *phs* genetic locus from *Salmonella typhimurium* and a role for a *phs* product in its own induction. J Bacteriol, 1993. **175**(19): p. 6368-6371.

18. Gao, W.M., et al., Knock-out of SO1377 gene, which encodes the member of a conserved hypothetical bacterial protein family COG2268, results in alteration of iron metabolism, increased spontaneous mutation and hydrogen peroxide sensitivity in *Shewanella oneidensis* MR-1. BMC Genomics, 2006. **7**: p. 76.

19. Gay, P., et al., Positive selection procedure for entrapment of insertion-sequence elements in gram-negative bacteria. J Bacteriol, 1985. **164**(2): p. 918-921.

20. Hedderich, R., et al., Anaerobic respiration with elemental sulfur and with disulfides. FEMS Micro. Rev., 1998. **22**(5): p. 353-381.

21. Heidelberg, J.F., et al., Genome sequence of the dissimilatory metal ion-reducing bacterium *Shewanella oneidensis.* Nat Biotechnol, 2002. **20**(11): p. 1118-1123.

22. Heinzinger, N.K., et al., Sequence analysis of the *phs* operon in *Salmonella typhimurium* and the contribution of thiosulfate reduction to anaerobic energy metabolism. J Bacteriol, 1995. **177**(10): p. 2813-2820.

23. Hensel, M., et al., The genetic basis of tetrathionate respiration in *Salmonella typhimurium.* Mol Microbiol, 1999. **32**(2): p. 275-287.

24. Hinsley, A.P. and B.C. Berks, Specificity of respiratory pathways involved in the reduction of sulfur compounds by *Salmonella enterica.* Microbiology, 2002. **148**(11): p. 3631-3638.

25. Ho, S.N., et al., Site-directed mutagenesis by overlap extension using the polymerase chain reaction. Gene, 1989. **77**(1): p. 51-59.

26. Jackson, B.E. and M.J. McInerney, Thiosulfate disproportionation by *Desulfotomaculum thermobenzoicum*. Appl Environ Microbiol, 2000. **66**(8): p. 3650-3653.

27. Jormakka, M., et al., Molecular mechanism of energy conservation in polysulfide respiration. Nat Struct Mol Biol, 2008. **15**(7): p. 730-737.

28. Kelly, D.P. and A.P. Wood, Synthesis and determination of thiosulfate and polythionates. Inorganic Microbial Sulfur Metabolism, 1994. **243**: p. 475-501.

29. Kertesz, M.A., Riding the sulfur cycle - metabolism of sulfonates and sulfate esters in Gram-negative bacteria. FEMS Micro Rev, 2000. **24**(2): p. 135-175.

30. Kostka, J.E., G.W. Luther, and K.H. Nealson, Chemical and biological reduction of Mn(III)-pyrophosphate complexes - Potential importance of dissolved Mn(III) as an environmental oxidant. Geochimica Et Cosmochimica Acta, 1995. **59**(5): p. 885-894.

31. Kovach, M.E., et al., pBBR1MCS - a broad-host-range cloning vector. Biotechniques, 1994. **16**(5): p. 800.

32. Krafft, T., R. Gross, and A. Kroger, The function of *Wolinella succinogenes psr* genes in electron transport with polysulphide as the terminal electron acceptor. Eur J Biochem, 1995. **230**(2): p. 601-606.

33. Larkin, M.A., et al., ClustalW and ClustalX version 2. Bioinformatics, 2007. **23**(21): p. 2947-2948.

34. Lovley, D.R., D.E. Holmes, and K.P. Nevin, Dissimilatory Fe(III) and Mn(IV) reduction. Adv Microb Physiol, 2004. **49**: p. 219-286.

35. Lovley, D.R. and E.J. Phillips, Novel mode of microbial energy metabolism: organic carbon oxidation coupled to dissimilatory reduction of Iron or Manganese. Appl Environ Microbiol, 1988. **54**(6): p. 1472-1480.

36. Lovley, D.R., et al., Fe(III) and S^0 reduction by *Pelobacter carbinolicus*. Appl Environ Microbiol, 1995. **61**(6): p. 2132-2138.

37. Macy, J.M., et al., Growth of *Wolinella succinogenes* on H2S plus fumarate and on formate Plus sulfur as energy sources. Arch Microbiol, 1986. **144**(2): p. 147-150.

38. McClelland, M., et al., Complete genome sequence of *Salmonella enterica* serovar typhimurium LT2. Nature, 2001. **413**(6858): p. 852-856.

39. Miroshnichenko, M.L., et al., Biodiversity of thermophilic sulfur-reducing bacteria: New substrates and new habitats. Microbiology, 1998. **67**(5): p. 563-568.

40. Montgomery, H. and J. Dymock, The determination of nitrite in water. Analyst (London), 1961. **86**: p. 414-416.

41. Moser, D.P. and K.H. Nealson, Growth of the facultative anaerobe *Shewanella putrefaciens* by elemental sulfur reduction. Appl Environ Microbiol, 1996. **62**(6): p. 2100-2105.

42. Mowat, C.G., et al., Octaheme tetrathionate reductase is a respiratory enzyme with novel heme ligation. Nat Struct Mol Biol, 2004. **11**(10): p. 1023-1024.

43. Myers, C.R. and J.M. Myers, Role of menaquinone in the reduction of fumarate, nitrate, Iron(III) and Manganese(IV) by *Shewanella putrefaciens* MR-1. FEMS Microbiol Lett, 1993. **114**(2): p. 215-222.

44. Myers, C.R. and K.H. Nealson, Bacterial Manganese reduction and growth with Manganese oxide as the sole electron acceptor. Science, 1988. **240**(4857): p. 1319-1321.

45. Oren, A. and M. Shilo, Anaerobic heterotrophic dark metabolism in the Cyanobacterium *Oscillatoria limnetica* - Sulfur respiration and lactate fermentation. Arch Microbiol, 1979. **122**(1): p. 77-84.

46. Payne, A.N. and T.J. DiChristina, A rapid mutant screening technique for detection of technetium [Tc(VII)] reduction-deficient mutants of *Shewanella oneidensis* MR-1. FEMS Microbiol Lett, 2006. **259**(2): p. 282-287.

47. Perry, K.A., et al., Mediation of Sulfur Speciation by a Black-Sea facultative anaerobe. Science, 1993. **259**(5096): p. 801-803.

48. Quandt, J. and M.F. Hynes, Versatile suicide vectors which allow direct selection for gene replacement in gram-negative bacteria. Gene, 1993. **127**(1): p. 15-21.

49. Ringel, M., et al., Growth of *Wolinella succinogenes* with elemental sulfur in the absence of polysulfide. Arch Microbiol, 1996. **165**(1): p. 62-64.

50. Saffarini, D.A., et al., Anaerobic respiration of *Shewanella putrefaciens* requires both chromosomal and plasmid-borne genes. FEMS Microbiol Lett, 1994. **119**(3): p. 271-277.

51. Schauder, R. and A. Kroger, Bacterial Sulfur Respiration. Arch Microbiol, 1993. **159**(6): p. 491-497.

52. Schauder, R. and E. Muller, Polysulfide as a possible substrate for Sulfur-reducing bacteria. Arch Microbiol, 1993. **160**(5): p. 377-382.

53. Schut, G.J., S.L. Bridger, and M.W. Adams, Insights into the metabolism of elemental sulfur by the hyperthermophilic archaeon *Pyrococcus furiosus*: characterization of a coenzyme A- dependent NAD(P)H sulfur oxidoreductase. J Bacteriol, 2007. **189**(12): p. 4431-4441.

54. Stookey, L.L., Ferrozine - a new spectrophotometric reagent for Iron. Anal Chem, 1970. **42**(7): p. 779-781.

55. Taillefert, M., et al., *Shewanella putrefaciens* produces an Fe(III)-solubilizing organic ligand during anaerobic respiration on insoluble Fe(III) oxides. Journal of Inorganic Biochemistry, 2007. **101**(11-12): p. 1760-1767.

56. Taratus, E.M., S.G. Eubanks, and T.J. DiChristina, Design and application of a rapid screening technique for isolation of selenite reduction-deficient mutants of Shewanella putrefaciens. Microbiol Res, 2000. **155**(2): p. 79-85.

57. Venkateswaran, K., et al., Polyphasic taxonomy of the genus *Shewanella* and description of *Shewanella oneidensis* sp. nov. Int J Syst Evol Microbiol, 1999. **49**: p. 705-724.

58. Wall, J.D. and L.R. Krumholz, Uranium reduction. Annu Rev Microbiol, 2006. **60**: p. 149-166.

59. Zhang, M.N., et al., Dissolution morphology of Iron (oxy)(hydr)oxides exposed to the dissimilatory Iron-reducing bacterium *Shewanella oneidensis* MR-1. Geomicrobiol J, 2009. **26**(2): p. 83-92.

CHAPTER 3

OUTER MEMBRANE-ASSOCIATED SERINE PROTEASE INVOLVED IN ADHESION OF *SHEWANELLA ONEIDENSIS* MR-1 TO FE(III) OXIDES

Abstract

The facultative anaerobe *Shewanella oneidensis* MR-1 respires a variety of anaerobic electron acceptors, including insoluble Fe(III) oxides. *S. oneidensis* employs a number of novel strategies for respiration of insoluble Fe(III) oxides, including localization of respiratory proteins to the cell outer membrane (OM). The molecular mechanism by which *S. oneidensis* adheres to and respires Fe(III) oxides, however, remains poorly understood. In the present study, whole cell fractionation and MALDI-TOF-MS/MS techniques were combined to identify a serine protease (SO3800) associated with the *S. oneidensis* OM. SO3800 contained predicted structural motifs similar to cell surface-associated serine proteases that function as bacterial adhesins in other gram-negative bacteria. The gene encoding SO3800 was deleted from the *S. oneidensis* genome and the resulting mutant strain (ΔSO3800) was tested for its ability to adhere to and respire Fe(III) oxides. ΔSO3800 was severely impaired in its ability to adhere to Fe(III)-oxides, yet retained wild-type Fe(III) respiratory capability. Laser Doppler velocimetry and cryoetch-High Resolution-SEM experiments indicated that ΔSO3800 displayed a lower cell surface charge and a higher amount of surface-associated exopolysaccharides. Results of this study indicate that *S. oneidensis* may

respire insoluble Fe(III) oxides at a distance, negating the requirement for attachment prior to electron transfer.

Introduction

Microbial Fe(III) respiration is central to a wide variety of environmentally significant processes, including the biogeochemical cycling of carbon and metals, the degradation of natural and contaminant organic matter, the weathering of clays and minerals, the biomineralization of minerals such as magnetite, and the reductive precipitation (immobilization) of toxic metals and radionuclides (11, 26). Fe(III)-respiring bacteria are ubiquitous in nature and may be found in marine, freshwater and terrestrial environments, including metal- and radionuclide-contaminated subsurface aquifers (16, 26). Fe(III)-respiring bacteria are also deeply rooted and scattered throughout the domains *Bacteria* and *Archaea* (possibly indicating an ancient metabolic process) and include hyperthermophiles, psychrophiles, acidophiles and extreme barophiles (26). Despite their potential environmental and evolutionary significance, the molecular mechanism of microbial Fe(III) respiration remains poorly understood

The γ-proteobacterium *Shewanella oneidensis* MR-1 is a facultative anaerobe that displays remarkable respiratory versatility. *S. oneidensis* respires a variety of terminal electron acceptors during anaerobic respiration, including soluble and insoluble forms of the transition metals Fe(III) and Mn(IV) (3, 11, 26). *S. oneidensis* couples metal reduction to the oxidation of hydrogen and organic carbon and thus impacts the biogeochemical cycling of carbon and metals in redox-stratified aqueous environments. Fe(III)-respiring bacteria are presented with a unique physiological problem: Fe(III) exists as highly crystalline (oxy)hydroxides at circumneutral pH, rendering them

inaccessible to traditional respiratory enzymes located in the inner membrane (IM) or periplasmic space. To overcome this physiological problem, *S. oneidensis* is postulated to employ a number of novel respiratory strategies, including: 1) localization of proteins to the cell surface where they may directly contact and deliver electrons to insoluble Fe(III) oxides (2, 12, 30, 45); 2) non-reductive dissolution of insoluble Fe(III)oxides to soluble Fe(III) forms that are taken up and reduced by IM or periplasmic Fe(III) reductases (42); and 3) delivery of electrons to extracellular, insoluble Fe(III) oxides via electron shuttling pathways (8, 31, 33, 44).

Several recent studies have provided genetic evidence supporting the view that metal-respiring *Shewanella* localize terminal Fe(III) reductases to their cell surface via type II protein secretion-mediated pathways (12, 38). Type II protein secretion-deficient mutants are unable to respire Fe(III) oxides, and the cell surface proteins missing from type II protein secretion-deficient mutants include the Fe(III)-reducing, decaheme *c*-type cytochrome MtrC. Antibody recognition force microscopy has demonstrated that MtrC is exposed on the *S. oneidensis* cell surface(30), and phage display and molecular dynamics simulation modeling has indicated that MtrC contains a putative Fe(III)-binding motif, an indication that *S. oneidensis*-Fe(III) oxide attachment may be facilitated by cell surface-exposed MtrC (28). The ability of *mtrC*-deficient mutant strains to adhere to insoluble Fe(III) oxides has yet to be examined.

A second potential mechanism for bacterial adhesion to insoluble Fe(III) oxides involves interaction with Fe(III)-specific, OM-associated adhesins. A major group of bacterial adhesins is found in the subtilisin-like, serine protease (subtilase) superfamily of proteins. Serine proteases display limited overall sequence similarity and are found

scattered throughout both the prokaryotic and eukaryotic domains (47). Prokaryotic serine proteases containing a signal peptide for translocation are generally secreted (or in some cases, autotransported via Type V protein secretion) outside the cell where they can remain attached to the cell surface and carry out a myriad of functions, including foreign protein degradation for amino acid uptake, degradation of eukaryotic host cell enzyme inhibitors, maturation of cell surface proteins and toxins, and adhesion to solid surfaces (40). Bacterial adhesins identified as serine protease autotransporters from enteric bacteria (SPATEs), for example, are autotransported to the OM where their N-terminal passenger domain extends outside the cell and attaches to host cells as a first step in pathogenesis (47). Autotransporting serine proteases identified in non-enteric bacteria include *Bordatella pertussis* BrkA, a serum resistance protein which facilitates attachment to epithelial cells in the human throat, (35) and an OM protease of *Treponema denticola* that adheres to hydroxyapatite during colonization of teeth in the human oral cavity (13). Bacterial adhesion to solid surfaces may also be mediated by electrostatic interaction between negatively charged functional groups on the cell surface and positively charged functional groups on the solid surface (e.g., Fe(III) oxides) (15). The electrostatic charge of bacterial cell surfaces is similar for a wide range of both gram-positive and gram-negative bacteria (46).

The main objectives of the present study were to 1) identify subtilisin-like, serine proteases associated with the cell surface protein fraction of *S. oneidensis*, 2) generate in-frame deletions of the corresponding serine protease-encoding genes, and 3) test the resulting serine protease-deficient mutants for cell surface charge, exopolysaccharide production, and adhesion to and respiration of insoluble Fe(III) oxides.

Materials and Methods

Bacterial strains and growth conditions. For genetic manipulations, *S. oneidensis* MR-1 was cultured at 30°C in Luria Bertani medium (10 g L^{-1} NaCl, 5 g L^{-1} yeast extract, 10 g L^{-1} tryptone). For anaerobic growth experiments, cells were cultured in a defined salts medium (SM) (10) supplemented with lactate (18 mM) or formate (30 mM) as carbon/energy source. Anaerobic growth experiments were carried out in 13 mL Hungate tubes (Bellco Glass, Inc) filled with 10 mL of SM and sealed with black butyl rubber stoppers under an N_2 atmosphere. Electron acceptors were added from filter-sterilized stocks (synthesized as described previously (10, 37): O_2 (atmospheric); NO_3^-, 10 mM; Fe(III) citrate, 50 mM; hydrous ferric oxide (HFO), Mn(III)-pyrophosphate, 10 mM; 40 mM; trimethylamine-*N*-oxide (TMAO), 25 mM; $S_2O_3^{2-}$, 10 mM; $S_4O_6^{2-}$, 2 mM; fumarate, 30 mM; dimethylsulfoxide (DMSO), 25 mM; and S^0, 20 mM. When required, gentamycin (Gm) was supplemented at 15 μg mL^{-1}. For growth of *Escherichia coli* β2155 λ pir (4), diaminopimelate (DAP) was supplemented at 100 μg mL^{-1}.

Analytical Techniques. Cell growth was monitored by direct cell counts via epifluorescence microscopy and by measuring terminal electron acceptor depletion or end product accumulation. Acridine orange-stained cells were counted (Carl Zeiss AxioImager Z1 Microscope) according to previously described procedures (27). Cell numbers at each time point were calculated as the average of 10 counts from two parallel yet independent anaerobic incubations. NO_2^- was measured spectrophotometrically with sulfanilic acid-*N*-1-naphthyl-ethylene-diamine dihydrochloride solution (32). Fe(III) reduction was monitored by measuring Fe(II) production with the ferrozine technique

(41). Mn(III)-pyrophosphate concentration was measured colorimetrically as previously described (23). $S_2O_3^{2-}$ and $S_4O_6^{2-}$ concentrations were measured by cyanolysis as previously described (21). Growth on O_2, TMAO, DMSO, and fumarate were monitored by optical density at 600 nm (OD_{600}). Control experiments consisted of incubations with cells that were heat-killed at 80°C for 30 minutes prior to inoculation.

Isolation, identification, and amino acid sequence analysis of SO3800. Wild-type *S. oneidensis* MR-1 cells were cultivated and harvested as previously described (12). Cells were cultivated to late exponential growth phase and peripherally attached proteins were released using a KCl wash buffer (0.5 M KCl, 100 mM Tris-HCl, 1 mM EDTA). Peripheral proteins were concentrated using ultrafiltration. Concentrated protein samples were normalized for protein content (for wild type and mutant strains) and separated electrophoretically according to standard techniques (24) using 8-16% linear gradient Tris-HCl polyacrylamide gels (Bio-Rad) In-gel zymogram assays for protease detection were carried out in a similar fashion with the exception that 10% gels containing casein replaced linear gradient Tris-HCl gels. Zymogram assays were performed according to the manufacturers instructions.

Protein bands were excised from SDS-PAGE gels and identified by peptide mass fingerprinting and MALDI-TOF MS/MS analyses. Samples were reduced (20 mM tributylphosphine), alkylated (40 mM iodoacetamide) and digested in-gel with trypsin (Sigma-Aldrich, St. Louis, MO). Tryptic fragments were analyzed by an AB4700 Proteomic Analyzer (Applied Biosystems) operated in reflector mode. Spectra were analyzed using GPS explorer software (Applied Biosystems) and the MASCOT™ database (Matrix Science Inc., Boston, MA) Proteins displaying sequence similarity to

SO3800 were identified using blastp available at the National Center for Biotechnology Information (NCBI) (1). Conserved protein domains were identified with Pfam (http://pfam.sanger.ac.uk) (14) and Prosite (http://www.expasy.org/prosite/) (18)

In-frame gene deletion mutagenesis. The gene encoding SO3800 was deleted in-frame from the *S. oneidensis* genome as described previously (4). Briefly, regions corresponding to ~750 bp upstream and downstream of the SO3800 open reading frame were PCR-amplified with iProof ultra high-fidelity polymerase (Bio-Rad). The deletion construct was cloned into suicide vector pKO2.0 (pKOΔSO3800) and mobilized into wild-type *S. oneidensis*. Transconjugates were identified on solid medium containing Gm and confirmed via PCR. Following counterselection on solid medium containing sucrose (10% w/v), a single mutant strain (designated ΔSO3800) containing the expected deletion was isolated and confirmed via PCR and direct DNA sequencing (University of Nevada, Reno Genomics Facility).

Bacterial cell microelectrophoresis. Bacterial cell electrophoretic mobility experiments were performed on *S. oneidensis* wild-type and ΔSO3800 mutant strains via laser Doppler velocimetry (Zetasizer 3000HS_A, Malvern Instruments Ltd., Malvern, United Kingdom). Cell mobility measurements were performed over a wide range of KCl concentrations (5 to 300 mM, pH 5.5-5.8). Prior to measurement at each ionic strength, three conductance readings were made, polarizing the electrodes at each new concentration. Zero-field measurements of cell motility in the absence of an applied electrical field were carried out and subtracted from the mobility estimates. Reported mobility estimates and associated standard errors resulted from a total of twelve measurements (sum of three independent measurements carried out on four separate cell

batches). Cell surface charge and electrophoretic softness were determined according to Ohshima's soft-particle theory (34).

Determination of cell-hematite attachment isotherms. *S. oneidensis* wild-type and ΔSO3800 mutant strains were cultivated overnight in LB at 30 °C. 1 mL of the culture was centrifuged (16000 × g) and washed twice in phosphate buffer (12). Strains were grown in SM with lactate and fumarate to late-logarithmic phase, centrifuged at 3000 × g for 30 min and washed and resuspended in anaerobic background electrolyte (50 mM KCl). After washing, the cell suspensions were adjusted to 1.8×10^8 cells mL^{-1} via dilution with KCl, and the pH was adjusted to pH 7 via addition of 0.1 N KOH. For adsorption isotherm experiments, wild-type and ΔSO3800 cells were added to 5 mL KCl buffer to yield desired final cell concentrations (1.8×10^8 cells mL^{-1}). Cell suspensions were incubated anaerobically (atmosphere of 90% N_2, 10% H_2) for 2 h to reach pre-determined equilibria (data not shown) in the presence and absence of hematite (2 mg mL^{-1} final concentration). Hematite stock solutions were prepared by dissolving 1 g hematite (α-Fe_2O_3) into 10 mL of anaerobic 50 mM KCl buffer (pH 7). At pre-selected time intervals, samples were taken from the hematite-cell suspensions and centrifuged at 800 × g. The resulting supernatant was centrifuged again at 800 × g. The OD_{600} of the resulting supernatants were determined to estimate the concentration of cells remaining in solution. Cell adhesion to hematite was calculated by subtracting the concentration of cells remaining in the cell suspension supplemented with hematite from an otherwise identical suspension with hematite omitted.

Visualization of cell attachment. Visualization of attached *S. oneidensis* wild-type and ΔSO3800 mutant strains was carried out in the following manner. Test substrata

of 13 mm diameter were pressed from hematite (α-Fe_2O_3) and corundum (α-Al_2O_3) powders and subsequently heated to 550 °C for 24 hours to remove organic contamination and to ensure fully oxidized surfaces. Suspensions of washed, fumarate-grown cells were diluted in 5 mM anaerobic PIPES buffer (pH = 7) to a cell density of 1×10^4 cells mL^{-1}. Adhesion assays were performed in Falcon Multiwell™ 6 well tissue culture plates: three samples of each oxide were placed in separate wells and 5 mL of the cell suspension was added under anaerobic conditions and allowed to attach for 15 min. The cells were removed and washed five times with 5 mL of sterile PIPES buffer to remove all unattached cells. Cells were then stained with 4'-6-diamidino-2-phenylindole, dihydrochloride (DAPI) and observed with an Olympus BX61 epifluorescent microscope equipped with a 60X LUMPlanFL water immersion lens (NA=0.9) and appropriate filter block. Images were captured with an Hamamatsu ORCAII-ER high-resolution digital CCD camera. Attached cells were enumerated using ImageJ (http://rsb.info.nih.gov/ij/). In separate experiments, attached cells were also counter stained with tetramethyl rhodamine isothiocyanate-conjugated *Cancavalia ensiformis* lectin-A (TRITC-ConA) to visualize any exopolysaccharides associated with cell surfaces.

Cryoetch-high resolution SEM (cryoetch-HRSEM). Overall architecture of the *S. oneidensis* wild-type and ΔSO3800 mutant cell surfaces were visualized via cryoetch-HRSEM. For low temperature sample preparation, 2.5 μL of concentrated cell pellet was pipetted onto 3 mm gold planchets (Balzers, 012 0130T) and inverted to collect the pellet mass on the droplet surface. The sample was then plunge-frozen in liquid ethane (-183.3 ^oC) and stored under liquid nitrogen (LN_2). The sample was transferred to a pre-cooled (-170 ^oC) Oxford CT-3500 cryostage, where the specimen surface was fractured with a pre-

chilled blade and washed with liquid N_2. Immediately following fracture, the stage shutters were closed and the cryostage transferred to a Denton DV-602 chromium coater, where the sample was held under a constant vacuum of 4 x 10^{-7} torr. Cryoetching was performed in the DV-602 by increasing the sample temperature from –180 ^{o}C to –105 ^{o}C using an Oxford ITC 502 temperature controller and holding the sample temperature at –105 ^{o}C for 15-17 minutes. The etched sample was sputter coated with 2 nm of chromium and transferred to the upper stage of a Topcon DS-130 FESEM. Low temperature cryoetch-HRSEM images were collected from whole-cell pellet samples. Imaging was performed at 25 kV following 30 minutes of temperature stabilization at –120 ^{o}C.

Results

Predicted structural features of SO3800. The polypeptide encoded by genomic locus SO3800 was identified via MALDI-TOF-MS/MS as a predominant protein of the peripheral protein fraction of *S. oneidensis*. Analysis of the predicted amino acid sequence of SO3800 revealed conserved Pfam and ProSite domains corresponding to subtilisin subclass serine proteases, including Peptidase S8 and S53 conserved domains (Figure. 3.1). SO3800 contained the conserved catalytic triad of amino acids (aspartate, histidine, serine; DHS) characteristic of DHS clade subtilisins, and the order of the three catalytic residues provided additional evidence that SO3800 is a member of the subtilisin clade. Protease activity was confirmed via in-gel zymogram assays, which demonstrated that SO3800 catalyzed casein degradation (Figure. 3.2). SO3800 contained predicted structural motifs similar to those found in a broad class of proteins that function as adhesins in other gram-negative bacteria, including SPATEs from *E. coli* (AIDA-1

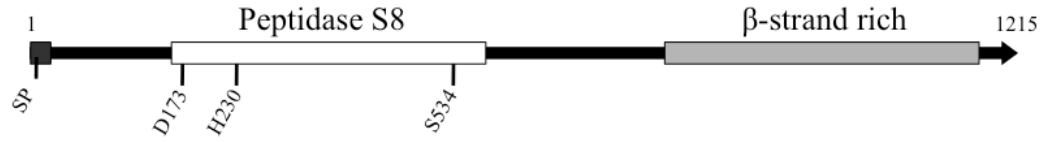

Figure 3.1. Conserved domains in SO3800. The conserved Pfam domain PF00082 is represented as a white box and contains the catalytic, active site residues D173, H230 and S534 indicative of classical S8 family serine proteases (subtilisins). The C-terminal portion of the protein contains a beta-strand rich domain that shares sequence similarity to other bacterial OM-associated adhesins.

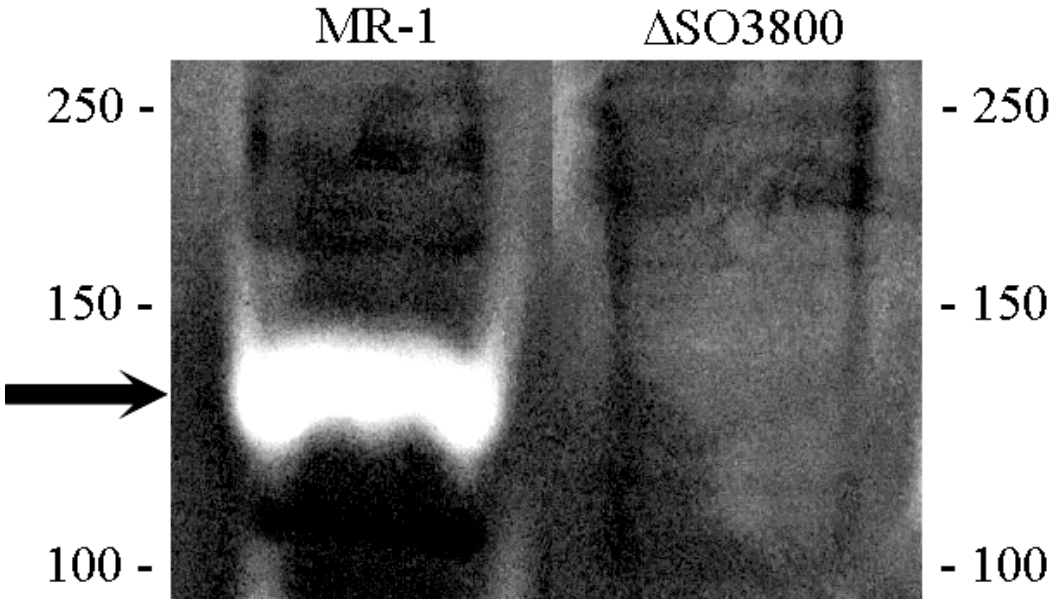

Figure 3.2. Zymogram analysis of SO3800 from the peripheral protein fraction of *S. oneidensis* MR-1. Proteins were removed from the surface of late logarithmically-grown cells, separated by electrophoretically by SDS-PAGE and stained for protease activity. The large (126 kDa) predominant band (indicated with an arrow in lane 1) was identified via MALDI-TOF-MS/MS as SO3800. The corresponding clearing zone indicative of SO3800 protease activity is missing from the peripheral protein fraction of the ΔSO3800 mutant strain (Lane 2). Molecular weight markers are indicated in kilodaltons.

adhesin-like protein; T-COFFEE score: 100) and *Y. pestis* (YadA-like adhesin; T-COFFEE score: 54), and the non-SPATE BrkA, (T-COFFEE score: 100), a *B. pertussis* serum resistance protein expressed during pathogenesis.

Anaerobic respiratory capability of *S. oneidensis* deletion mutant ΔSO3800. The gene encoding SO3800 was deleted via application of a newly constructed gene deletion system. The resulting deletion mutant ΔSO3800 was confirmed via direct DNA sequencing (data not shown). ΔSO3800 retained the ability to respire anaerobically on a suite of nine anaerobic electron acceptors, including insoluble Fe(III)-oxides, soluble Fe(III)-citrate, Mn(III)-pyrophosphate, fumarate, TMAO, DMSO, NO_3^-, and $S_2O_3^{2-}$ (Figure. 3.3).

Eletrophoretic mobility of *S. oneidensis* wild-type and Δ SO3800 mutant strains. *S. oneidensis* wild type and Δ SO3800 mutant cells displayed negative electrophoretic mobility at all KCl concentrations tested (range 5 – 250 mM) (Figure. 3.4). For fumarate-grown wild-type cells, electrophoretic mobility (μ) dropped rapidly from $-0.714 \pm 0.05 \times 10^{-8}$ m^2 V^{-1} s^{-1} (mean ± standard error of the mean) at 5 mM KCl to $-0.116 \pm 0.01 \times 10^{-8}$ m^2 V^{-1} s^{-1} at 27 mM. At ionic strengths >27 mM for which estimates were made, μ dropped less rapidly until at 80 mM, μ was not significantly different from zero. In contrast, ΔSO3800 cell mobility at 5 mM ($-0.316 \pm 0.01 \times 10^{-8}$ m^2 V^{-1} s^{-1}) was significantly reduced compared to the wild type cells. Furthermore, at ionic strengths >100 mM, Δ SO3800 cells retained an electrophoretic mobility significantly more negative than zero ($-0.089 \pm 0.01 \times 10^{-8}$ and $-0.091 \pm 0.01 \times 10^{-8}$ m^2 V^{-1} s^{-1} at 100 and 250 mM respectively).

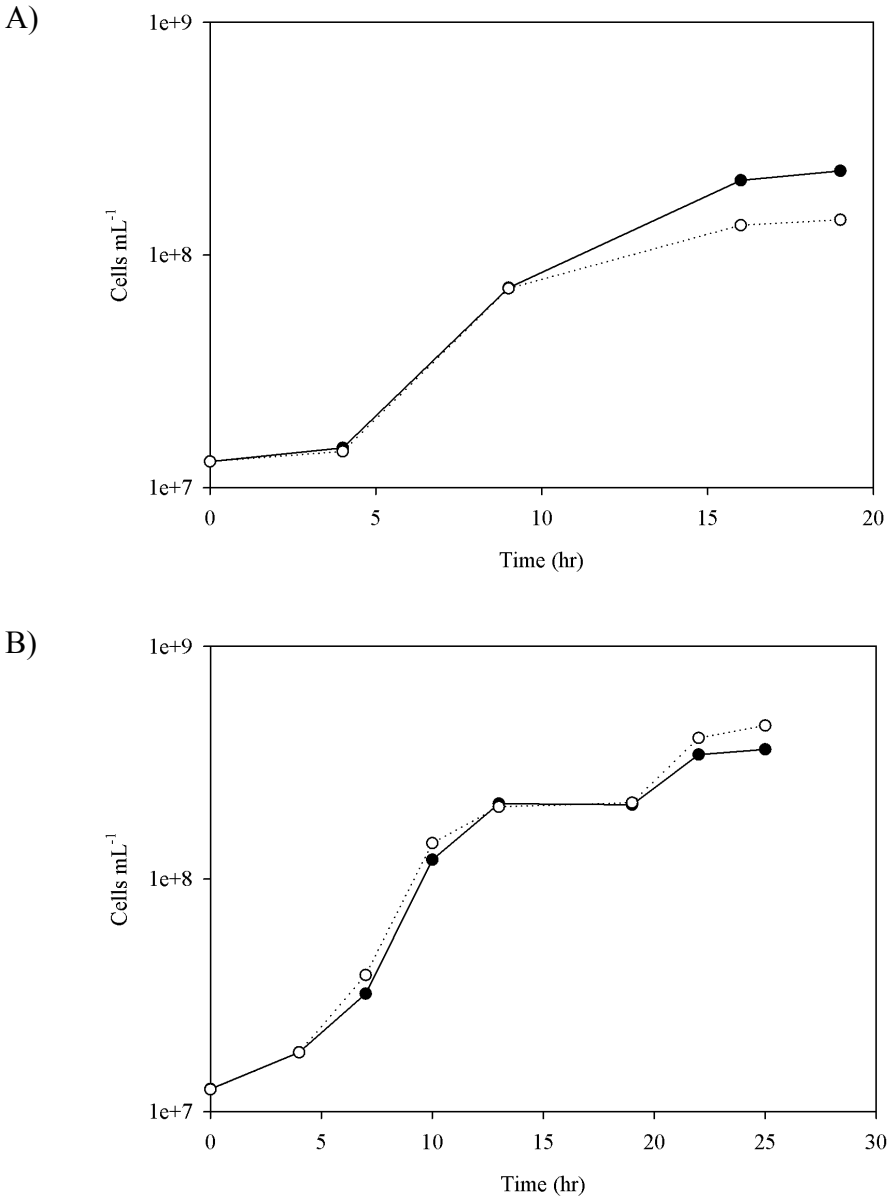

Figure 3.3. Growth on anaerobic electron acceptors. wild-type (filled circles), ΔSO3800 (open circles). A) cell density as a function of time with DMSO as electron acceptor B) cell density as a function of time with fumarate as electron acceptor. C) Mn(III) concentration as a function of time with Mn(III)-pyrophosphate as electron acceptor. D) Fe(II) concentration as a function of time with Fe(III)-citrate as electron acceptor. E) Fe(II) concentration as a function of time with HFO as electron acceptor. F) cell density as a function of time with NO_3^- as electron acceptor. G) cell density as a function of time with TMAO as electron acceptor. In some cases, error bars are smaller than the symbol.

C)

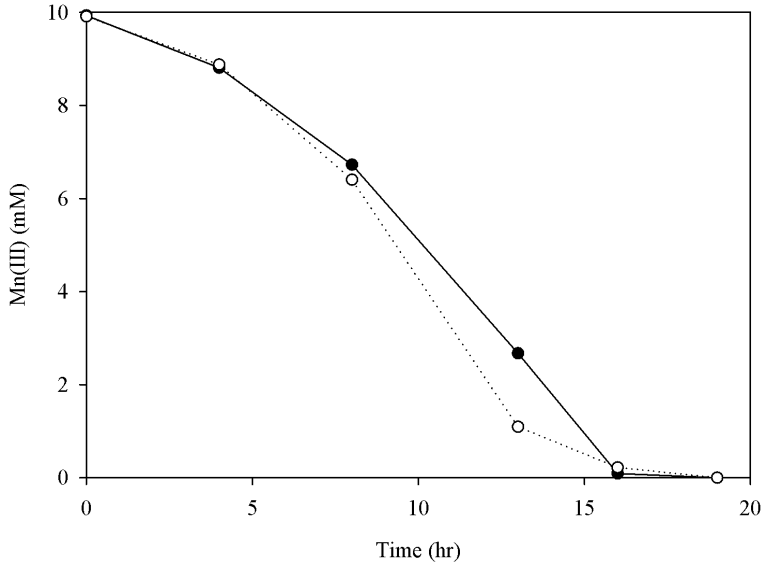

D)

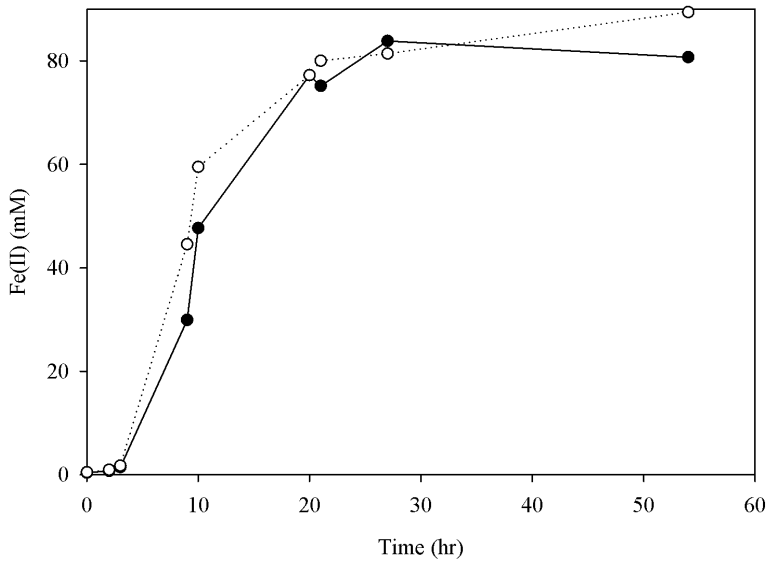

Figure 3.3 Continued

E)

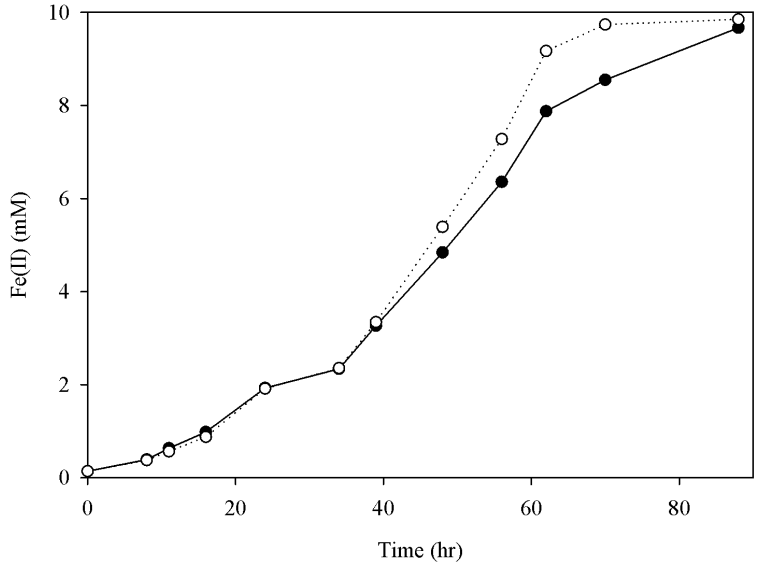

F)

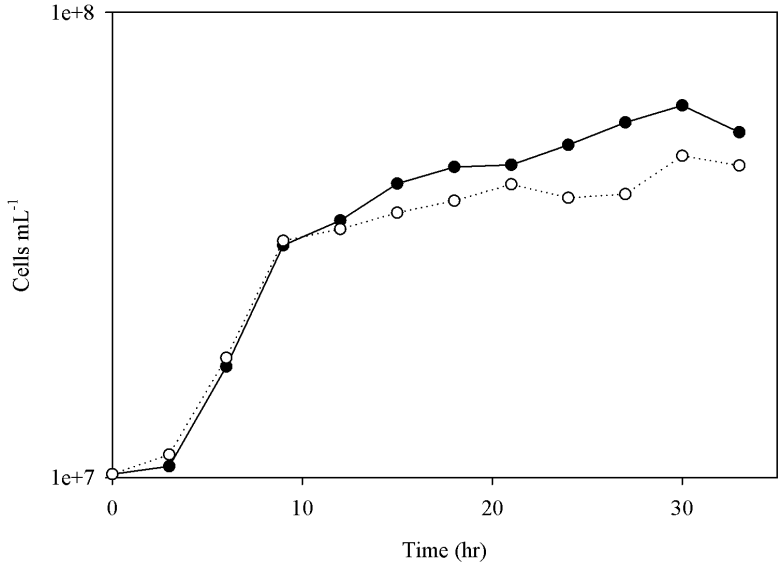

Figure 3.3 continued

G)

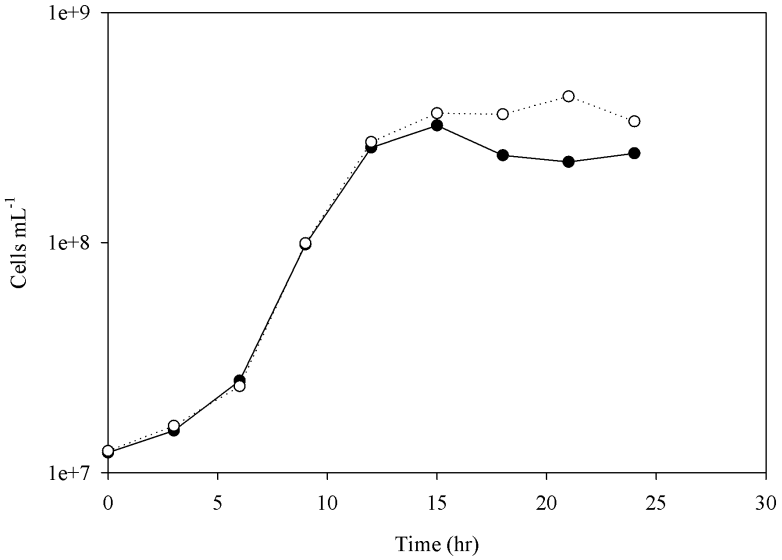

Figure 3.3 continued

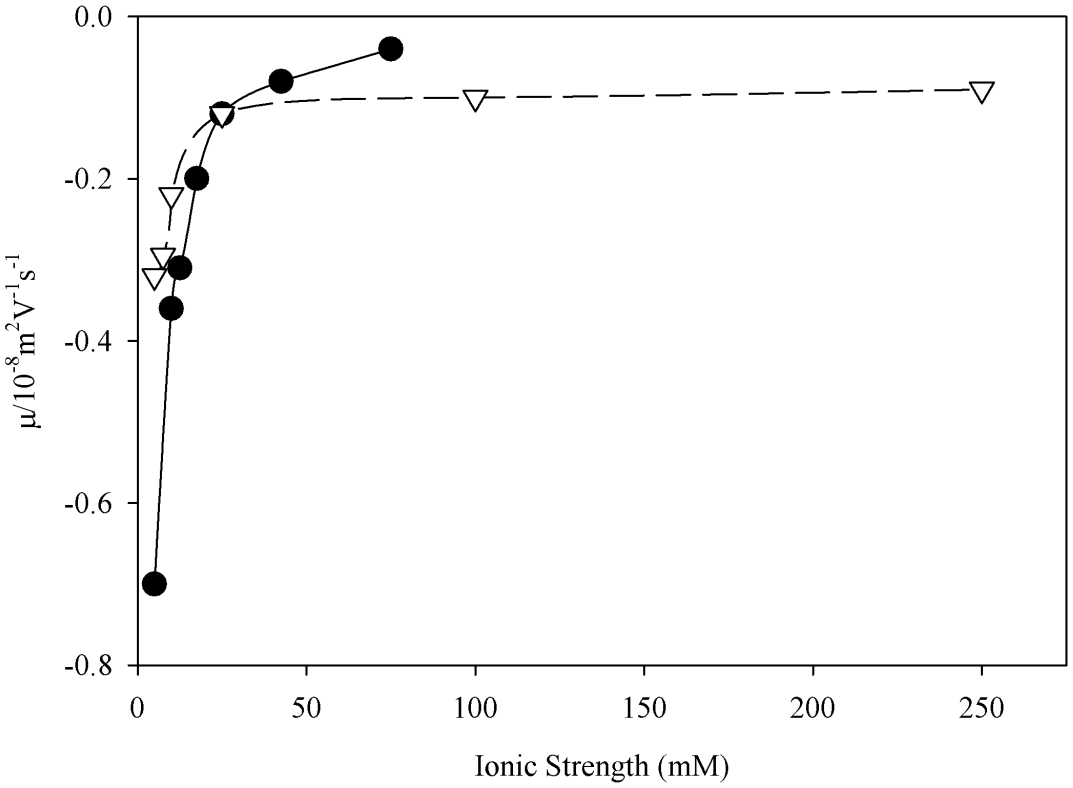

Figure 3.4. Electrophoretic mobility of fumarate-grown *S. oneidensis* MR-1 and ΔSO3800 mutant strains. Electrophoretic mobility was tested via laser Doppler velocimetry at varying ionic strengths. Δ SO3800 cells (open triangles) displayed significantly lower values than *S. oneidensis* wild-type cells (closed circles), especially at higher ionic strengths (> 100 mM).

Electrophoretic mobility estimates of the two cell sets were well-described by the soft particle theory (coefficients of determination, r^2, of 0.996, 0.972 for wild-type and ΔSO3800, respectively). Consistent with an effective μ of zero at ionic strengths above 80 mM, electrophoretic softness (λ^{-1}) estimates for wild type cells suggest a relatively hard, ion-impenetrable cell surface ($\lambda^{-1} = 0.4 \pm 0.6$ nm). The cells also display a relatively high fixed charge density (ρ_{fix}) of -8.7 ± 1.7 mM. ΔSO3800 expresses a significantly softer, more ion-penetrable surface ($\lambda^{-1} = 2.0 \pm 0.5$ nm ΔSO3800) than wild type cells. In addition, the softer cell surface of ΔSO3800 has a 5-fold lower ρ_{fix} of -1.9 ± 0.5 mM.

Adhesion of *S. oneidensis* wild-type and ΔSO3800 mutant strains to Fe(III) oxides. The ability of *S. oneidensis* wild-type and ΔSO3800 mutant strains to adhere to hematite (α-Fe_2O_3) and corundum (α-Al_2O_3) was tested. In terms of an adsorption isotherm, fumarate-grown ΔSO3800 cells adhered to hematite at levels approximately 35% of that displayed by fumarate-grown *S. oneidensis* wild-type cells. (Figure. 3.5). To confirm that ΔSO3800 was impaired in its ability to adhere to hematite, cell adhesion was quantified by direct cell counting on the surface of hematite and corundum particles. On hematite, the mean cell density observed across three parallel yet independent experiments was 1.16×10^6 cells cm^{-2} for *S. oneidensis* wild-type cells and 0.55×10^6 cells cm^{-2} for ΔSO3800 mutant cells (i.e., ΔSO3800 cell density on hematite was 37% of wild-type). For corundum the difference between means was smaller, 0.88×10^6 compared to 0.81×10^6 cells cm^{-2} for the wild type and mutant cells respectively (i.e., ΔSO3800 cell density on corundum was 92% of wild-type). Differences in adhered cell densities between replicates were ≤ 10% in all cases (data not shown). The difference in

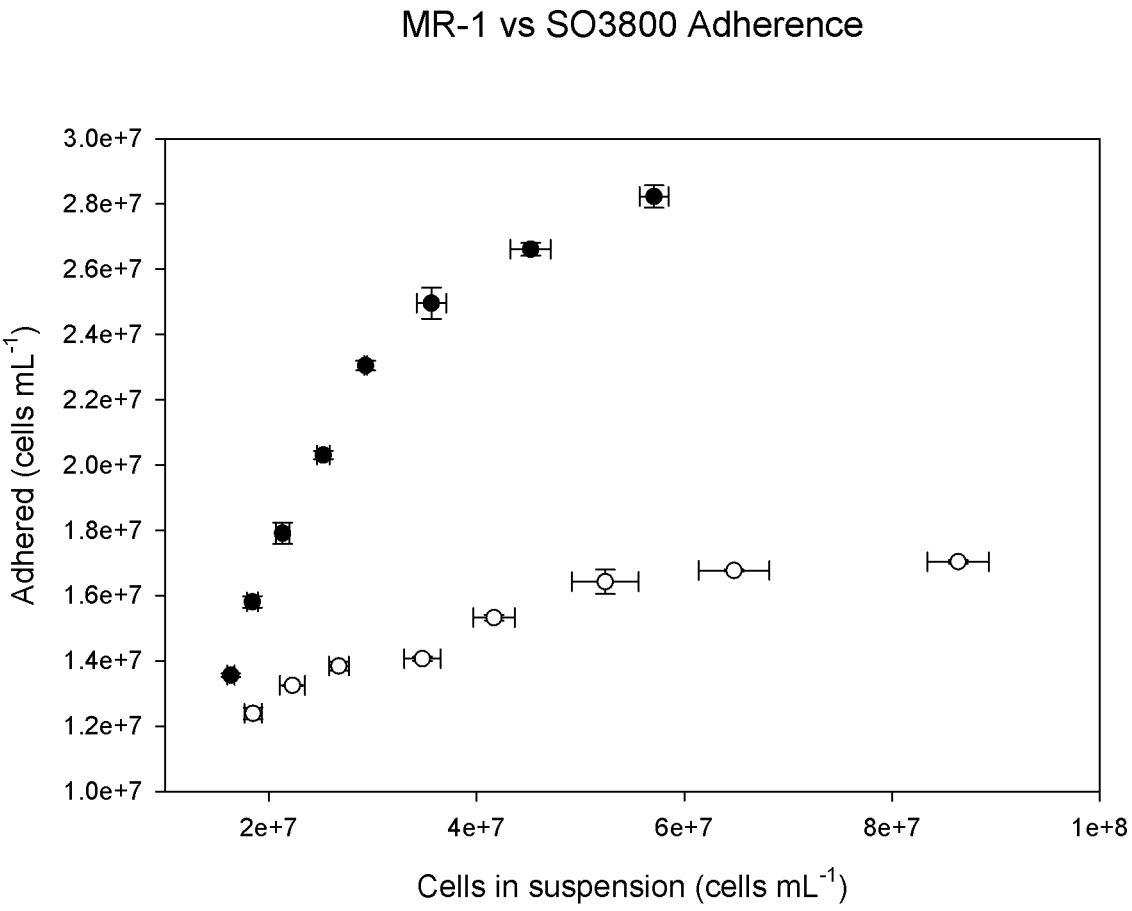

Figure 3.5. Hematite adhesion isotherms. Cell concentrations of free (x-axis) versus adhered (y-axis) cells after incubation with hematite in suspension. Symbols are the same as in Figure 3.3.

cell density between the *S. oneidensis* wild-type and ΔSO3800 mutant cells was therefore greater by approximately three-fold on the hematite surface than corundum

Detection of exopolymers on the *S. oneidensis* wild-type and ΔSO3800 mutant cell surfaces. Lectin (TRITC-ConA) staining serves as a sensitive probe for the presence of capsular exopolysaccharides on the *S. oneidensis* cell surface. Fluorescent micrographs of TRITC-ConA counter-stained, DAPI-stained cells of *S. oneidensis* wild-type and ΔSO3800 mutant strains indicated that the *S. oneidensis* wild type cell surface contains little, if any capsular exopolysaccharides, while the surface of ΔSO3800 binds significantly more TRITC-ConA stain, consistent with an increased accumulation of capsular exopolysaccharides on the ΔSO3800 cell surface (Figure. 3.6)

Cryoetch-HRSEM requires neither fixation nor dehydration of cells and thus permits visualization of cells in a fully hydrated state. Surfaces of fumarate-grown *S. oneidensis* wild-type cells are free of exopolymers (Figure. 3.7A, B), an observation confirmed at high magnification (Figure. 3.7C). The only surface-associated features observed on wild type cells are polar flagella (Figure. 3.7B); otherwise the cell surface remains largely featureless. The surfaces of ΔSO3800 cells are distinctly different than the *S. oneidensis* wild-type cells (Figure. 3.7D-F). ΔSO3800 cells displayed pilus-like structures not observed with wild-type cells, and ΔSO3800 displayed a textured cell surface compared to the smooth appearance of the *S. oneidensis* wild-type cells.

Discussion

A main pathway for Fe(III) oxide reduction by *S. oneidensis* is postulated to entail direct contact between the cell and Fe(III) oxide surfaces (11, 26). Close association of

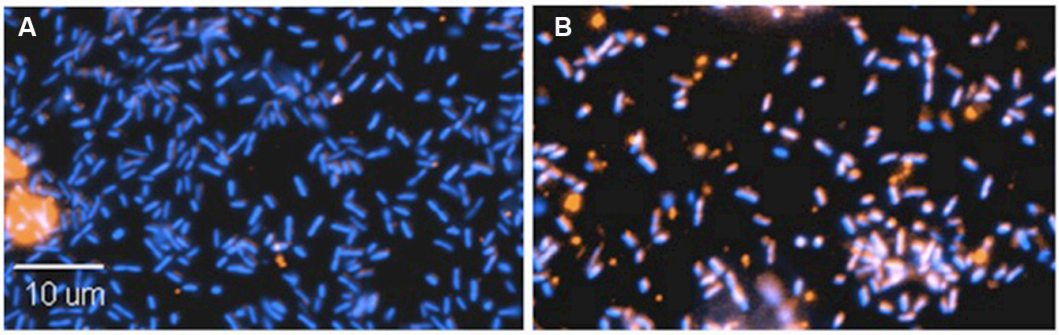

Figure 3.6. Fluorescent micrograph of *S. oneidensis* wild-type (panel A) and ΔSO3800 (panel B) cells adhered to hematite surfaces. Cells were double-stained with DAPI (blue stain) and TRITC-ConA (red stain, to visualize cell surface exopolysaccharides). The ΔSO3800 mutant strain bound significantly more TRITC-ConA stain, an indication of increased cell surface-associated exopolysaccharide.

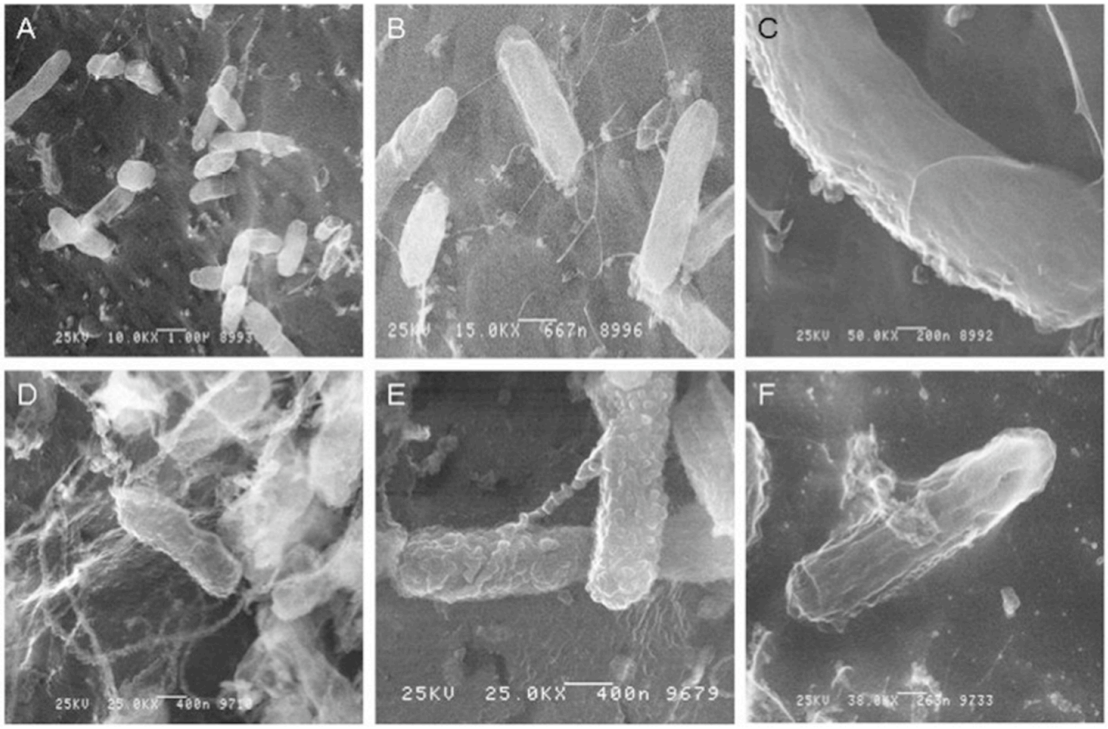

Figure 3.7. Cryoetch-HRSEM of *S. oneidensis* wild-type and ΔSO3800 cells. Fumarate-grown cells were visualized by cryoetch-HRSEM. Wild-type cells were devoid of any prominent cell surface features (A-C), while Δ SO3800 cells displayed pilus-like structures and a textured surface (D-F).

the cell and Fe(III) oxide surfaces is required to facilitate electron transfer from surface-exposed, *c*-type cytochromes MtrC and OmcA (39) . A distance of < 15 Å is required for direct electron transfer from the catalytic heme group of MtrC to hematite (22). MtrC and OmcA are also hypothesized to bind Fe(III) oxides directly (30, 45). A specific bond may be formed between MtrC or OmcA and the hematite surface (29), an adhesion strategy that may aid in electron transfer to insoluble Fe(III) oxides. A recent study based on phage display and molecular dynamics simulation modeling has predicted that a conserved amino acid sequence (Thr-Pro-Thr) found adjacent to the terminal heme group in both MtrC and OmcA may function as a hematite-binding motif (28). The mechanism by which *S. oneidensis* whole cells adhere to hematite surfaces, however, remains poorly studied. An adhesion deficient strain of *S. algae* BrY, RAD20, expressed lower levels of OM proteins and was significantly less hydrophobic than wild-type, thereby suggesting that hydrophobic OM proteins may alter the surface properties of *Shewanella* species (9). In addition, Type IV pili (43) and flagella (6) have also been implicated in attachment of bacterial cells to mineral surfaces.

S. oneidensis protein SO3800 was identified in an initial screen of potential Fe(III)-binding adhesins located in the peripheral protein fraction of *S. oneidensis*. SO3800 contained predicted structural motifs similar to serine protease-like adhesins found in other gram-negative bacteria, including the SPATES YadA of *Y. pestis* and AIDA-1 of enteropathic *E. coli* (47). SO3800 displayed proteolytic activity with casein as substrate and contained predicted structural features found in some, but not all, serine protease-like autotransporters (e.g., S8 and S53 peptidase conserved domains, β strand-rich C-terminal region and N-terminal signal peptide) (47). In-frame gene deletion

mutant ΔSO3800 was severely impaired in its ability to adhere to hematite in suspension or on pressed hematite surfaces (adhesion levels approximately 35-37% of the wild-type strain). The mechanism by which SO3800 facilitates adhesion of *S. oneidensis* to Fe(III) oxides is not well understood, but may include 1) a direct mechanism in which the overall electrostatic charge (or an Fe(III)-binding motif) of SO3800 facilitates adhesion to the hematite surface, or 2) an indirect mechanism in which SO3800 protease activity remodels the *S. oneidensis* cell surface (e.g., removes excess EPS) to facilitate binding of other proteins to hematite. SO3800 does not contain a Thr-Pro-Thr motif, an indication that a direct Fe(III)-binding motif of SO3800 will be different than that predicted for MtrC(28). Evidence supporting the indirect mechanism includes the observed decrease in cell surface charge, increase in electrophoretic softness and increase in capsular exopolysaccharide of ΔSO3800 compared to the wild-type strain. The SO3800-catalyzed removal of EPS, for example, may allow surface-exposed, MtrC and OmcA to directly adhere and transfer electrons to hematite surfaces.

ΔSO3800 cells were severely impaired in their ability to adhere to insoluble Fe(III)-oxide surfaces, yet they retained the ability to respire all anaerobic electron acceptors, including insoluble Fe(III) oxides. One interpretation of these results is that SO3800 facilitates adhesion to and respiration of insoluble Fe(III) oxides under growth conditions not used in the present study. An alternate explanation is that adhesion of *S. oneidensis* to Fe(III) oxides is not required for respiration of Fe(III) oxides at wild-type rates, an indication that electron transfer to Fe(III) oxides may proceed through indirect pathways such as Fe(III) solubilization(42) or electron shuttling reactions (11, 31, 33). In a recent study, MtrC- and OmcA-catalyzed Fe(III) oxide reduction rates measured *in*

vitro could not account for Fe(III) oxide reduction rates measured for OM fractions or whole cells of *S. oneidensis in vivo*.(36). These results were also interpreted as evidence that *S. oneidensis* respires insoluble Fe(III) oxides at a distance via indirect electron shuttling pathways, negating the requirement for adhesion prior to electron transfer.

The relative contributions of the direct contact, electron shuttling and Fe(III)-solubilizing pathways to the overall rate of microbial Fe(III) reduction in the environment are not well understood. The environmental factors dictating which strategy dominates, or if multiple pathways are used simultaneously, remain unclear. Such information is crucial to predicting the rates of biogeochemical processes that are linked to microbial Fe(III) reduction, including the reductive mobilization of insoluble metals, the reductive precipitation of contaminant radionuclides, and the oxidative degradation of natural and contaminant organic matter. In the direct contact pathway, for example, the rate of electron transfer to Fe(III) oxides may be limited by Fe(III) oxide surface area, a limitation relieved by the electron shuttling and Fe(III)-solubilizing pathways. Redox-active, electron shuttling compounds (humic acids, fulvic acids, phenazines) are found in significant concentrations in both marine and freshwater systems and may represent a dominant pathway for microbial Fe(III) reduction (7, 8, 17, 19, 20, 25, 33). Only recently has the Fe(III)-solubilizing pathway been recognized as a potential means of providing Fe(III)-respiring bacteria with a readily accessible electron acceptor (5, 42). Current work with *S. oneidensis* is focused on identifying those growth conditions that require SO3800 for Fe(III) oxide respiration, and determining the molecular mechanism by which SO3800 facilitates adhesion of *S. oneidensis* cells to Fe(III) oxide surfaces.

REFERENCES

1. Altschul, S.F., et al., Gapped BLAST and PSI-BLAST: a new generation of protein database search programs. Nucleic Acids Research, 1997. **25**(17): p. 3389-3402.

2. Beliaev, A.S., et al., MtrC, an outer membrane decahaem c cytochrome required for metal reduction in *Shewanella putrefaciens* MR-1. Molecular Microbiology, 2001. **39**(3): p. 722-30.

3. Burnes, B.S., M.J. Mulberry, and T.J. DiChristina, Design and application of two rapid screening techniques for isolation of Mn(IV) reduction-deficient mutants of *Shewanella putrefaciens*. Applied and Environmental Microbiology, 1998. **64**(7): p. 2716-2720.

4. Burns, J.L. and T.J. DiChristina, Anaerobic respiration of elemental sulfur and thiosulfate by *Shewanella oneidensis* MR-1 requires psrA, a homolog of the phsA gene of *Salmonella enterica* Serovar Typhimurium LT2. Applied and Environmental Microbiology, 2009. **75**(16): p. 5209-5217.

5. Carey, E.A. and M. Taillefert, The role of soluble Fe(III) in the cycling of iron and sulfur in coastal marine sediments. Limnology and Oceanography, 2005. **50**(4): p. 1129-1141.

6. Childers, S.E., S. Ciufo, and D.R. Lovley, *Geobacter metallireducens* accesses insoluble Fe(III) oxide by chemotaxis. Nature, 2002. **416**(6882): p. 767-769.

7. Coates, J.D. and L.A. Achenbach, Microbial perchlorate reduction: rocket-fueled metabolism. Nat Rev Microbiol, 2004. **2**(7): p. 569-80.

8. Coates, J.D., et al., Recovery of humic-reducing bacteria from a diversity of environments. Appl Environ Microbiol, 1998. **64**(4): p. 1504-9.

9. Das, A. and F. Caccavo, Jr., Dissimilatory Fe(III) oxide reduction by *Shewanella alga* BrY requires adhesion. Curr Microbiol, 2000. **40**(5): p. 344-7.

10. DiChristina, T.J. and E.F. DeLong, Isolation of anaerobic respiratory mutants of *Shewannella putrefaciens* and genetic analysis of mutants deficient in anaerobic growth on Fe3+. Journal of Bacteriology, 1994. **176**(5): p. 1468-1474.

11. DiChristina, T.J., J.K. Fredrickson, and J.M. Zachara, Enzymology of electron transport: energy generation with geochemical consequences. Reviews in Mineralogy and Geochemistry, 2005. **59**: p. 27-52.

12. DiChristina, T.J., C.M. Moore, and C.A. Haller, Dissimilatory Fe(III) and Mn(IV) reduction by *Shewanella putrefaciens* requires *ferE*, a homolog of the *pulE* (*gspE*) type II protein secretion gene. Journal of Bacteriology, 2002. **184**(1): p. 142-151.

13. Ellen, R.P., J.R. Dawson, and P.F. Yang, Treponema denticola as a model for polar adhesion and cytopathogenicity of spirochetes. Trends Microbiol, 1994. **2**(4): p. 114-9.

14. Finn, R.D., et al., The Pfam protein families database. Nucleic Acids Research, 2008. **36**: p. D281-D288.

15. Fowle, D.A. and J.B. Fein, Competitive adsorption of metal cations onto two gram positive bacteria: Testing the chemical equilibrium model. Geochimica Et Cosmochimica Acta, 1999. **63**(19-20): p. 3059-3067.

16. Hau, H.H. and J.A. Gralnick, Ecology and biotechnology of the genus *Shewanella.* Annual Review of Microbiology, 2007. **61**: p. 237-258.

17. Hernandez, M.E., A. Kappler, and D.K. Newman, Phenazines and other redox-active antibiotics promote microbial mineral reduction. Appl Environ Microbiol, 2004. **70**(2): p. 921-928.

18. Hulo, N., et al., The PROSITE database. Nucleic Acids Research, 2006. **34**: p. D227-D230.

19. Kappler, A., et al., Electron shuttling via humic acids in microbial iron(III) reduction in a freshwater sediment. Fems Microbiology Ecology, 2004. **47**(1): p. 85-92.

20. Kappler, A. and K.L. Straub, Geomicrobiological cycling of iron. Molecular Geomicrobiology, 2005. **59**: p. 85-108.

21. Kelly, D.P. and A.P. Wood, Synthesis and Determination of Thiosulfate and Polythionates. Inorganic Microbial Sulfur Metabolism, 1994. **243**: p. 475-501.

22. Kerisit, S., et al., Molecular computational investigation of electron-transfer kinetics across cytochrome-iron oxide interfaces. Journal of Physical Chemistry C, 2007. **111**(30): p. 11363-11375.

23. Kostka, J.E., G.W. Luther III, and K.H. Nealson, Chemical and biological reduction of Mn(III)-pyrophosphate complexes: Potential importance of dissolved Mn(III) as an environmental oxidant. Geochimica et Cosmochimica Acta, 1995. **59**(5): p. 885-894.

24. Laemmli, U.K., Cleavage of structural proteins during the assembly of the head of bacteriophage T4. Nature, 1970. **227**(5259): p. 680-5.

25. Lovley, D.R., et al., Humic substances as electron acceptors for microbial respiration. Nature, 1996. **382**(6590): p. 445-448.

26. Lovley, D.R., D.E. Holmes, and K.P. Nevin, Dissimilatory Fe(III) and Mn(IV) reduction. Advances in Microbial Physiology, 2004. **49**: p. 219-285.

27. Lovley, D.R. and E.J. Phillips, Novel mode of microbial energy metabolism: organic carbon oxidation coupled to dissimilatory reduction of Iron or Manganese. Appl Environ Microbiol, 1988. **54**(6): p. 1472-1480.

28. Lower, B.H., et al., In vitro evolution of a peptide with a hematite binding motif that may constitute a natural metal-oxide binding archetype. Environ Sci Technol, 2008. **42**(10): p. 3821-7.

29. Lower, B.H., et al., Specific bonds between an iron oxide surface and outer membrane cytochromes MtrC and OmcA from Shewanella oneidensis MR-1. J Bacteriol, 2007. **189**(13): p. 4944-52.

30. Lower, B.H., et al., Antibody recognition force microscopy shows that outer membrane cytochromes OmcA and MtrC are expressed on the exterior surface of *Shewanella oneidensis* MR-1. Appl Environ Microbiol, 2009. **75**(9): p. 2931-5.

31. Marsili, E., et al., *Shewanella* secretes flavins that mediate extracellular electron transfer. Proceedings of the National Academy of Sciences of the United States of America, 2008. **105**(10): p. 3968-3973.

32. Montgomery, H. and J.F. Dymock, Determination of Nitrite in Water. Analyst, 1961. **86**(102): p. 414-&.

33. Newman, D.K. and R. Kolter, A role for excreted quinones in extracellular electron transfer. Nature, 2000. **405**(6782): p. 94-97.

34. Ohshima, H., On the general expression for the electrophoretic mobility of a soft particle. Journal of Colloid and Interface Science, 2000. **228**(1): p. 190-193.

35. Oliver, D.C., et al., A conserved region within the Bordetella pertussis autotransporter BrkA is necessary for folding of its passenger domain. Mol Microbiol, 2003. **47**(5): p. 1367-83.

36. Ross, D.E., S.L. Brantley, and M. Tien, Kinetic characterization of terminal reductases OmcA and MtrC involved in respiratory electron transfer for dissimilatory iron reduction in *Shewanella oneidensis* MR-1. Appl Environ Microbiol, 2009: p. doi 10.1128/AEM.00544-09.

37. Saffarini, D.A., T.J. DiChristina, and K.H. Nealson, Anaerobic respiration by *Shewanella putrefaciens* requires both chromosomal and plasmid-borne genes. FEMS Microbiol Lett, 1994. **119**: p. 271-278.

38. Shi, L., et al., Direct involvement of type II secretion system in extracellular translocation of *Shewanella oneidensis* outer membrane cytochromes MtrC and OmcA. Journal of Bacteriology, 2008. **190**(15): p. 5512-5516.

39. Shi, L., et al., Respiration of metal (hydr)oxides by *Shewanella* and *Geobacter:* a key role for multihaem *c*-type cytochromes. Mol Microbiol, 2007. **65**(1): p. 12-20.

40. Siezen, R.J., B. Renckens, and J. Boekhorst, Evolution of prokaryotic subtilases: genome-wide analysis reveals novel subfamilies with different catalytic residues. Proteins, 2007. **67**(3): p. 681-94.

41. Stookey, L.L., Ferrozine - a new spectrophotometric reagent for iron. Analytical Chemistry, 1970. **42**(7): p. 779-781.

42. Taillefert, M., et al., *Shewanella putrefaciens* produces an Fe(III)-solubilizing ligand during anaerobic respiration on insoluble Fe(III) oxides Journal of Inorganic Biochemistry, 2007. **101**(11): p. 1760-1767.

43. Thormann, K.M., et al., Initial Phases of biofilm formation in *Shewanella oneidensis* MR-1. J Bacteriol, 2004. **186**(23): p. 8096-104.

44. Turick, C.E., L.S. Tisa, and F. Caccavo, Jr., Melanin production and use as a soluble electron shuttle for Fe(III) oxide reduction and as a terminal electron acceptor by Shewanella algae BrY. Appl Environ Microbiol, 2002. **68**(5): p. 2436-44.

45. Xiong, Y.J., et al., High-affinity binding and direct electron transfer to solid metals by the *Shewanella oneidensis* MR-1 outer membrane *c*-type cytochrome OmcA. Journal of the American Chemical Society, 2006. **128**(43): p. 13978-13979.

46. Yee, N., J.B. Fein, and C.J. Daughney, Experimental study of the pH, ionic strength, and reversibility behavior of bacteria-mineral adsorption. Geochimica Et Cosmochimica Acta, 2000. **64**(4): p. 609-617.

47. Yen, Y.T., et al., Common themes and variations in serine protease autotransporters. Trends Microbiol, 2008. **16**(8): p. 370-9.

CHAPTER 4

A CONSERVED CYSTEINE (CYS42) OF OUTER MEMBRANE PROTEIN MTRB IS REQUIRED FOR METAL RESPIRATION BY *SHEWANELLA ONEIDENSIS* MR-1

Abstract

Shewanella oneidensis MR-1 respires a variety of compounds as terminal electron acceptor for anaerobic respiration, including insoluble Fe(III) and Mn(IV) oxides. MtrB contains an N-terminal Cys-X-X-Cys motif also found in thioredoxin- and peroxidase-family proteins. An in-frame gene deletion mutant of *mtrB* was unable to respire insoluble Fe(III) or Mn(IV) oxides, yet retained wild-type respiratory ability on other electron acceptors, including nitrate, fumarate, thiosulfate trimethylamine-N-oxide and dimethylsulfoxide. Both cysteine residues were strictly conserved in all MtrB homologs found in recently sequenced *Shewanella* spp. Cys42 and Cys45 were independently changed to alanine using site-directed mutagenesis. A C42A mutant displayed a similar respiratory phenotype to that of the deletion mutant, while a C45A mutant resembled wild-type MR-1. The site-directed mutants also displayed unique outer membrane protein profiles. The C42A mutant displayed a protein profile similar to the in-frame deletion mutant while the C45A mutant displayed an aberrant outer membrane protein profile. All three MtrB mutants (null, C42A, and C45A) displayed increased cytochrome abundance in outer membrane fractions. Additionally, the C42A mutant displayed a marked decrease in *mtrB* expression as measured by QRT-PCR. These results

demonstrate that Cys42 but not Cys45 is required for Fe(III) respiration and suggest that MtrB may be involved in sensing the presence of transition metals for anaerobic respiration.

Introduction

Metal-respiring bacteria occupy a central position in a variety of environmentally important processes including the biogeochemical cycling of metals and carbon, biocorrosion of steel surfaces, bioremediation of radionuclide-contaminated aquifers, and electricity generation in microbial fuel cells (11, 13, 30). Metal-respiring bacteria are presented, however, with a unique physiological challenge: they are required to respire anaerobically on electron acceptors (e.g., Fe(III) oxides, elemental sulfur) that are highly insoluble at circumneutral pH and unable to enter the cell and contact inner membrane-localized respiratory systems. To overcome these physiological problems, metal-respiring bacteria are postulated to employ a variety of novel respiratory strategies not found in other bacteria, including 1) direct enzymatic reduction at the cell surface, 2) electron shuttling between the cell and metal surfaces, 3) metal solubilization by bacterially-produced organic ligands followed by respiration of the soluble organic-metal complexes, and 4) the use of nanowires to conduct electrons from the cell surface to solid metal oxide surfaces (14, 18, 24, 32, 55). Despite the environmental significance of microbial metal respiration, the molecular mechanism remains poorly understood.

S. oneidensis MR-1 contains a highly branched electron transport chain organized in a modular fashion. Primary dehydrogenases oxidize electron donors (e.g. lactate, formate, H_2) and transfer electrons to an inner membrane (IM)-bound quinone pool.

Reduced quinols (either ubiquinol or menaquinol) subsequently transfer electrons to an IM-bound tetraheme *c*-type cytochrome, CymA (35, 36, 40, 49-52). Quinols may also directly transfer electrons to quinol oxidase components of other respiratory terminal reductase complexes such as TorABC (trimethylamine-*N*-oxide oxidoreductase) (9) or PsrABC (thiosulfate and elemental sulfur reductase) (7). CymA functions as a central branch point in the anaerobic respiratory chain in *S. oneidensis*. CymA deletion mutants are unable to respire Fe(III), Mn(IV), Nitrate (NO_3^-), Nitrite (NO_2^-), dimethylsulfoxide (DMSO) or fumarate (36, 50, 51). For the reduction of metal oxides, CymA is postulated to transfer electrons to a series of soluble, periplasmically-localized *c*-type cytochromes including Small tetraheme cytochrome (STC), and a decaheme cytochrome MtrA. Electrons are transferred across the outer membrane (OM) via OM-associated proteins MtrB (an integral OM beta-barrel protein) and MtrC and OmcA (peripheral OM decaheme cytochromes) (3-6, 15, 20, 21, 39, 41, 42, 44, 57, 59). In vitro studies suggest that both MtrC and OmcA may directly bind and reduce Fe(III) oxides albeit with different binding constants and consequently different reduction rates (15, 48). In a recent study, MtrB is postulated to form a complex with OM cytochromes OmcA and MtrC as well as periplasmic protein MtrA to construct an "electron conduit" for electrons traversing the OM (21). The precise roles MtrB, OmcA, MtrA and MtrC play in electron transfer to metal oxides however, remain unclear.

MtrB is an OM protein strictly required for metal respiration; MtrB deletion mutants mislocalize OM cytochromes OmcA and MtrC (37). MtrB is also required for the reduction of anthraquinone-2,6-disulfonate (AQDS), a small quinonoid compound which may act as an exogenous electron shuttle (53). MtrB contains a Cys-Lys-Gly-Cys

motif in the N-terminal region of the protein and the function of these cysteine residues is currently unknown. Beta barrel proteins typically do not contain cysteine residues, as it can interfere with the structure of the integral membrane proteins (43). Proteins containing Cys-X-X-Cys motifs (where X is any amino acid) perform a wide variety of functions in both prokaryotic and eukaryotic systems. These include the refolding of mismatched disulfide bonds (Protein Disulfide Isomerase, PDI (58)), general electron carrier (Thioredoxin (17)), and components responsible for sensing oxidative stress (OxyR (60)). The main objective of the present study is to determine if the conserved N-terminal cysteines of MtrB are required for anaerobic metal respiration in *S. oneidensis* MR-1.

Materials and Methods

Bacterial Strains and cultivation conditions

For genetic manipulations, *S. oneidensis* MR-1 was cultured at 30°C in Luria Bertani medium (10 g L^{-1} NaCl, 5 g L^{-1} yeast extract, 10 g L^{-1} tryptone). For anaerobic growth experiments, cells were cultured in a defined salts medium (SM) supplemented with lactate (18 mM) or formate (30 mM) as carbon/energy source (38). Anaerobic growth experiments were carried out in 13 mL Hungate tubes (Bellco Glass, Inc) filled with 10 mL of SM and sealed with black butyl rubber stoppers under an N_2 atmosphere. Electron acceptors were added from filter-sterilized stocks (synthesized as described previously (12): O_2 (atmospheric); NO_3^-, 10 mM; Fe(III) citrate, 50 mM; hydrous ferric oxide (HFO), Mn(III)-pyrophosphate, 10 mM; 40 mM; trimethylamine-*N*-oxide (TMAO), 25 mM; $S_2O_3^{2-}$, 10 mM; $S_4O_6^{2-}$, 2 mM; fumarate, 30 mM; dimethylsulfoxide (DMSO), 25 mM; and S^0, 20 mM. When required, gentamycin (Gm) was supplemented

at 15 μg mL^{-1}. For growth of *Escherichia coli* β2155 λ pir, diaminopimelate (DAP) was supplemented at 100 μg mL^{-1} (10).

Cell growth was monitored by direct cell counts via epifluorescence microscopy and by measuring terminal electron acceptor depletion or end product accumulation. Acridine orange-stained cells were counted (Carl Zeiss AxioImager Z1 Microscope) according to previously described procedures (31). Cell numbers at each time point were calculated as the average of 10 counts from two parallel yet independent anaerobic incubations. NO_2^- was measured spectrophotometrically with sulfanilic acid-*N*-1-naphthyl-ethylene-diamine dihydrochloride solution (34). Fe(III) reduction was monitored by measuring Fe(II) production with the ferrozine technique (54). Mn(III)-pyrophosphate concentration was measured colorimetrically as previously described (28). $S_2O_3^{2-}$ and $S_4O_6^{2-}$ concentrations were measured by cyanolysis as previously described (26). Growth on O_2, TMAO, DMSO, and fumarate were monitored by optical density at 600 nm (OD_{600}). Control experiments consisted of incubations with cells that were heat-killed at 80°C for 30 minutes prior to inoculation.

Nucleotide and amino acid sequence analyses

Genome sequence data for *S. oneidensis* MR-1 (23), *S. putrefaciens* 200, *S. putrefaciens* CN32, *S. putrefaciens* W3-18-1, *S. amazonensis* SB2B, *S. denitrificans* OS217, *S. baltica* OS155, *S. baltica* OS195, *S. baltica* OS185, *S. baltica* OS223, *S. frigidimarina* NCIMB400, *S. pealeana* ATCC 700345, *S. woodyi* ATCC 51908, *S.* sp. ANA-3, *S.* sp. MR-4, *S.* sp. MR-7, *S. loihica* PV-4, *S. halifaxens* HAW-EB4, *S. piezotolerans* WP3, *S. sediminis* HAW-EB3, and *S. benthica* KT99 were obtained from

the National Center for Biotechnology Information (NCBI, http://www.ncbi.nlm.nih.gov). *S. oneidensis* MR-1 MtrB homologs in other *Shewanella* spp were identified via BLAST analysis (1). Multiple alignments of MtrB homologs from *Shewanella* spp. were generated using ClustalW (56). LOGO diagrams (8) were generated from http://weblogo.berkeley.edu using ClustalW alignment files.

In-frame gene deletion and site-directed mutagenesis

mtrB was removed from the *S. oneidensis* genome via application of a newly constructed gene deletion system (7). Briefly, regions corresponding to ~750 bp upstream and downstream of the *mtrB* open reading frame (ORF) were independently PCR-amplified and subsequently joined using overlap-extension PCR. The resulting fragment was cloned into suicide vector pKO2.0, which does not replicate in *S. oneidensis*. This construct (pKO-MTRB) was mobilized into wild-type MR-1 via conjugal transfer from an *E. coli* donor strain. *S. oneidensis* strains with the plasmid integrated into the genome were selected on solid LB medium containing gentamycin (15 μg mL^{-1}). Single integrations were verified via PCR with primers flanking the recombination region. Plasmids were resolved from the genomes of single integrants by plating on solid LB medium containing sucrose (10% w/v) with NaCl omitted. In-frame deletions were verified by PCR and direct DNA sequencing (University of Nevada, Reno Genomics Center).

Single amino acid mutations in MtrB (C42A or C45A) were constructed using the Quikchange Lightning site-directed mutagenesis kit (Stratagene). The *mtrB* ORF and regions corresponding to ~750 bp upstream and downstream were PCR-amplified as a

single fragment and subsequently cloned into the broad host range cloning vector pBBR1MCS (29). Mutagenesis primers (C42A-Sense, C42A-Antisense, C45A-Sense, C45A-Antisense, Table 4.1) were designed according to the manufacturer's instructions. Mutagenesis PCR reactions were carried out according to the manufacturer's instructions and subsequently transformed into XL10 Gold Kan^R competent cells (Stratagene). Correct amino acid mutations (C42A or C45A) were verified by direct DNA sequencing using primers MTRB-SeqF and MTRB-SeqR (Table 4.1, University of Nevada, Reno Genomics Center). Correct constructs were subsequently cloned into pKO2.0 in an analogous manner as described above. Mutated *mtrB* ORFs were "knocked-in" as described previously, to alleviate any problems associated with *in trans* complementation and verified by PCR and direct DNA sequencing (7).

Quantitative Real-Time PCR and Gene expression analyses

S. oneidensis MR-1 and mutant strains MTRB1, C42A, and C45A were cultured in SM with 30 mM fumarate as terminal electron acceptor. Cells were grown to mid-log phase growth and total RNA was harvested using PureZol (Bio-Rad, Hercules, CA) according to the manufacturer's instructions. Total RNA was processed with the QiaSpin RNeasy kit with on-column DNaseI treatment (QIAGEN). Total cDNA was synthesized using the High Capacity cDNA archive kit (Applied Biosystems) according to the manufacturer's instructions. Quantitative real-time PCR data was obtained using custom TaqMan® assays designed for *mtrA*, *mtrB*, *mtrC*, *omcA*, and *gyrB*. Cycling routines consisted of 95 C for 20 sec. and 40 cycles of 95 °C for 1 second and 60 °C for 20 sec and were performed using a StepOne Plus Real-Time Sequence detection system

Table 4.1. Primers used in this study

Name	Sequence
MTRBD1	GACTGGATCCCTC CTC TAA GAG TCC AAT GGC TGG C
MTRBD2	CAG CAT CAG CAT TTG TGC GGT GTA GCC TGT GTT GGC TAA TAA CGC TAG AGT
MTRBD3	ACT CTA GCG TTA TTA GCC AAC ACA GGC TAC ACC GCA CAA ATG CTG ATG CTG
MTRBD4	GACTGTCGACACA TTT AGC CAA GCC CTA AGC CGT
MTRBDTF	CAG AGC AAG TCG AAG CCA CCT TAG
MTRBDTR	CCA TCG GTA CTA TGG CAA ACA GAG C
C42A-SENSE	GTGAAATTATCCGCATGGAGCGCAAAAGGCTGCGTCGTTGAAACG
C42A-ANTISENSE	CGTTTCAACGACGCAGCCTTTTGCGCTCCATGCGGATAATTTCAC
C45A-SENSE	GCATGGAGCTGTAAAGGCGCAGTCGTTGAAACGGGCACA
C45A-ANTISENSE	TGTGCCCGTTTCAACGACTGCGCCTTTACAGCTCCATGC
MTRB-SEQF	GAT CAC TCT AGC GTT ATT AGC CAA C
MTRB-SEQR	GTT GCT TGA ACC TGC TGT TAT C

(Applied Biosystems). Gene expression data was obtained using the comparative ($\Delta\Delta C_T$) method in the StepOne Plus software. Wild-type MR-1 was used as the reference sample and *gyrB* was used as the endogenous control. PCR reactions were performed in triplicate.

Peripheral Protein Extraction and Identification

Wild-type *S. oneidensis* MR-1 cells were cultivated and harvested as previously described (14). Cells were cultivated to late exponential growth phase and peripherally attached proteins were released using a KCl wash buffer (0.5 M KCl, 100 mM Tris-HCl, 1 mM EDTA). Peripheral proteins were concentrated using ultrafiltration. Concentrated protein samples were normalized for protein content (for wild type and mutant strains) and separated electrophoretically according to standard techniques using 8-16% linear gradient Tris-HCl polyacrylamide gels (Bio-Rad). SDS-PAGE gels were stained for total protein using Bio-Safe Coomassie Blue (Bio-Rad) or for *c*-type cytochrome heme peroxidase activity (16).

Protein bands were excised from SDS-PAGE gels and identified by peptide mass fingerprinting and MALDI-TOF MS/MS analyses. Samples were reduced (20 mM tributylphosphine), alkylated (40 mM iodoacetamide) and digested in-gel with trypsin (Sigma-Aldrich, St. Louis, MO). Tryptic fragments were analyzed by an AB4700 Proteomic Analyzer (Applied Biosystems) operated in reflector mode. Spectra were analyzed using GPS explorer software (Applied Biosystems) and the MASCOT™ database (Matrix Science Inc., Boston, MA)

Results

MtrB homologs contain a conserved Cys-X-X-Cys Motif. Multiple sequence alignments of MtrB homologs from sequenced *Shewanella* spp. displayed a conserved motif in the N-terminus consisting of two cysteine residues separated by two other amino acids. The second amino acid (lysine) in the motif was also strictly conserved. The third amino acid displayed the only variance. 12 out of 20 sequenced MtrB homologs contained glycine as the third residue while 5 out of 20 contained arginine. 2 out of 20 contained asparagine and a single member (*S. frigidimarina* NCIMB400) contained alanine. These results are represented as a LOGO diagram in Figure 4.1. *S. denitrificans* did not contain a MtrB homolog and is therefore not respresented in the LOGO diagram or percentages listed above.

Figure 4.1. LOGO Diagram of CXXC region of MtrB. Diagram generated from multiple alignments of MtrB homologs from all metal-respiring *Shewanella* spp. Letter height corresponds to percentage of sequences with specific residue at the indicated position. Numbering is according to *S. oneidensis* MR-1.

Construction of in-frame deletion and site-directed mutant strains. *mtrB* was removed from the *S. oneidensis* genome by application of the newly constructed gene deletion system (7). Site-directed mutants C42A and C45A were constructed in an analogous manner, except that individual nucleotides were changed via site-directed mutagenesis and the in-frame deletion mutant (MtrB1) was used as the recipient strain, and the construct containing modified *mtrB* sequences plus upstream and downstream DNA was mobilized and selected for insertion. Mutant strains were verified via direct DNA sequencing (data not shown) and RT-PCR (to confirm expression of upstream and downstream genes).

In-frame deletion mutant MtrB1 and site-directed mutant C42A (but not C45A) display anaerobic respiratory deficiencies. Wild-type *S. oneidensis*, deletion mutant MtrB1, site-directed mutants C42A and C45A, and complemented mutant MTRB+ were tested for anaerobic respiration on a combination of two electron donors (lactate and formate) and a set of alternate electron acceptors. MtrB1 and C42A were severely impaired in their ability to respire Fe(III), Mn(III) and Mn(IV) (Figure. 4.2). Growth on alternate terminal electron acceptors including NO_3^-, $S_2O_3^{2-}$, fumarate, DMSO, TMAO, and S^0 was unaffected.

Outer membrane protein profiles of MtrB1 and site-directed mutant strains C42A and C45A. Loosely attached peripheral proteins were removed from the surface of wild-type MR-1 and mutant strains (MtrB1, C42A and C45A). Proteins were separated by SDS-PAGE and stained for *c*-type cytochrome-linked heme peroxidase activity (Figure. 4.4). All strains tested displayed a prominent *c*-type cytochrome at approximately 80 kDa, however in both MTRB1 and C42A the cytochrome was

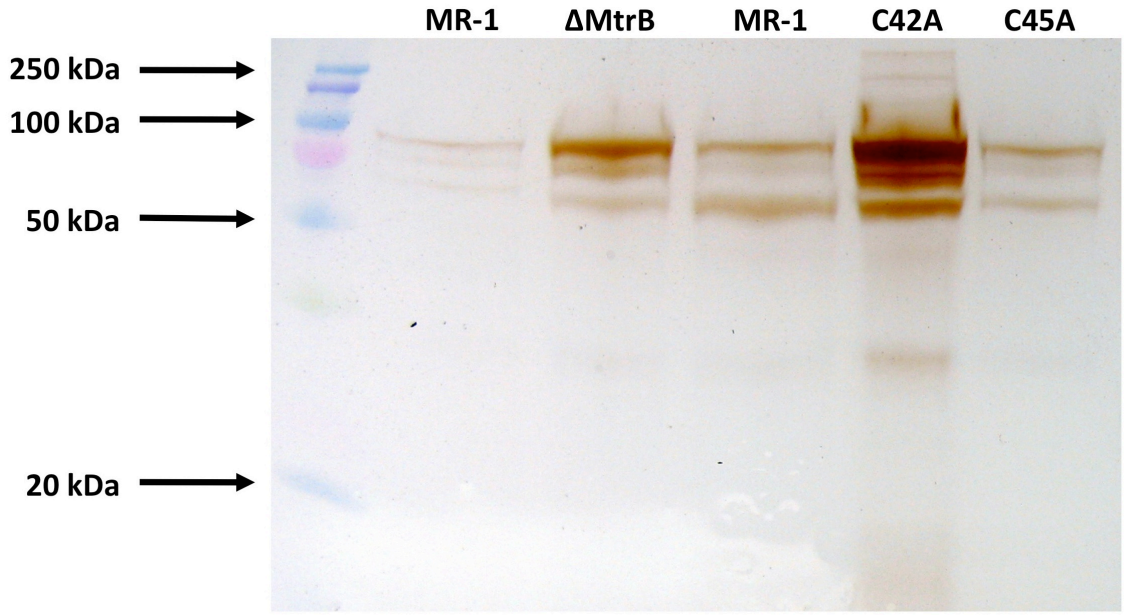

Figure 4.2. *c*-type cytochrome-linked heme peroxidase activity stain of peripheral protein fractions. Peripheral protein fractions were washed from wild-type *S. oneidensis* (MR-1) and mutant strains and separated via SDS-PAGE. Molecular weight markers are indicated to the left of the gel lanes.

significantly more abundant (Figure 4.3). All lanes contained the same amount of total protein, as determined by a modified Lowry method.

Identification of increased abundance *c*-type cytochrome from MtrB1 and C42A. Protein bands displaying increased abundance in MtrB1 and C42A were excised from gels stained with Bio-Safe Coomassie and prepared for identification as described above. Peptide samples were identified via multi-stage MALDI-TOF MS/MS in triplicate. The band displaying increased *c*-type cytochrome abundance from MtrB1 and C42A was identified as the decaheme outer membrane cytochrome OmcA. OmcA was also identified from the corresponding band in wild-type MR-1 and C45A.

QRT-PCR of genes in the *mtr* operon in MtrB1 and site-directed mutant strains. Wild-type MR-1 and mutant strains were grown to mid-log phase using lactate and fumarate as electron donor and acceptor, respectively. Total RNA was harvested and subsequently purified of any contaminating genomic DNA by treatment with DNaseI. Gene expression levels were quantified using the $\Delta\Delta C_T$ method (22, 33) via relative fluorescence during QRT-PCR. Transcripts for *mtrA*, *mtrB*, *mtrC*, and *omcA* were detected in all strains (no *mtrB* transcript was detected in MTRB1) and expression values were normalized to an endogenous control gene (*gyrA*) and also normalized to the wild-type MR-1 values. Expression of *mtrB* in the C42A mutant strain was decreased approximately 10 fold compared to wild-type MR-1 and C45A, while expression of other genes was unaffected (Figure. 4.4)

Discussion

Shewanella spp. are an environmentally diverse group of bacteria responsible for a variety of biogeochemical processes including the weathering of clays,

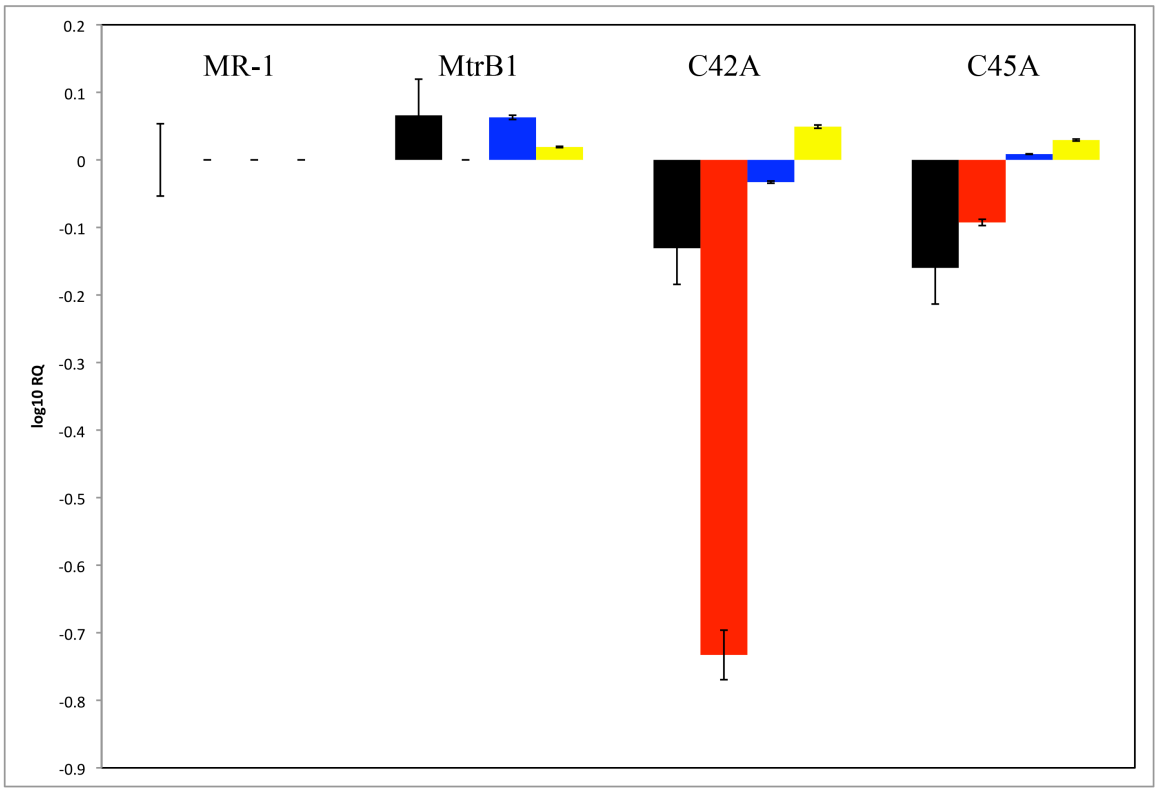

Figure 4.3. Relative quantitation results from individual *mtr* genes from wild-type *S. oneidensis* and MtrB mutant strains. Bars represent relative fluorescence change monitored during QRT-PCR relative to the MR-1 reference sample and normalized to the *gyrB* expression level. *mtrA* – black, *mtrB* – red, *mtrC* – blue, and *omcA* – yellow.

biotransformation of transition metals including Iron and Manganese, mobilization of sulfur, and respiration of contaminant radionuclides. Compared to the wealth of knowledge about alternative respiratory processes including SO_4^{2-} respiration, nitrogen fixation and even relatively newly discovered processes such as methanogenesis and anaerobic ammonia oxidation, a gene or protein responsible for metal respiration has yet to be conclusively identified. Metal respiration in *Shewanella* spp. requires the OM decaheme *c*-type cytochromes MtrC and OmcA and periplasmically-localized decaheme *c*-type cytochrome MtrA. Additionally, integral OM protein MtrB is also strictly required for Fe(III) and Mn(IV) respiration in *S. oneidensis* MR-1 and deletion mutants are severely impaired in metal reduction activity. MtrB contains a conserved N-terminal CXXC protein motif similar to those found in thioredoxin and peroxidase proteins. Interestingly, cysteine residues are usually absent from beta barrel proteins due to structural considerations.

Cys-X-X-Cys (where X represents any amino acid) motifs are typically found in redox-active proteins such as thioredoxins and in proteins responsible for properly folding disulfide bonds (DSBs) (45, 47). CXXC-motif proteins refold disulfide bonds or transfer electrons in a multistep process. First, a single cysteine residue thiol group in the thioredoxin (or similar) protein attacks the disulfide bond in the target protein and forms an intermolecular disulfide. This disulfide is attacked by the second cysteine residue (resolving cysteine) and subsequently forms an intramolecular disulfide bond in the thioredoxin protein, while forming a dithiol in the target protein (2, 46, 47). A total of two electrons are transferred in the process and results in a strained conformation in the thioredoxin protein, which is significantly more stable in the dithiol form (25). Proteins

responsible for forming DSBs operate in the opposite fashion (preferring an oxidized conformation) and form DSBs by removing electrons from a dithiol-containing protein (25). DSB proteins and thioredoxin proteins both contain a proline residue between the two cysteines in the CXXC motif. This proline causes a kink in the peptide backbone and results in strained conformation for each protein. The position of the proline residue (CPGC in thioredoxin and CGPC in DsbA) determines whether a dithiol or disulfide formation is preferred (25, 47).

Additionally, CXXC-containing proteins such as peroxidases may act as redox sensors by oxidation of conserved cysteine residues to reversible sulfenic (R-SOH) and irreversible sulfinic ($R\text{-}SO_2H$) and sulfonic ($R\text{-}SO_3H$) states of the thiol group (19). The best characterized system is the hydrogen peroxide (H_2O_2)-sensing protein OxyR and the corresponding *oxyR* regulon in *E. coli*. OxyR exists as a tetramer and contains conserved residues Cys199 and Cys208. Under H_2O_2-stress conditions, Cys199 is oxidized to the R-SOH form and inititates formation of an intramolecular disulfide bond with Cys208. This alters the DNA binding characteristics of OxyR which affects expression of genes required for detoxification of reactive oxygen species (ROS) (60). Alternatively, Cys199 may be oxidized to the R-SOH form and interact directly without forming an intramolecular disulfide (27).

CXXC-motifs are also found in proteins that coordinate metal or metal-containing cofactors such as Zinc (Zn^{2+}), Heme (*c*-type cytochromes), or Iron-Sulfur (FeS) clusters (19). Although cofactors may be directly bound to proteins via conserved cysteine residues (e.g. *c*-type cytochromes), additional residues such as proximal and distal histidines or additional cysteine residues (for FeS clusters) are often required to bind the

cofactor and ensure functionality (19). Proteins that bind Zn^{2+} may also act as transcriptional regulators in response to oxidative stress. When cysteine residues coordinating Zn^{2+} ions become oxidized, Zn^{2+} is removed from the protein, which then undergoes a conformational change, resulting in altered DNA binding properties and subsequent transcriptional changes (19, 27, 60).

Recently, protein homologs to MtrB and MtrA were identified in a wide range of bacterial phyla, suggesting that trans-OM electron transfer may not be restricted to metal respiring bacteria (21). Additionally, MtrB contains a conserved N-terminal Cys-X-X-Cys motif which has been proposed as a metal-binding site in previous studies (3). Interestingly, other MtrB (or PioB, from Fe(II)-oxidizing bacteria) homologs do not contain the conserved CXXC motif in the N-terminus and, when combined with results from the present study, these results suggest that MtrB may provide a unique function in *Shewanella* spp. as compared to other bacteria containing the OM "electron conduit." C42A mutations in MtrB from *S. oneidensis* MR-1 displayed similar phenotypes to MtrB-null mutations, indicating that C42 is strictly required for MtrB function. Because C45A mutations did not disrupt MtrB function, it is unlikely that the CXXC motif in MtrB functions similar to those found in thioredoxins or proteins involved with DSB folding. Additionally, peroxidases or other proteins involved in sensing oxidative stress also require both cysteine residues for function, but limited function has been reported when the resolving cysteine is modified to serine (47). Results from the present study potentially represent a new class of CXXC motifs where only a single cysteine is required for function. Current work is aimed at determining the function of C42 of MtrB in metal respiration in *Shewanella oneidensis* MR-1.

REFERENCES

1. Altschul, S.F., et al., Gapped BLAST and PSI-BLAST: a new generation of protein database search programs. Nucleic Acids Research, 1997. **25**(17): p. 3389-3402.

2. Bardwell, J.C.A. and J. Beckwith, The Bonds That Tie - Catalyzed Disulfide Bond Formation. Cell, 1993. **74**(5): p. 769-771.

3. Beliaev, A.S. and D.A. Saffarini, *Shewanella putrefaciens mtrB* encodes an outer membrane protein required for Fe(III) and Mn(IV) reduction. Journal of Bacteriology, 1998. **180**(23): p. 6292-7.

4. Beliaev, A.S., et al., MtrC, an outer membrane decahaem c cytochrome required for metal reduction in *Shewanella putrefaciens* MR-1. Molecular Microbiology, 2001. **39**(3): p. 722-30.

5. Borloo, J., et al., A kinetic approach to the dependence of dissimilatory metal reduction by *Shewanella oneidensis* MR-1 on the outer membrane cytochromes c OmcA and OmcB. FEBS J, 2007. **274**(14): p. 3728-38.

6. Bretschger, O., et al., Current production and metal oxide reduction by Shewanella oneidensis MR-1 wild type and mutants. Applied and Environmental Microbiology, 2007. **73**(21): p. 7003-7012.

7. Burns, J.L. and T.J. DiChristina, Anaerobic respiration of elemental sulfur and thiosulfate by *Shewanella oneidensis* MR-1 requires psrA, a homolog of the phsA gene of *Salmonella enterica* Serovar Typhimurium LT2. Applied and Environmental Microbiology, 2009. **75**(16): p. 5209-5217.

8. Crooks, G.E., et al., WebLogo: A sequence logo generator. Genome Research, 2004. **14**(6): p. 1188-1190.

9. Dale, J.R., R. Wade, Jr., and T.J. Dichristina, A conserved histidine in cytochrome c maturation permease CcmB of *Shewanella putrefaciens* is required for anaerobic growth below a threshold standard redox potential. Journal of Bacteriology, 2007. **189**(3): p. 1036-1043.

10. Dehio, C. and M. Meyer, Maintenance of broad-host-range incompatibility group P and group Q plasmids and transposition of Tn5 in *Bartonella henselae* following conjugal plasmid transfer from *Escherichia coli.* Journal of Bacteriology, 1997. **179**(2): p. 538-540.

11. DiChristina, T., et al., *Microbial metal reduction by members of the genus Shewanella: novel strategies for anaerobic respiration.*, in *Biogeochemistry of Anoxic Marnie Basins*, L. Neretin, Editor. 2006, Kluwer Publishing Co.: Dordrecht, NL.

12. DiChristina, T.J. and E.F. DeLong, Isolation of anaerobic respiratory mutants of *Shewannella putrefaciens* and genetic analysis of mutants deficient in anaerobic growth on Fe3+. Journal of Bacteriology, 1994. **176**(5): p. 1468-1474.

13. DiChristina, T.J., J.K. Fredrickson, and J.M. Zachara, Enzymology of electron transport: energy generation with geochemical consequences. Reviews in Mineralogy and Geochemistry, 2005. **59**: p. 27-52.

14. DiChristina, T.J., C.M. Moore, and C.A. Haller, Dissimilatory Fe(III) and Mn(IV) reduction by *Shewanella putrefaciens* requires *ferE*, a homolog of the *pulE* (*gspE*) type II protein secretion gene. Journal of Bacteriology, 2002. **184**(1): p. 142-151.

15. Eggleston, C.M., et al., Binding and direct electrochemistry of OmcA, an outer-membrane cytochrome from an iron reducing bacterium, with oxide electrodes: A candidate biofuel cell system. Inorganica Chimica Acta, 2008. **361**(3): p. 769-777.

16. Francis, R.T. and R.R. Becker, Specific Indication of Hemoproteins in Polyacrylamide Gels Using a Double-Staining Process. Analytical Biochemistry, 1984. **136**(2): p. 509-514.

17. Gleason, F.K. and A. Holmgren, Thioredoxin and Related Proteins in Procaryotes. Fems Microbiology Reviews, 1988. **54**(4): p. 271-298.

18. Gorby, Y.A., et al., Electrically conductive bacterial nanowires produced by *Shewanella oneidensis* strain MR-1 and other microorganisms. Proceedings of the National Academy of Sciences of the United States of America, 2006. **103**(30): p. 11358-11363.

19. Green, J. and M.S. Paget, Bacterial redox sensors. Nature Reviews Microbiology, 2004. **2**(12): p. 954-966.

20. Hartshorne, R.S., et al., Characterization of Shewanella oneidensis MtrC: a cell-surface decaheme cytochrome involved in respiratory electron transport to extracellular electron acceptors. Journal of Biological Inorganic Chemistry, 2007. **12**(7): p. 1083-1094.

21. Hartshorne, R.S., et al., Characterization of an electron conduit between bacteria and the extracellular environment. Proc Natl Acad Sci U S A, 2009.

22. Heid, C.A., et al., Real time quantitative PCR. Genome Research, 1996. **6**(10): p. 986-994.

23. Heidelberg, J.F., et al., Genome sequence of the dissimilatory metal ion-reducing bacterium Shewanella oneidensis. Nat Biotechnol, 2002. **20**(11): p. 1118-23.

24. Jones, M., et al., *Shewanella oneidensis* mutants selected for their inability to produce soluble organic-Fe(III) are unable to respire Fe(III) as anaerobic electron acceptor. Environmental Microbiology, 2010.

25. Kadokura, H., F. Katzen, and J. Beckwith, Protein disulfide bond formation in prokaryotes. Annual Review of Biochemistry, 2003. **72**: p. 111-135.

26. Kelly, D.P. and A.P. Wood, Synthesis and Determination of Thiosulfate and Polythionates. Inorganic Microbial Sulfur Metabolism, 1994. **243**: p. 475-501.

27. Kim, S.O., et al., OxyR: A molecular code for redox-related signaling. Cell, 2002. **109**(3): p. 383-396.

28. Kostka, J.E., G.W. Luther, and K.H. Nealson, Chemical and Biological Reduction of Mn(Iii)-Pyrophosphate Complexes - Potential Importance of Dissolved Mn(Iii) as an Environmental Oxidant. Geochimica Et Cosmochimica Acta, 1995. **59**(5): p. 885-894.

29. Kovach, M.E., et al., pBBR1MCS: a broad-host-range cloning vector. Biotechniques, 1994. **16**(5): p. 800-2.

30. Lovley, D.R., D.E. Holmes, and K.P. Nevin, Dissimilatory Fe(III) and Mn(IV) reduction. Advances in Microbial Physiology, 2004. **49**: p. 219-285.

31. Lovley, D.R. and E.J.P. Phillips, Novel Mode of Microbial Energy-Metabolism - Organic-Carbon Oxidation Coupled to Dissimilatory Reduction of Iron or Manganese. Applied and Environmental Microbiology, 1988. **54**(6): p. 1472-1480.

32. Marsili, E., et al., *Shewanella* secretes flavins that mediate extracellular electron transfer. Proceedings of the National Academy of Sciences of the United States of America, 2008. **105**(10): p. 3968-3973.

33. Meijerink, J., et al., A novel method to compensate for different amplification efficiencies between patient DNA samples in quantitative real-time PCR. Journal of Molecular Diagnostics, 2001. **3**(2): p. 55-61.

34. Montgomery, H. and J.F. Dymock, Determination of Nitrite in Water. Analyst, 1961. **86**(102): p. 414-&.

35. Murphy, J.N. and C.W. Saltikov, The *cymA* gene, encoding a tetraheme *c*-type cytochrome, is required for arsenate respiration in *Shewanella* species. Journal of Bacteriology, 2007. **189**(6): p. 2283-2290.

36. Myers, C.R. and J.M. Myers, Cloning and sequence of cymA a gene encoding a tetraheme cytochrome c required for reduction of iron(III), fumarate, and nitrate by Shewanella putrefaciens MR-1. Journal of Bacteriology, 1997. **179**(4): p. 1143-1152.

37. Myers, C.R. and J.M. Myers, MtrB is required for proper incorporation of the cytochromes OmcA and OmcB into the outer membrane of Shewanella putrefaciens MR-1. Appl Environ Microbiol, 2002. **68**(11): p. 5585-94.

38. Myers, C.R. and K.H. Nealson, Bacterial manganese reduction and growth with manganese oxide as the sole electron acceptor. Science, 1988. **240**(4857): p. 1319-1321.

39. Myers, J.M. and C.R. Myers, Isolation and sequence of *omcA*, a gene encoding a decaheme outer membrane cytochrome c of *Shewanella putrefaciens* MR-1, and detection of omcA homologs in other strains of *S. putrefaciens*. Biochim Biophys Acta, 1998. **1373**(1): p. 237-51.

40. Myers, J.M. and C.R. Myers, Role of the tetraheme cytochrome CymA in anaerobic electron transport in cells of Shewanella putrefaciens MR-1 with normal levels of menaquinone. Journal of Bacteriology, 2000. **182**(1): p. 67-75.

41. Myers, J.M. and C.R. Myers, Role for outer membrane cytochromes OmcA and OmcB of *Shewanella putrefaciens* MR-1 in reduction of manganese dioxide. Appl Environ Microbiol, 2001. **67**(1): p. 260-9.

42. Myers, J.M. and C.R. Myers, Overlapping role of the outer membrane cytochromes of *Shewanella oneidensis* MR-1 in the reduction of manganese(IV) oxide. Lett Appl Microbiol, 2003. **37**(1): p. 21-5.

43. Paschen, S.A., et al., Evolutionary conservation of biogenesis of beta-barrel membrane proteins. Nature, 2003. **426**(6968): p. 862-866.

44. Pitts, K.E., et al., Characterization of the *Shewanella oneidensis* MR-1 decaheme cytochrome MtrA: expression in *Escherichia coli* confers the ability to reduce soluble Fe(III) chelates. Journal of Biological Chemistry, 2003. **278**(30): p. 27758-65.

45. Rietsch, A. and J. Beckwith, The genetics of disulfide bond metabolism. Annual Review of Genetics, 1998. **32**: p. 163-184.

46. Rietsch, A., et al., Reduction of the periplasmic disulfide bond isomerase, DsbC, occurs by passage of electrons from cytoplasmic thioredoxin. Journal of Bacteriology, 1997. **179**(21): p. 6602-6608.

47. Ritz, D. and J. Beckwith, Roles of thiol-redox pathways in bacteria. Annual Review of Microbiology, 2001. **55**: p. 21-48.

48. Rosso, K.M., D.M.A. Smith, and M. Dupuis, An ab initio model of electron transport in hematite (alpha-Fe2O3) basal planes. Journal of Chemical Physics, 2003. **118**(14): p. 6455-6466.

49. Schuetz, B., et al., Periplasmic electron transfer via the *c*-type cytochromes MtrA and FccA of *Shewanella oneidensis* MR-1. Applied and Environmental Microbiology, 2009. **75**(24): p. 7789-7796.

50. Schwalb, C., S.K. Chapman, and G.A. Reid, The membrane-bound tetrahaem c-type cytochrome CymA interacts directly with the soluble fumarate reductase in *Shewanella.* Biochem Soc Trans, 2002. **30**(4): p. 658-62.

51. Schwalb, C., S.K. Chapman, and G.A. Reid, The tetraheme cytochrome CymA is required for anaerobic respiration with dimethyl sulfoxide and nitrite in *Shewanella oneidensis.* Biochemistry, 2003. **42**(31): p. 9491-9497.

52. Shi, L., et al., Respiration of metal (hydr)oxides by *Shewanella* and *Geobacter:* a key role for multihaem *c*-type cytochromes. Mol Microbiol, 2007. **65**(1): p. 12-20.

53. Shyu, J.B.H., D.P. Lies, and D.K. Newman, Protective role of *tolC* in efflux of the electron shuttle anthraquinone-2,6-disulfonate. Journal of Bacteriology, 2002. **184**(6): p. 1806-1810.

54. Stookey, L.L., Ferrozine - a new spectrophotometric reagent for iron. Analytical Chemistry, 1970. **42**(7): p. 779-781.

55. Taillefert, M., et al., *Shewanella putrefaciens* produces an Fe(III)-solubilizing ligand during anaerobic respiration on insoluble Fe(III) oxides Journal of Inorganic Biochemistry, 2007. **101**(11): p. 1760-1767.

56. Thompson, J.D., D.G. Higgins, and T.J. Gibson, Clustal-W - Improving the Sensitivity of Progressive Multiple Sequence Alignment through Sequence Weighting, Position-Specific Gap Penalties and Weight Matrix Choice. Nucleic Acids Research, 1994. **22**(22): p. 4673-4680.

57. Wigginton, N.S., et al., Electron tunneling properties of outer-membrane decaheme cytochromes from *Shewanella oneidensis.* Geochimica Et Cosmochimica Acta, 2007. **71**(3): p. 543-555.

58. Wilkinson, B. and H.F. Gilbert, Protein disulfide isomerase. Biochimica Et Biophysica Acta-Proteins and Proteomics, 2004. **1699**(1-2): p. 35-44.

59. Zhang, H., et al., In Vivo Identification of the Outer Membrane Protein OmcA-MtrC Interaction Network in *Shewanella oneidensis* MR-1 Cells Using Novel Hydrophobic Chemical Cross-Linkers. J Proteome Res, 2008.

60. Zheng, M., F. Aslund, and G. Storz, Activation of the OxyR transcription factor by reversible disulfide bond formation. Science, 1998. **279**(5357): p. 1718-1721.

CHAPTER 5

CONCLUSIONS

Shewanella oneidensis MR-1 respires a variety of compounds as terminal electron acceptor during anaerobic respiration. *S. oneidensis* is postulated to respire highly crystalline Fe(III) oxides via one or more of the following mechanisms: 1) direct contact between the cell and mineral oxide allows direct electron transfer between redox active protein complexes present on the cell surface and the solid Fe(III), 2) the use of soluble, redox active electron shuttles which are reduced inside the cell, diffuse to the mineral surface, transfer electrons to the oxide and subsequently return to the cell to be re-reduced, 3) The use of electrically conductive "nanowires" which carry electrons great distances from the cell surface and directly transfer electrons to the mineral oxide, and 4) secretion of a small organic ligand that chelates Fe(III) and delivers it to the cell, where it may be internalized and reduced by periplasmically localized Fe(III) terminal reductases. Previous studies indicate that *Shewanella* spp. and *Geobacter* spp. utilize different mechanisms for respiring Fe(III) oxides as *Geobacter* strictly requires direct contact, while *Shewanella* may respire Fe(III) at a distance.

This study presents conflicting data about the molecular mechanism of anaerobic Fe(III) respiration. *S. oneidensis* MR-1 uses a Type II protein secretion system to localize an Fe(III) terminal reductase (FeR) to the outer face of the outer membrane of the cell. This Fe(III) reductase complex is mislocalized and functional in the periplasmic space in

a T2SS mutant strain, suggesting that the multicomponent reductase is secreted in complete and folded form. The T2SS mutant strain is severely impaired in Fe(III) respiratory ability, suggesting that without the direct contact of FeR proteins to Fe(III) oxide surfaces, no respiration can occur. However, a serine protease adhesin mutant is deficient in adhesion to Fe(III) oxides, yet retains Fe(III) respiratory capability, suggesting that direct contact between the cell and mineral surfaces is not required. Additionally, because electron transfer between surface exposed heme groups in OM cytochromes OmcA and MtrC and Fe(III) oxide surfaces is only efficient when the heme groups are within ~14 angstroms of the mineral surface, any surface exopolysaccharide or exopolymer would likely interfere with the ability of the heme groups to make contact with the insoluble Fe(III).

Electron shuttles (e. g. riboflavin, menaquinone, and melanin) have recently been proposed as viable alternatives to direct electron transfer. Electron shuttles alleviate many problems associated with microbial metal respiration, including the need for direct contact between the cell surface and the mineral. Riboflavin may be secreted by *S. oneidensis* as a combination shuttle/chelator ("shelator") whereby it nonreductively dissolves solid Fe(III), returns to the cell as a soluble Fe(III)-riboflavin complex and is reduced by a *Shewanella* FeR. Recent data suggest, however, that riboflavin may be too energetically costly to produce and excrete in significant quantities required for electron shuttling, especially in nutrient limited environments. Furthermore, riboflavin is relatively insoluble at circumneutral pH and would likely precipitate in the *S. oneidensis* environment. Alternate electron shuttles including menaquinone and melanin have been attributed to cell culture artifacts such as cell lysis. *Shewanella alga* BrY only produced

melanin as an electron shuttle growth medium was supplemented with L-Tyrosine at 2 g per liter (11 mM). These levels are not physiologically relevant, considering that cells would have to produce and secrete millimolar levels of tyrosine to trigger melanin production *in vivo*.

With the recent release of 22 genome sequences for members of the *Shewanella* genus, a reliable and efficient method for generating deletions of candidate FeR proteins is needed. In the present study, hallmark components from different plasmid vectors were combined to generate a new suicide vector for constructing markerless, in-frame gene deletions. The newly constructed vector contains the R6K origin of replication (which *Shewanella* spp. are unable to replicate), the RP4 mobilization origin, a gentamycin resistance cassette, and *sacB* (encoding levansucrase, which, when expressed, is lethal in gram-negative bacteria). The pKO2.0 vector was tested via deletion of the putative thiosulfate reductase, PsrA. *psrA* was removed from the *S. oneidensis* genome via stepwise selection, counterselection mechanism. The resulting mutant PSRA1 was unable to respire $S_2O_3^{2-}$ or S^0 as terminal electron acceptor while respiration on all other electron acceptors was unaffected. RT-PCR confirmed that the remaining genes in the *psr* operon were still transcribed and the single gene deletion did not affect their expression. In addition, pKO2.0 was also used to "knock-in" the wild-type *psrA* gene at the same locus where *psrA* was removed. This further extends the functionality of the gene-deletion system by allowing complementation of the deleted gene without the adverse effects associated with *in trans* expression of complemented genes from broad host range plasmids. Because PsrA is localized to the cytoplasmic membrane, but oriented to the periplasmic space, PSRA1 provides valuable information

to the mechanism of S^0 respiration. S^0 exists as an insoluble S_8 ring that is presumably unable to cross the outer membrane and be reduced inside the cell. Interestingly, all bacterial species that respire S^0 also respire Fe(III) (which is also insoluble and unable to enter the cell). Because PSRA1 was abolished in not only $S_2O_3^{2-}$ respiration but also S^0 respiration, the S^0 reduction mechanism likely involves an abiotic (purely chemical) terminal reduction step where end products of the PsrA enzymatic reaction diffuse from the cell and reduce the insoluble S^0. Trace amounts of $S_2O_3^{2-}$ present in media containing S^0 are reduced by PsrA to SO_3^{2-} and S^{2-}; the lone pair of SO_3^{2-} can perform a nucleophilic attack to open the S^0 ring and remove a chain terminating S atom from the polysulfide chain to form additional $S_2O_3^{2-}$. The resulting $S_2O_3^{2-}$ may then be reduced by PsrA to sustain the intermolecular sulfur cycle. Because PsrA deletion mutants retained Fe(III) respiratory ability, it is unlikely that sulfide (S^{2-}) acts as an electron shuttle to insoluble Fe(III) oxides.

MtrB was removed from the MR-1 genome using the recently developed gene deletion system and tested for its ability to respire Fe(III) oxides. The MtrB-null mutant strain (MTRB1) was severely impaired for both solid and soluble Fe(III) respiration. Interestingly, MtrB contains a conserved N-terminal CXXC motif similar to those found in thioredoxin and peroxidase proteins. β -barrel proteins typically do not contain cysteine residues due to restrictions in forming secondary structure inside membranes. The conserved cysteine residues were independently changed to alanine and the resulting mutant strains were also tested for the ability to respire Fe(III). Surprisingly, only the more N-terminal cysteine mutation displayed a mutant phenotype, suggesting a potentially novel mechanism different than that of thioredoxins or peroxidases. OM

protein profiles from the null and site directed mutant strains differed significantly from wild type and potentially represent the biochemical function of MtrB and its conserved cysteine residues. Decaheme cytochrome OmcA was strikingly more abundant in peripheral protein fractions from both MTRB1 and C42A mutant strains. These data suggest that MtrB plays a role in OM scaffolding with OmcA as the likely partner. Additionally, the C42A mutant strain displayed a 10 fold decrease in *mtrB* expression, implying an autoregulatory mechanism for MtrB. Taken together, the overall role MtrB plays in Fe(III) respiration in *S. oneidensis* MR-1 is a globally important one. Not only does MtrB function as a scaffold protein for potential OM Fe(III) reductases, but also as a regulatory protein which may sense redox conditions and alter gene expression accordingly. Additionally, because MtrB mutants are completely deficient in Fe(III) respiration, other mechanisms including both endogenously produced electron shuttles (e.g. quinones and riboflavin) and nanowires seem unlikely as predominant reduction pathways terminating with Fe(III). As a final caveat, MtrB displays structural homology to known Fe(III) import proteins FecA (importing Fe(III)-citrate) and FepA (importing Fe(III)-pyoverdine) from other bacteria. Collectively, this suggests that MtrB is an OM Fe(III)-chelate transporter that operates in a similar manner to those Fe(III) transporters required for assimilatory Fe(III) reduction. MtrB likely functions as a redox probe on the OM of the cell and works with an unknown transcription factor to regulate expression of metal respiration genes. MtrB also likely works in conjunction with OmcA, as OmcA mutants display little to no deficiency in Fe(III) respiratory ability. OmcA may sense redox conditions using the 10 covalently bound heme groups that have varying redox potentials. The oxidation of these heme groups may cause conformational changes in

OmcA that are ultimately sensed by MtrB and activate the appropriate transcriptional response.

APPENDIX

PURIFICATION OF NATIVE, TAG-FREE CYSTATHIONINE BETA-LYASE (METC) FROM *SHEWANELLA ONEIDENSIS* MR-1 USING THE PROFINITY EXACT FUSION-TAG AND PROFINIA PROTEIN PURIFICATION SYSTEM

Introduction

Bacteria are ubiquitous in the natural environment and occupy nearly every known ecological niche, including extreme environments that are inhospitable to other organisms. The unique biological adaptations that underlie this ecological flexibility and the rapid progress of sequencing efforts to map diverse bacterial genomes makes many microbes attractive candidates as model systems in the laboratory. An important area of research focuses on investigating microorganisms with the potential for bioremediation of organic and inorganic environmental contaminants.

Shewanella oneidensis MR-1 is a non-pathogenic gram-negative bacterium that is an important model organism for bioremediation studies due to its versatile metabolic and respiratory capabilities. *S. oneidensis* can grow both aerobically and anaerobically and respires a variety of compounds as terminal electron acceptors such as solid metals (Fe(III) and Mn(IV) oxides), radionuclides (U(VI) and Tc(VII)), and several others that span the redox continuum (NO_3^-, Fumarate, Dimethylsulfoxide, S^0) (DiChristina, Fredrickson, Zachara 2005). Despite intensive research into microbial metal respiration, the molecular mechanism of electron transfer to insoluble metal oxides remains poorly understood. *S. oneidensis* MR-1 is postulated to employ a number of novel mechanisms for transferring electrons to the cell surface where outer membrane (OM)-localized

proteins can transfer electrons to insoluble metals (DiChristina, Fredrickson, Zachara 2005). Because of the unique physiology of *S. oneidensis*, studies characterizing proteins in the central metabolism and electron transport chain can provide valuable insight into the molecular mechanism of metal respiration and thus presents an opportunity to investigate how environmental factors can impact the biology of a microorganism. Until recently, these studies have been hampered by the difficulty of generating sufficient quantities of pure, native proteins for crystallography and *in vitro* enzymatic studies.

Cystathionine β-lyase (MetC, CBL) is a crucial enzyme involved in methionine biosynthesis (Dwivedi *et. al.* 1982). MetC is pyridoxal-5'-phosphate-dependent and cleaves cystathionine at the beta-linkage between the carbon and sulfur atoms, generating L-Homocysteine, which is further methylated to form L-Methionine (Martel *et. al.* 1987). MetC can also act as a Carbon-Sulfur (C-S) lyase for other substrates containing C-S linkages (e.g. L-Cysteine, L-Cystine). MetC may therefore play an important role in the central metabolism of *S. oneidensis* by regulating sulfur-containing compounds that can affect redox-balance. *Escherichia coli* CBL has been previously crystallized and its structure determined to 1.83 Å (Laber *et. al.* 1996). Although *S. oneidensis* MR-1 MetC displays an amino acid similarity of 67% (eval=6.7^{-103}) to *E. coli* MetC, the structure and functional characteristics unique to the *S. oneidensis* MetC protein are not well understood. A common requirement for any downstream biochemical and structural studies of proteins is the ability to generate milligram quantities of sufficiently pure and active protein.

Purification of soluble, cytoplasmic proteins is traditionally performed using affinity chromatography following overexpression of a recombinant fusion protein in *E.*

coli. Fusion tags often include glutathione-S-transferase (GST)- or polyhistidine (HIS)-sequences used to bind the target protein to an immobilized liganed on an affinity column. Most commonly used fusion tags remain attached to the target protein following purification and thus may inhibit crystallographic or functional assays. Thus, it is often necessary to introduce an enzymatic cleavage site between the target protein sequence and the fusion tag to facilitate purification of tag-free protein in a two-step process; however, this is often laborious and time-consuming. The Profinity eXact fusion-tag employs a novel one-step affinity and tag-removal system that produces native protein free of the fusion tag, often in less than one hour (Oganesyan and Strong, Technote 5652).

The Profinia purification system performs automated affinity chromatography of recombinant fusion-tagged proteins and optionally, a subsequent integrated desalting step. The Profinia system uses pre-programmed methods and pre-packed affinity cartridges and is capable of generating milligram quantities of protein. The Profinity eXact fusion-tag purification system is ideally suited for use with the Profinia system, enabling one-step, automated affinity purifications with subsequent cleavage of the fusion-tag and exchange of the native, tag-free protein into the buffer of choice.

In this study, expression vectors containing the *S. oneidensis* MR-1 *metC* coding region were constructed with an N-terminal Profinity eXact fusion-tag. Purifications were performed and were optimized on multiple scales using both chemical and mechanical lysis (sonication) methods. In addition, the impact of cleavage time was examined and protein yield, purity and activity were monitored following each expression experiment. Following optimization at a small scale, a scale-up experiment

was performed. In these scale-up experiments, protein increased proportionally, while purity remained comparable to that of the small-scale purifications. These studies thus demonstrate the effectiveness of using the Profinity eXact technology with the preprogrammed methods on an automated chromatography system for the rapid generation of milligram quantities of pure, tag-free protein for downstream functional assays.

Methods

Cloning of *metC* gene into eXact expression vector pPAL7. The *metC* open reading frame was PCR-amplified with iProof Ultra high-fidelity polymerase using primers containing *Hind*III (5' end) and *Xho*I (3' end) as directed in the Profinity eXact system manual. Supercoiled pPAL7 vector and *metC* DNA were double digested with *Hind*III and *Xho*I in compatible buffer and ligated to form pPAL-MC. A second clone (pPAL-MCL) was constructed in an analogous manner, except that the 5' primer contained an additional 6 nucleotides coding for a Thr-Ser Linker (for optimal cleavage as recommended). Ligation products were transformed into an *E. coli* host strain (NovaBlue) via electroporation (Bio-Rad). Clones were verified via restriction analysis and subsequently transformed into BL21(DE3)pLysS expression strains (for strict control of *metC* expression). pLysS encodes T7 lysozyme which binds to T7 RNA polymerase to tightly control expression of cloned inserts in T7-based expression systems (Novagen).

Protein expression and extraction. BL21(DE3)pLysS strains carrying pPAL-MC (BL-MC) and pPAL-MCL (BL-MCL) were cultured in the presence of ampicillin (100 ug mL^{-1}) and chloramphenicol (25 ug mL^{-1}). Overnight seed cultures were grown at

37°C (200 rpm) and used to inoculate expression cultures. Expression cultures were grown at 30°C (175 rpm) to OD_{600} ~1.0. IPTG was added to a final concentration of 1 mM and cultures were induced for 10 hr. Following expression, cell cultures were harvested via centrifugation (10,000*g*, 4°C, 10 min). For chemical lysis, cells were resuspended in Profinia Bacterial Lysis Reagent (Bio-Rad) (10 mL per gram wet cell weight). Cell suspensions were incubated with Benzonase (Novagen, 25 U mL^{-1}, 25°C, 10 min) to reduce viscosity. Lysates were cleared via centrifugation (20,000*g*, 4°C, 20 min) and the resulting supernatants were filtered (0.45 μm PES filters). For mechanical lysis, cells were resuspended in the recommended Profinity eXact 1X Bind/Wash buffer (100 mM Na_2HPO_4, 10 mL per gram wet cell weight). Samples were sonicated on ice at 100% intensity in 30 sec. pulses (60W) (total processing time 10 min) using an S4000 sonicator (Misonix). Lysates were centrifuged and cleared as described above.

Affinity Purification. Cleared lysates were purified using the Profinia Purification System using the preprogrammed Profinity eXact Methods. These methods consisted of using either 1 mL Bioscale Mini eXact plus 10 mL Bioscale Mini P6 desalting cartridges or 5 mL eXact plus 50 mL desalting cartridges. Buffers were prepared at the following concentrations according to the Profinity eXact system manual: Bind/Wash Buffer (100 mM NaH_2PO_4, pH 7.2); Elution Buffer (100 mM NaH_2PO_4, 100 mM NaF, pH 7.2); Desalting Buffer (137 mM NaCl, 2.7 mM KCl, 4.3 mM Na_2HPO_4, 8.1 mM KH_2PO_4, pH 7.4). Samples were applied to Profinity eXact affinity cartridges using the standard flow rate (1.0 mL min^{-1}). Fractions for the column flow-through, washs, and elution were collected via automatic peak detection. Purified protein was collected in a

total of 4 mL for 1 mL eXact cartridge purifications and in a total of 10 mL for 5 mL eXact cartridge purifications.

SDS-PAGE and Experion Pro260 Analysis. SDS-PAGE analysis was performed using Criterion Tris HCL 4-20% linear gradient gels (Bio-Rad). Gels were stained with Bio-Safe Coomassie Blue G-250 stain following standard protocols and imaged with a GelDoc XR system using Quantity One 1-D analysis software (Bio-Rad). Samples were prepared with a 6-fold dilution into Laemmli sample buffer and 30 μL of sample or 10 μL of Precision Plus Protein Kaleidoscope Standard was loaded per lane. Protein quantity and purity was determined using the Bio-Rad Experion Automated Electrophoresis system with the Pro260 analysis kit according to the standard protocol. Protein concentrations were independently confirmed using the Bio-Rad RC DC Protein Assay kit according to the instructions provided with the kit.

Native-PAGE and Cystathionine β-lyase (CBL) activity assay. Native-PAGE analysis was performed using Criterion Tris HCL 8-16% linear gradient gels (Bio-Rad). Samples were diluted 1:2 into Native sample buffer 45 μL of sample or 10 μL of Precision Plus Protein Kaleidoscope Standard was loaded per lane. Gels were stained with Bio-Safe Coomassie Blue G-250 stain following standard protocols (in order to detect the total protein in each lane) or with CBL activity stain (100 mM Tris-HCl, 10 mM L-Cysteine, 500 μM $Pb(NO_3)_2$, pH 8.2). For detection with the CBL activity stain, gels were washed three times in dH_2O (15 min, with shaking) then visualized with CBL activity stain (30 min, 25^oC, no shaking). Gels were imaged with a GelDoc XR system using Quantity One 1-D analysis software. Positive CBL activity results in an insoluble lead sulfide precipitate in the gel (which appears black in gel images).

Protein identification by MALDI-TOF MS/MS. Eluted proteins were confirmed by Matrix-assisted Laser Desorption-Ionization Time of Flight tandem mass spectrometry (MALDI-TOF MS). Proteins were excised from polyacrylamide gels and reduced (Tributylphosphine, 20 mM), alkylated (Iodoacetamide, 40 mM), and digested in-gel with trypsin (Sigma-Aldrich). The trypsin-digested fragments were concentrated using C_{18} ZipTips (Millipore) and spotted onto a 192-well Applied Biosystems (ABI) MALDI plate for multi-stage MALDI-TOF analysis (Georgia Tech Mass Spectrometry Facility). MALDI-TOF MS/MS analysis was carried out with an ABI Voyager 4700 MALDI-TOF-TOF system operated in reflector mode. Peptide ions were analyzed with GPS Explorer software package using the MASCOT™ Database.

Results

Chemical vs. Sonication lysis procedeures. To determine the optimal methods for isolation of total cell protein, both chemical and mechanical (sonication) lysis procedures were compared. Results (Figure 1) demonstrate that both the chemical and sonication lysis methods were equally efficient for isolating soluble MetC protein from multiple samples including both trial scale (250 mL) and preparatory (1 L) culture volumes. Data from both chemical and sonication lysis procedures and both culture volumes are displayed in Table 1.

Native MetC is efficiently cleaved from the eXact column. A variety of proteins require a spacer or linker between the eXact affinity tag and the native protein sequence to promote efficient cleavage from the column. To determine if a linker was required, two clones were constructed, one containing only native MetC amino acid sequence (pPAL-MC), and another containing the recommended Threonine-Serine linker

(pPAL-MCL). In trial-scale experiments (250 mL culture volume), protein purification from each clone resulted in nearly identical yields and purity (data not shown). Native MetC is highly desirable for downstream applications and the clone without the linker region (pPAL-MC) was chosen for further study.

MetC requires minimal time for efficient cleavage from the eXact column. In an effort to further optimize the purification scheme, a series of column incubation times were examined. Profinia eXact methods were programmed with 12 min, 30 min, and 2 hr incubation times, followed by elution and desalting. One liter cultures were grown as described above and prepared by sonication (50 mL total lysate). 10 mL volumes were loaded onto 1 mL eXact columns followed by 10 mL desalting columns. Comparable yields and purity were obtained for each incubation time (Table 2, Figure 2).

Large Scale Purification of MetC. To obtain sufficient quantities of MetC for further downstream applications, a large-scale purification with a 3 liter culture volume was performed. Cells were grown as described above and lysed using sonication. Lysate (200 mL) was prepared as described and loaded onto a 5 mL eXact affinity column followed by a 50 mL desalting column. The column was incubated for 30 minutes to allow for sufficient cleavage, and eluted (10 mL). The large-scale purification resulted in excellent yield (8.71 mg total protein, 0.871 mg mL^{-1}) with no loss in purity (87.2%) (Figure 3). The Profinia-eXact combination is sufficient to produce large quantities of protein from cell lysate in a minimal amount of time (< 2 hours).

Recombinant MetC is active in vitro. Protein fractions were loaded onto both Native and denaturing polyacrylamide gels to determine activity (Native-PAGE) and size and purity (SDS-PAGE). Activities of wild-type MetC (from *S. oneidensis* crude lysate)

and purified recombinant MetC were detected as black precipitates (corresponding to the cleavage of thiol from L-Cysteine and subsequent reaction with lead nitrate to form an insoluble lead-sulfide), while other fractions from the purification displayed C-S lyase activity at a higher position in the gel (resulting from the fusion to the eXact tag) (Figure 4A). SDS-PAGE gels were stained for total protein only, and purified MetC displayed a band at the expected size (~40 kDa) (Figure 4B). The purity of the *S. oneidensis* MetC band was confirmed by MALDI-TOF MS/MS (Figure 4C).

Discussion

Purification of tag-free native protein is an important step in elucidating steps in biochemical pathways. Here we report the purification of cystathionine beta-lyase from a gram-negative bacterium, *Shewanella oneidensis* MR-1. The enzyme may play an important role in regulating redox balance in an organism with an extensive respiratory chain, which terminates with both soluble and insoluble terminal electron acceptors. Purified protein allows for a more in-depth study into biochemical processes related to maintaining redox balance, specifically the availability of thiol-containing compounds. The combination of the eXact fusion-tag and Profinia automated purification system allowed us to purify MetC in a relatively short amount of time, with high purity, and in large quantity.

References

DiChristina, TJ, JK Fredrickson, and JM Zachara. 2005. Enzymology of electron transport: Energy generation with geochemical consequences. Reviews in mineralogy and Geochemistry. **59:**27-52.

Dwivedi, CM, RC Ragin, JR Uren. 1982. Cloning, purification and characterization of beta-cystathionase from *Escherichia coli*. Biochemistry. **21**(13):3064-3069.

Laber, B, T Clausen, R Huber, A Messerschmidt, U Egner, A Müller-Fahrnow, and HD Pohlenz. 1996. Cloning, purification, and crystallization of *Escherichia coli* cystathionine beta-lyase. FEBS Letters **379**(1):94-96.

Martel, A, C Bouthier de la Tour, and F Le Goffic. 1987. Pyridoxal 5'phospate binding site of *Escherichia coli* beta-cystathionase and cystathionine gamma synthase comparison of their sequences. Biochem. Biophys. Res. Commun. **147**(2):565-571.

Table A.1.

Clone	250 mL Culture Chemical Lysis (10 mL Lysate)			1 L Culture Chemical Lysis (50 mL Lysate)			250 mL Culture Sonicated (10 mL Lysate)			1 L Culture Sonicated (50 mL Lysate)		
	Conc.	**Purity**	**Total Protein**	**Conc.**	**Purity**	**Total Protein**	**Conc.**	**Purity**	**Total Protein**	**Conc.**	**Purity**	**Total Protein**
pPAL-MC	0.075	92.9	0.3	0.6	91.2*	2.4	0.072	91.6	0.28	0.72	87.0	2.88

Table A.1. Trial-scale (1 mL eXact column) protein performance data. Concentrations are given as mg mL^{-1}. Purity is represented as percentages. Total protein is given in mg.

Table A.2

Clone	12 minutes			30 minutes			2 hours		
	Conc.	**Purity**	**Total Protein**	**Conc.**	**Purity**	**Total Protein**	**Conc.**	**Purity**	**Total Protein**
pPAL-MC	0.09	86.4	0.36	0.08	87.3	0.36	0.12	85	0.48

Table A.2. Time-course incubation (1 mL eXact Column) protein performance data. Concentrations are given as mg mL^{-1}. Purity is represented as percentages. Total protein is given in mg.

Figure A.1.

A

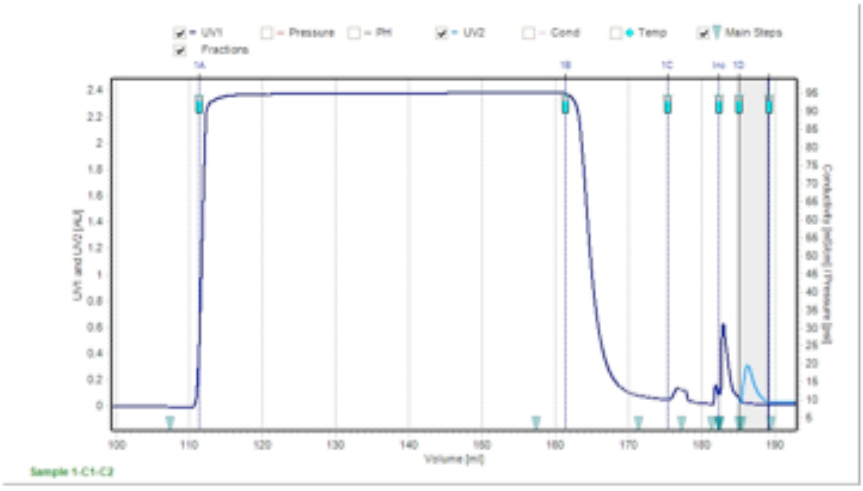

B

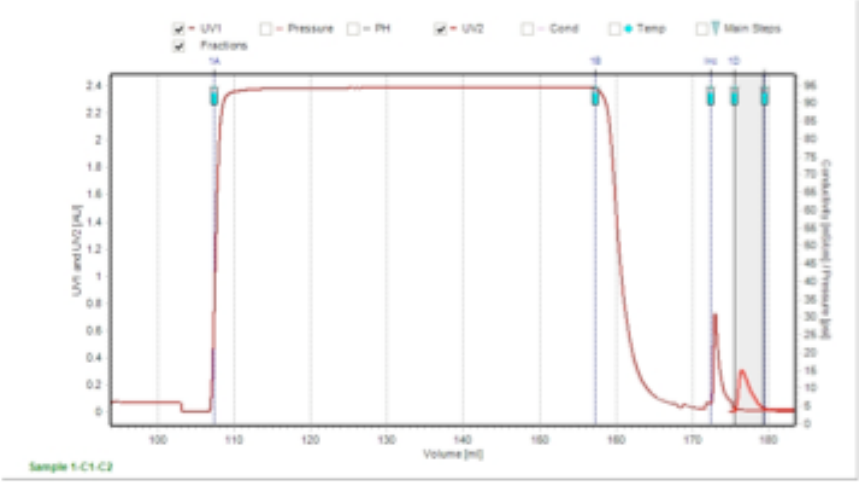

Figure A.1. Trial-scale purification of MetC with 1 mL eXact column. A. Chromatogram of lysate prepared by chemical lysis of 1L culture (Affinity trace (UV1) in dark blue, Desalting trace (UV2) in light blue). **B.** Chromatogram of lysate prepared by sonication of 1L culture (Affinity trace (UV1) in dark red, Desalting trace (UV2) in red). Collected fractions are indicated above graphs. Inc. = Column Incubation.

Figure A.2.

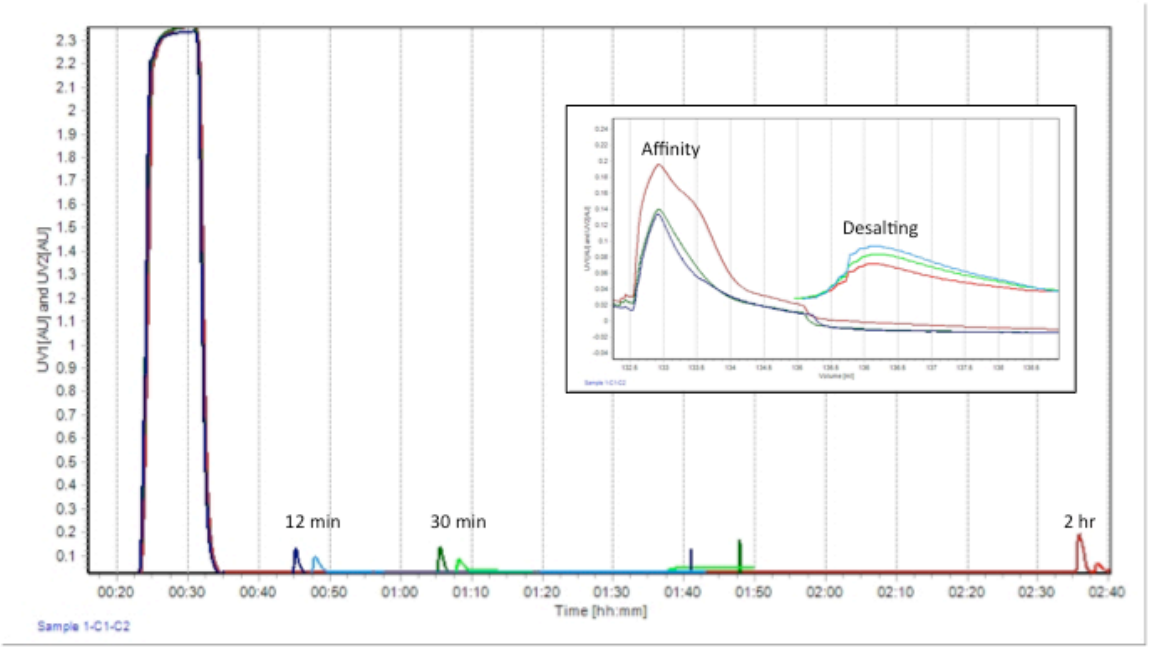

Figure A.2. Trial-scale purification of MetC with varying column incubation times. Combined chromatogram of purifications varying column incubation time with affinity traces (dark blue, dark green, dark red) 12 min, 30 min, 2 hr, respectively) and desalting traces (light blue, light green, light red) displayed based on total processing time (main image) or based on total processing volume (inset). Peaks in the main image between 1:40 and 1:50 correspond to column cleaning steps for the 12 min and 30 min incubations.

Figure A.3.
A

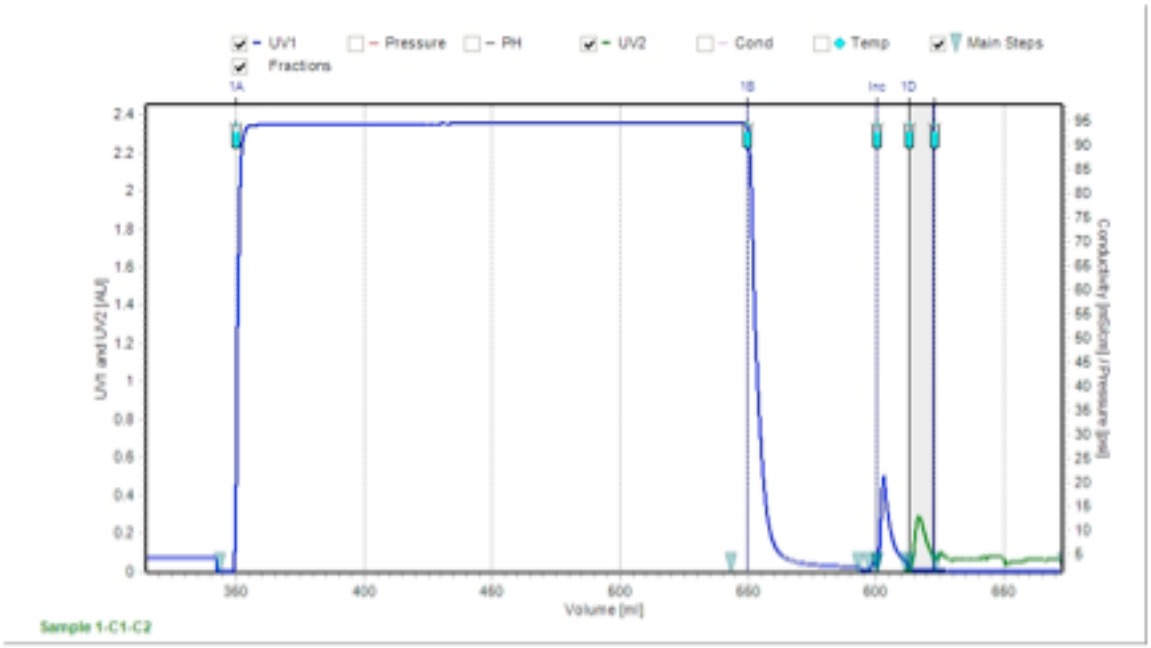

B

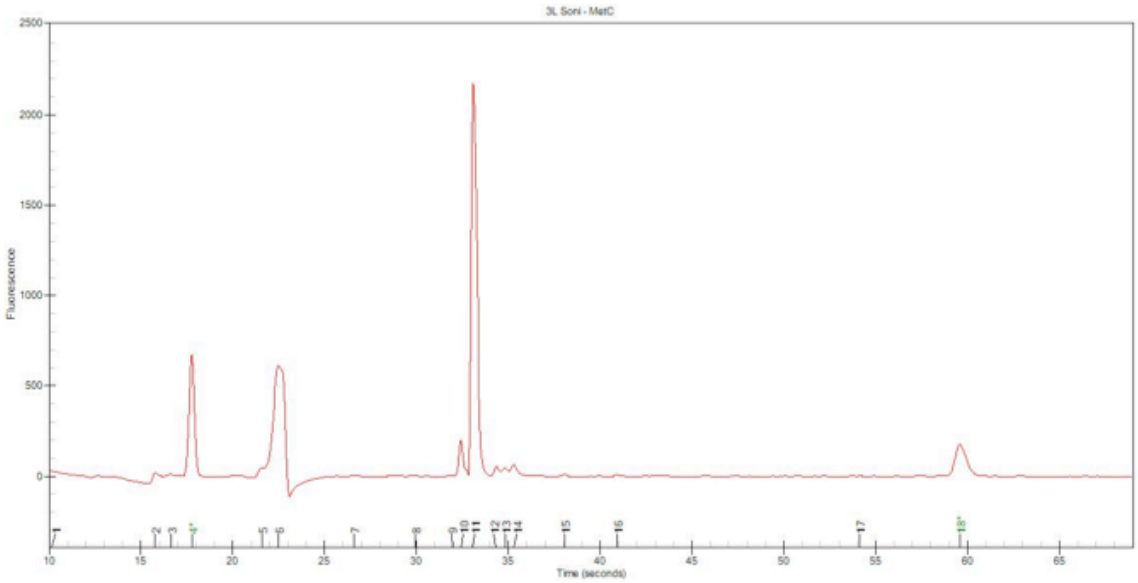

Figure A.3. Large scale purification of MetC with 5 mL eXact column. A. Chromatogram of 200 mL sonicated lysate (3L culture volume). Affinity (UV1) trace in blue, desalting (UV2) trace in green. Collected fractions are indicated above the graph. **B.** Representative Experion electropherogram of eluted MetC protein (87.2% purity at 0.871 mg mL^{-1} protein concentration)

Figure A.4.
A

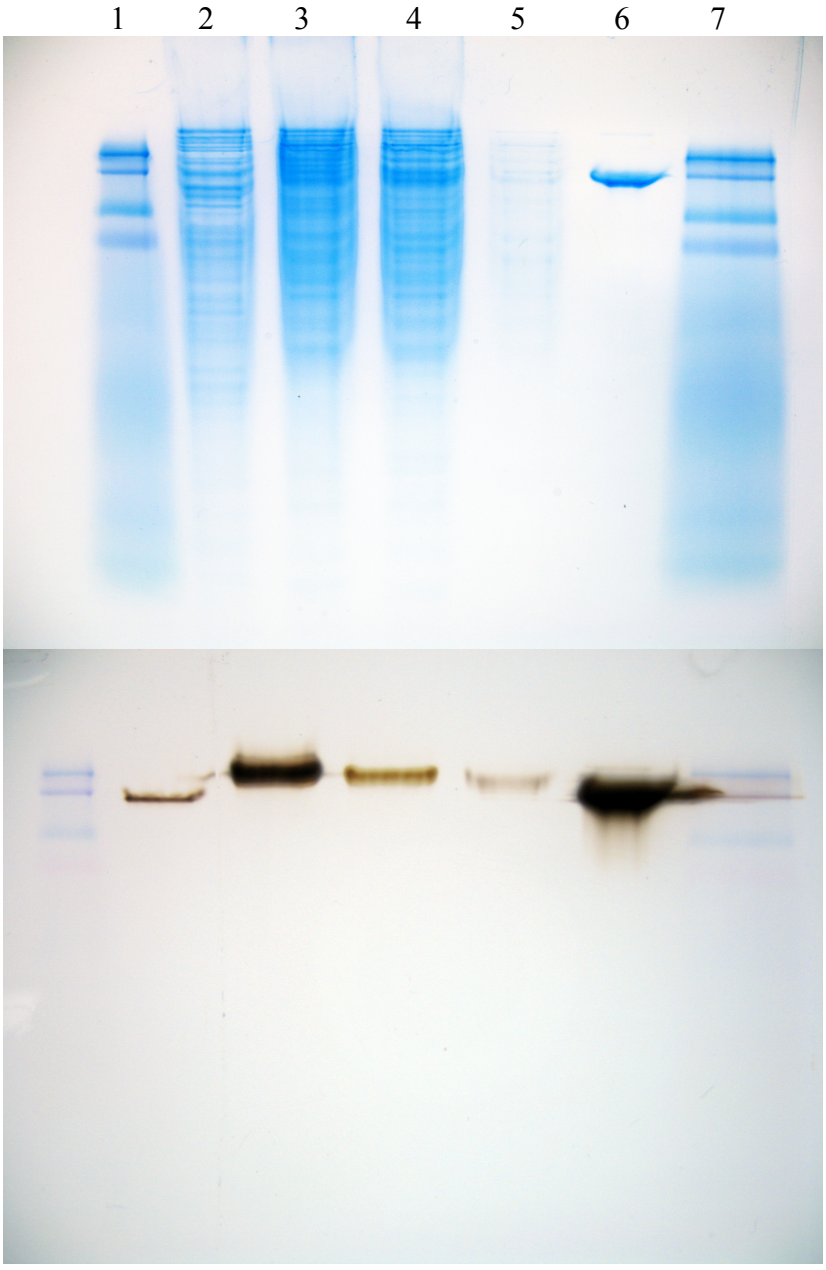

Figure A.4. Native- and SDS-PAGE Analysis. A. Native-PAGE of *S. oneidensis* MR-1 crude lysate and collected fractions from 3L purification (Lanes: 1- Precision Plus Kaleidoscope Marker, 2- MR-1 Crude Lysate, 3- MetC Load, 4-MetC Flowthrough, 5-MetC Wash, 6- MetC Eluted Protein, 7- Precision Plus Kaleidoscope Marker) Left Panel: Bio-Safe Coomassie G-250 stained gel, Right Panel: Cystathionine beta-Lyase activity

stained gel. Black precipitates correspond to the cleavage of thiol from L-cysteine and subsequent reaction with lead nitrate to form an insoluble lead sulfide. MR-1 lysate and eluted protein acivity bands are slightly lower due to absence of the eXact fusion-tag. **B.** Bio-Safe Coomassie G-250 stained SDS-PAGE Gel of crude lysate and collected fractions. Lanes are the same as in Panel A. **C.** MALDI-TOF MS spectrum of Eluted MetC protein. Spectrum and masses of peptides correspond to those predicted in the MASCOT™ database.

B

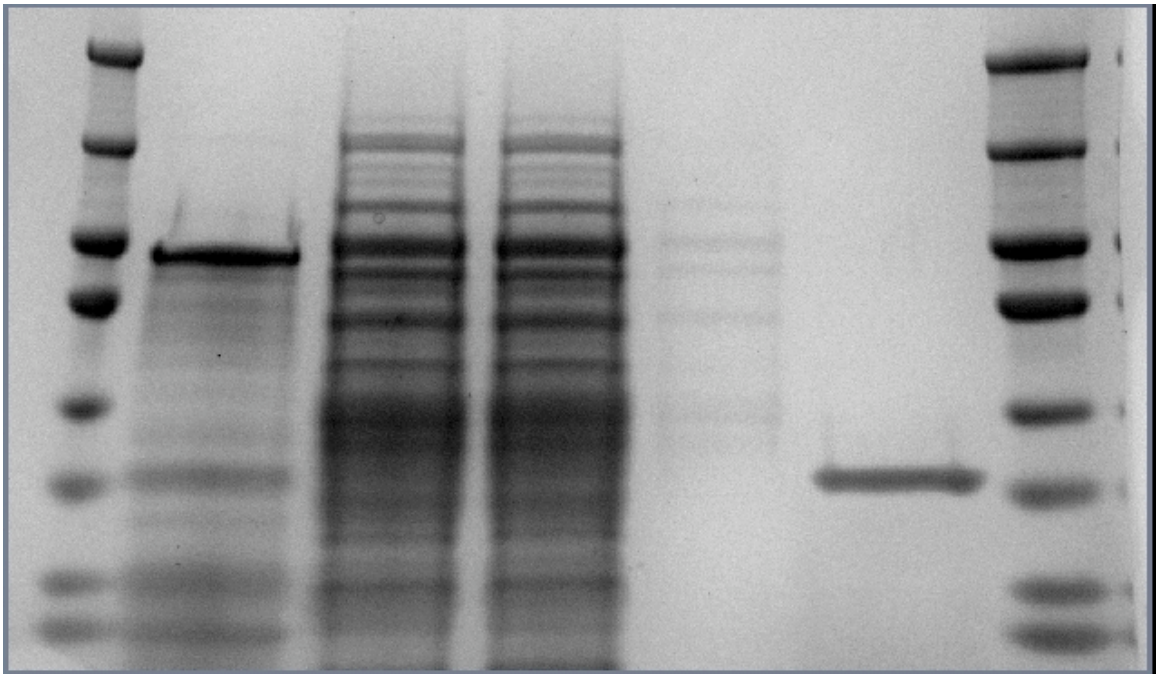

C

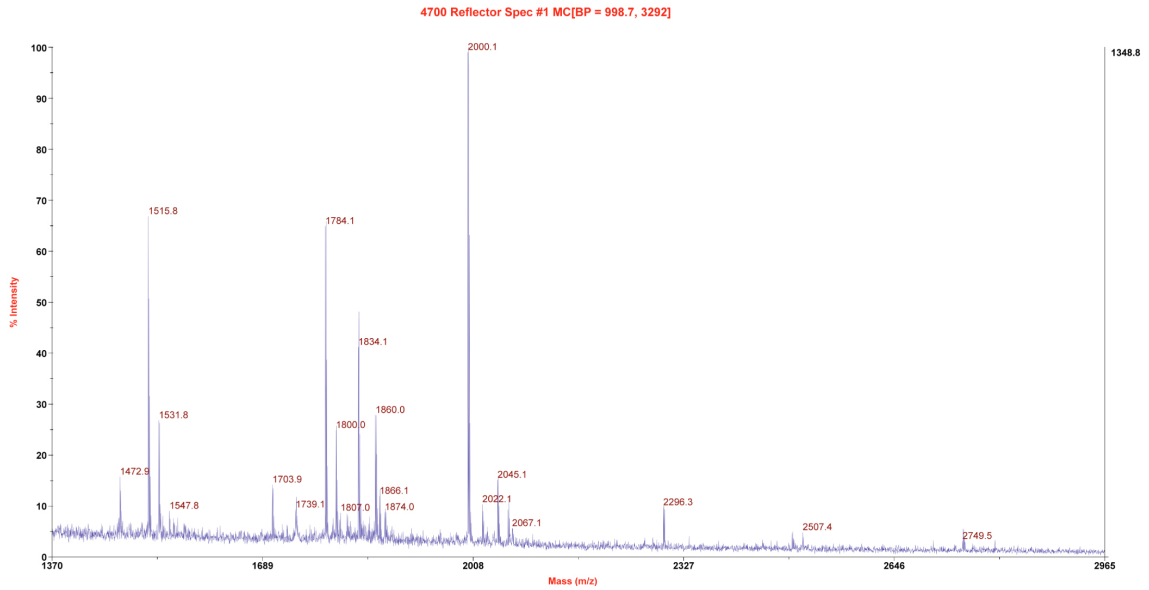

Figure A.4 continued